



***Institute of Atmospheric Optics
Russian Academy of Sciences
Laboratory of Coherent and
Adaptive Optics***

**Final Report
Contract F61775-98-WE071**

**Principal Investigator
Prof.Vladimir P.Lukin**

TOMSK-1999

19991117 119

AQF00-02-0462

Report for First Four Month Period

Contents

Contents	2
Introduction	3-4
Chapter 1. The Influence of Wave Front Dislocations on Phase Conjugation Instability with Thermal Blooming Compensation	5-33
1.1. Introduction	6-7
1.2. Model of Propagation	7-10
1.3. The Phase Conjugation Method	11-13
1.4. Screw Dislocations of the Wave Front	14-16
1.5. Phase Correction of Thermal Blooming	17-22
1.6. Conclusion	23
1.7. References for Chapter 2	24-26
Figures for Chapter1	27-33
Chapter 2. 2.1. Adaptive Optics Correction of Laser Beams on High Altitude Extended Paths and on Lower Atmosphere Paths with Real Beacons	36-45
2.1.1. Phase Fluctuations	37-38
2.1.2. Amplitude Fluctuations	38-45
2.2. Bandwidth Consideration	46-47
2.3. Anisoplanatic Degradation of Correction with Real Beacon	48-57
References for Chapter 2	58-59
Figures for Chapter 2	60-68

INTRODUCTION

This report is a summary of the first stage of scientific investigations performed in accordance with contract SPC 98-4041 between Institute of Atmospheric Optics SB RAN (IOA, Tomsk, Russia) and US Air Force Research Laboratory (AFB Kirtland, USA) via European Office of Aerospace Research and Development (EOARD, London, UK). This report was devoted to the numerical simulation for optical waves propagating in turbulent atmosphere under molecular absorption a high power laser radiation.

In accordance with the technical conditions the combined effect of thermal blooming and turbulence should be considered. These problems are exemplified in the two Chapters. To describe a real adaptive system it is necessary to take into account limits of its spatio-temporal resolution.

In Chapter 1 we consider the application of the phase conjugation method for the thermal blooming compensation. Analysis of the numerical experiment data has shown that the appearance of continuous auto-oscillations in adaptive system is connected with the occurrence of dislocations in the reference beam. The use of the Hartmann sensor with low spatial resolution and modal estimation of the phase results in smoothing the phase estimate and damps the AOS oscillations.

In the Chapter 2 we apply that even when the turbulent and nonlinear aberrations are of the same order, correction for thermal blooming is easier because scales of thermal aberrations are greater and frequencies lower. The only exception is a homogeneous path in the absence of scanning. In this case the strong thermal lens which appears near the beam focus may induce instability and decrease of control efficiency. For a moving object this effect can be disregarded.

So in the present report the main attention we devoted to the problem of compensation for turbulent aberrations.

Chapter 1. The Influence of Wave Front Dislocations on Phase Conjugation Instability with Thermal Blooming Compensation

The present part of report is devoted to the application of the phase conjugation method for the thermal blooming compensation. Analysis of the numerical experiment data has shown that the appearance of continuous auto-oscillations in adaptive system is connected with the occurrence of dislocations in the reference beam. The use of the Hartmann sensor with low spatial resolution and modal estimation of the phase results in smoothing the phase estimate and damps the AOS oscillations.

1.1. INTRODUCTION

The problem of the influence decrease of thermal distortions¹ on the high-power beam focusing by way of control of the wave front shape at the emitting aperture of the optical system is one of the most interesting fields of application of adaptive optics. The known methods of phase control can be presented in the form of three groups: 1) a priori control^{2,3}; 2) maximization of the focusing criterion⁴; 3) phase conjugation^{5,6,7}.

The present part is devoted to the application of the phase conjugation method for the thermal blooming compensation. This problem was discussed previously in a series of papers of different authors⁵⁻¹², and the results of these papers indicate that the application of phase conjugation to correct nonlinear distortions of high-power beams has some specific features including the instabilities of a different type. For homogeneous horizontal paths the instability appears as parameters oscillations of corrected and reference beams⁷, and for vertical paths the small-scale instability is developed.

In the above-mentioned papers it was assumed that the wave front of the reference radiation was determined in all the points of the aperture of the adaptive system and could be measured and reproduced with an arbitrary accuracy by means of some ideal sensor and wave front corrector. At the same time, in the paper¹³ it was shown that at strong distortions of the optical wave front the appearance of singular points was possible, where the intensity was equal to zero, and the wave front had the singularities in the form of screw dislocations and represented a multisheeted surface. This hypothesis was confirmed by laboratory¹⁴ and numerical experiments¹⁵. As noted in the papers, devoted to the problem of dislocations, the appearance of singular points can significantly affect the work of adaptive optical systems. However, up to now the investigations are lacking, which could allow one to understand in what way the adaptive system will work under such conditions. The purpose of our paper is the investigation of the influence of

dislocations on the efficiency of phase conjugation when compensating the nonstationary thermal blooming of cw beam.

1.2. Model of Propagation

Propagation of monochromatic linearly-polarized paraxial beam in an optically-inhomogeneous medium is described by the parabolic wave equation for a slow component of its complex amplitude¹⁶ $\mathbf{E} = \mathbf{e}_E \cdot E \cdot \exp(i\omega t - ikz)$:

$$2ik \frac{\partial E}{\partial z} = \nabla_{\perp}^2 E + k^2(n^2 - n_0^2)E \quad (1.1)$$

where $k = 2\pi/\lambda$ is the wave number; $\omega = c/\lambda$ is the frequency of electromagnetic oscillations; λ is the wavelength; $\nabla_{\perp}^2 = \partial^2/\partial x^2 + \partial^2/\partial y^2$ is the transverse Laplacian; \mathbf{e}_E is the polarization vector of electric field \mathbf{E} ; $n(x, y, z)$ is the refractive index. The boundary conditions for the complex amplitude are given as

$$E(\mathbf{r}, 0, t) = A(\mathbf{r}) \cdot \exp[i\varphi(\mathbf{r}, t)], \quad \mathbf{r} = (x, y) \quad (1.2)$$

where $A(x, y)$ is the amplitude distribution in the beam cross-section in the plane of emitting aperture; φ is its phase. For the cw Gaussian focused beam considered here we have:

$$A(\mathbf{r}) = A_0 \exp\left(-\frac{r^2}{2a_0^2}\right); \quad \varphi(\mathbf{r}, t) = \frac{kr^2}{2f} + \Phi(\mathbf{r}, t); \quad (1.3)$$

where a_0 is the beam radius at the intensity level $1/e$; f is the focal length; $\Phi(\mathbf{r}, t)$ is the phase correction. A_0 is the amplitude on the beam axis. The field of the refractive index in the high-power beam channel in the isobaric approximation is determined by temperature distribution in its cross-section, described by the nonstationary equation of forced heat transfer for the temperature field¹ T :

$$\frac{\partial T}{\partial t} + \mathbf{V}_{\perp} \nabla_{\perp} T = \frac{\alpha}{\rho C_p} W(\mathbf{r}, z, t),$$

$$T(\mathbf{r}, z, t = 0) = T_0, \quad (1.4)$$

where $W = EE^* \cdot 8\pi/cn_0$ is the beam intensity; $\mathbf{V}_{\perp} = (V_x, V_y)$ is the transverse component of wind velocity; α is the absorption coefficient; ρ is the density; C_p is the specific heat at constant pressure. For small variations of air temperature the connection between the temperature and the refractive index can be considered linear: $n - n_0 \approx n'_T(T_0) \cdot (T - T_0)$.

Assuming $n_0 \approx 1$, after substitution in Eq.(1.1), we have:

$$2ik \frac{\partial E}{\partial z} = \nabla_{\perp}^2 E + 2k^2 n'_T \cdot (T - T_0) \cdot E. \quad (1.5)$$

Thus, the nonstationary thermal blooming is described by the set of equations (1.4-1.5) together with the boundary condition (1.3).

Both the reflected (or scattered) radiation and the independent source can serve as the reference wave in the adaptive optical system (AOS). Here we consider only the case of the independent coherent reference beam, being propagated toward the corrected one along the same path. Such an AOS has been realized, for example, in the laboratory experiment⁹. Propagation of the complex amplitude of the reference beam $\mathbf{U} = \mathbf{e}_U \cdot U \cdot \exp(i\omega t + ikz)$ is described by the wave equation

$$-2ik \frac{\partial U}{\partial z} = \nabla_{\perp}^2 U + 2k^2 n'_T (T - T_0) U. \quad (1.6)$$

Boundary conditions were given so that in the absence of distortions the complex amplitudes of the high-power and reference beams were conjugated in the plane $z = 0$. Hence, their complex amplitudes must be conjugated also in the plane $z = f$, i. e.,

$$U(\mathbf{r}, f) = E_0^*(\mathbf{r}, f), \quad (1.7)$$

where $E_0(\mathbf{r}, f)$ is the solution of Eq.(1.5) at $T \equiv T_0$ with boundary conditions (1.3) at $\Phi \equiv 0$.

For numerical solution of equations describing the propagation of reference and high-power beams we used the splitting method^{7,17,18} with the symmetrized splitting operator. In this case all the fields are represented on the three-dimensional grid with the dimension (N_\perp, N_\perp, N_z) :

$$\begin{aligned} E_{I,J}(z_K) &= E(x_I, y_J, z_K) = E(\mathbf{r}_{I,J}, z_K), \\ x_I &= h_\perp \cdot (I - I_0); \quad I = 1, 2, \dots, N_\perp, \\ y_J &= h_\perp \cdot (J - J_0); \quad J = 1, 2, \dots, N_\perp, \\ z_K &= h_z \cdot (K - \tfrac{1}{2}); \quad K = 1, 2, \dots, N_z, \end{aligned} \tag{1.8}$$

where (I_0, J_0) are the values of indices corresponding to the origin of the coordinates, (h_\perp, h_\perp, h_z) are the distances between the nodes of the grid. The results of calculations given below were obtained at $N_\perp = 64$, $h_\perp = a_0/8$, $N_z = 16$, $h_z = f/16$.

1.3. The Phase Conjugation Method

The phase conjugation method is a special case of the more general method of wave front inversion based on reciprocity of electrodynamics equations. As applied to the used mathematical model, the reciprocity of the propagation equation means that if the complex amplitudes E and U are conjugated in the plane $z = 0$, then they are conjugated in the focal plane $z = f$, and *vice versa*:

$$E(\mathbf{r}, 0) = U^*(\mathbf{r}, 0) \Leftrightarrow E(\mathbf{r}, f) = U^*(\mathbf{r}, f) \quad (1.9)$$

Owing to the technical difficulties occurring in the wave amplitude control, in AOS we usually restrict ourselves to the phase control, that is, the phase conjugation method is used:

$$\text{Arg}(E(\mathbf{r}, z = 0)) = \text{Arg}(U^*(\mathbf{r}, z = 0)) = -\text{Arg}(U(\mathbf{r}, z = 0)) \quad (1.10)$$

If the distributions of amplitude modulus of the reference and corrected fields are approximately equal

$$A(\mathbf{r}) = |E(\mathbf{r}, 0)| \approx |U(\mathbf{r}, 0)|, \quad (1.11)$$

(or they differ by the constant multiplier), then one can look forward to high efficiency of such a purely phase control. The boundary condition for a corrected beam is of the form:

$$E(\mathbf{r}, 0) = A(\mathbf{r}) \cdot \exp(-i \cdot \text{Arg}(U(\mathbf{r}, 0))), \quad (1.12)$$

or

$$E(\mathbf{r}, 0) = A(\mathbf{r}) \cdot \exp(-i \cdot \arg(U(\mathbf{r}, 0))). \quad (1.13)$$

Mathematical formulation of the phase conjugation method (1.12) has the two peculiarities. First, the argument of the complex number is determined accurate to $2\pi m, m = \pm 1, \pm 2, \dots$; second, the argument of zero complex number is not determined.

If in the case of numerical simulation of an AOS the corrected field is determined through the principal value of the argument of the reference wave complex amplitude (1.13), then the first peculiarity is unessential. However, in controlling the wave front corrector to calculate the approximation of the required surface we need the unwrapped phase while the principal value of the argument is limited by the range $[-\pi, +\pi]$. To obtain the unwrapped phase the operation of "phase unwrapping" should be fulfilled. It is common practice in this case to calculate the phase differences and then the problem on the function reconstruction is solved on the basis of the values of its first differences in two directions. At numerical simulation the phase difference between the two adjacent nodes of the grid is determined as follows

$$\begin{aligned}\Delta_{I,J}^x &= \text{Arg}(U_{I+1,J}) - \text{Arg}(U_{I,J}) = \arg(U_{I+1,J}) + 2\pi m_{I+1,J} - \arg(U_{I,J}) - 2\pi m_{I,J} \\ &= \arg(U_{I+1,J}) - \arg(U_{I,J}) + 2\pi k_{I,J}^x, |k_{I,J}^x| \leq 1;\end{aligned}\quad (1.14)$$

and similarly $\Delta_{I,J}^y$. The values of $k_{I,J}^x, k_{I,J}^y \in \{-1, 0, +1\}$ are determined from the condition¹⁵ $|\Delta_{I,J}^x| \leq \pi, |\Delta_{I,J}^y| \leq \pi$. Similarly the phase differences can be determined as

$$\begin{aligned}\Delta_{I,J}^x &= \arg(U_{I+1,J} \cdot U_{I,J}^*) \\ \Delta_{I,J}^y &= \arg(U_{I,J+1} \cdot U_{I,J}^*)\end{aligned}\quad (1.15)$$

The problem of reconstruction of unwrapped phase from its differences calculated from the complex amplitude in the nodes of reference grid, is mathematically equivalent to the problem of phase reconstruction from phase differences obtained from the data of the shearing interferometer or estimated by the local phase tilt measured using the Hartmann sensor. Since the number of difference values is twice as large as the number of points, where the phase value must be obtained, such a problem is over determined and the supplementary conditions are conventionally superimposed, namely, minimizing of square law discrepancy¹⁹

$$\sum_{I,J} [(\phi_{I+1,J} - \phi_{I,J}) - \Delta_{I,J}^x]^2 + [(\phi_{I,J+1} - \phi_{I,J}) - \Delta_{I,J}^y]^2 \rightarrow \min \quad (1.16)$$

or minimizing of the integral variance of an error estimate²⁰

$$\left\langle \sum_{I,J} (\phi_{I,J} - \hat{\phi}_{I,J})^2 \right\rangle \rightarrow \min. \quad (1.17)$$

Here the statistical averaging is denoted by angular brackets, $\phi_{I,J}$ is the sought estimate of the phase, $\hat{\phi}_{I,J}$ is its exact value. In both cases the problem amounts to solution of the set of linear equations of the following form:

$$\phi_{I+1,J} + \phi_{I-1,J} + \phi_{I,J+1} + \phi_{I,J-1} - 4\phi_{I,J} = \Delta_{I,J}^x + \Delta_{I,J}^y - \Delta_{I-1,J}^x - \Delta_{I,J-1}^y. \quad (1.18)$$

When the differences are specified at the homogeneous grid, for solution of this problem we can use the method of the discrete Fourier transformation (DFT) and the Fourier fast transform algorithm^{21,22} (FFT) if the number of grid nodes satisfies the appropriate requirements. Solution of the set of Eqs (1.18) reconstructs the argument of complex amplitude except for an arbitrary constant

$$\begin{aligned} \text{Arg}(U_{I,J}) &= \phi_{I,J} + C \\ U_{I,J} &= |U_{I,J}| \cdot \exp[i(\phi_{I,J} + C)] \end{aligned} \quad (1.19)$$

and corresponds exactly to initial values of differences

$$\phi_{I+1,J} - \phi_{I,J} = \Delta_{I,J}^x, \phi_{I,J+1} - \phi_{I,J} = \Delta_{I,J}^y. \quad (1.20)$$

if the field U has no zeros.

1.4. Screw Dislocations of the Wave front

In the points where the complex amplitude (CA) of optical wave is exactly equal to zero, its argument is not determined. If this point lies on the line intersection, where the real and imaginary parts of CA change the sign, this point is the center of a screw dislocation of wave front. The existence of dislocations was predicted theoretically¹³ and was supported by the results of laboratory¹⁴ and numerical¹⁵ experiments.

Let us consider the vector field $\mathbf{g} = (g_x, g_y)$ determined as follows:

$$\begin{aligned} g_x(x, y) &= \lim_{\Delta x \rightarrow 0} \frac{1}{\Delta x} \arg[U(x + \frac{\Delta x}{2}, y)U^*(x - \frac{\Delta x}{2}, y)] \\ g_y(x, y) &= \lim_{\Delta y \rightarrow 0} \frac{1}{\Delta y} \arg[U(x, y + \frac{\Delta y}{2})U^*(x, y - \frac{\Delta y}{2})]. \end{aligned} \quad (1.21)$$

From the viewpoint of determination the field $g(p)$ is the gradient of the optical wave phase, and is truly of this kind if $U(\mathbf{r})$ nowhere becomes zero.

$$|U(\mathbf{r})| \neq 0 \Rightarrow \mathbf{g} = \nabla \cdot \text{Arg}(U(\mathbf{r})). \quad (1.22)$$

With dislocations, the field \mathbf{g} has peculiarities and ceases to be a purely potential field, and the contour integral

$$\oint_C \mathbf{g} \cdot d\mathbf{r} = \pm 2\pi \cdot (N_+ - N_-) \quad (1.23)$$

is determined by the number of dislocations twisted in positive (N_+) and negative (N_-) directions, which are inside this contour^{13,14}. In this case the phase difference expressed by the contour integral

$$\phi(\mathbf{r}_2) - \phi(\mathbf{r}_1) = \int_{\mathbf{r}_1}^{\mathbf{r}_2} \mathbf{g} d\mathbf{r} \quad (1.24)$$

depends on the integration method, and the equation

$$\nabla \phi = \mathbf{g} \quad (1.25)$$

has no solution.

It is well known that any vector field \mathbf{g} can be represented as a sum of irrotational \mathbf{g}_1 and solenoidal \mathbf{g}_2 components:

$$\mathbf{g} = \mathbf{g}_1 + \mathbf{g}_2 \quad (1.26)$$

and the solenoidal component can be excluded by the use of the divergence operator^{22,23,24}, so that the solution of the Poisson equation

$$\nabla^2 \phi = \text{div } \mathbf{g} = \text{div } \mathbf{g}_1 \quad (1.27)$$

corresponds to the potential part of the field \mathbf{g} :

$$\nabla \phi = \mathbf{g}_1. \quad (1.28)$$

Since the set of linear Eqs (1.18) is the finite-difference representation of the Poisson equation (1.27), the algorithm of reconstruction, solving the set of linear equations (1.18), "filters" the wave front dislocations, smoothing out the estimate of the phase of optical wave. A number of the results on numerical simulation of phase conjugation has been obtained based on the boundary condition of exact phase conjugation:

$$E_{I,J}(0) = A_{I,J} \cdot \exp[i \arg(U_{I,J}(0))] \quad (1.29)$$

As a rule, dislocations do not fall accurately on the grid nodes, and the boundary condition (1.29) is correct. However, the corresponding analytical boundary condition

$$E(\mathbf{r},0) = A(\mathbf{r}) \cdot \exp[i \arg(U(\mathbf{r},0))] \quad (1.30)$$

is not determined at the points where $U(\mathbf{r},0) = 0$. When at the same points $A(\mathbf{r}) \neq 0$, the continuity of the field $E(\mathbf{r},0)$ is disturbed and it becomes nondifferentiable. Although the grid boundary condition (1.29) can be considered as a result of the corrector application, with the element size, being equal to the distance between the grid nodes, care must be exercised when interpreting the results of numerical experiment since the corresponding analytical boundary condition (1.30) is incorrect. To gain greater insight

into why the characteristics of boundary condition of the type (1.29) show themselves with an appearance of dislocations in the reference beam, the numerical experiment was performed, in which we calculated the beam diffraction with the Gaussian intensity profile with the boundary condition of the form:

$$E(\mathbf{r}, 0) = A(\mathbf{r}) \exp[i \cdot \arg(x + iy)]. \quad (1.31)$$

As is evident from¹³, the field

$$U(\mathbf{r}, z) = e^{i\gamma} (B_x x + i \cdot B_y y), \quad (1.32)$$

where γ, B_x, B_y are the real constants, satisfies the parabolic wave equation in vacuum and has its dislocation in the origin of coordinates. Thus, the boundary condition (1.31) describes the field with dislocation at the point $\mathbf{r} = 0$. In this case its intensity is everywhere different from zero.

Figure 1.1 gives the 2D intensity repartition of such a beam for different values of $z' = z/z_d$, where $z_d = ka_0^2$ is the diffraction length. In the center of the beam the intensity gap is shaped reaching practically zero value at $z' = 0.1$. The similar effect is observed at compensation of thermal blooming when dislocations appear in the reference beam.

1.5. Phase Correction of Thermal Blooming

We have conducted the two types of numerical experiments on application of the phase conjugation method for correction of thermal blooming. In one case for the corrected beam we used the boundary condition of exact conjugation (30), and in the other case – the boundary condition (1.3). The phase correction $\Phi(\mathbf{r}, t)$ was obtained as a result of simulation of the Hartmann sensor and subsequent model estimating of the reference beam phase^{26, 27}.

In both cases we have simulated the "fast" adaptive system, focusing the Gaussian beam to the target plane, which is at the distance $f = \frac{1}{\sqrt{10}} z_d$. In the diffraction-limited case the intensity in the focus of such optical system is 10 times as large as the axial intensity on the emitting aperture. In the focal plane we recorded the peak intensity W_{\max} and the radiation power P falling within circle with radius $a_f = a_0 \cdot f / z_d$ which was equal to the radius of undistorted beam at the intensity level $1/e$. About 63% of the undistorted beam power falls within this circle. Simultaneously we recorded the appearance and coordinates of dislocations of the reference beam wave front in the plane $z = 0$. For this purpose in each node of the grid falling in the circle of radius $2a_0$ the value

$$\Sigma_{I,J} = \Delta_{I,J}^x + \Delta_{I+1,J}^y - \Delta_{I,J+1}^x - \Delta_{I,J}^y \quad (1.33)$$

was calculated corresponding to the integral (1.23) by the contour shaped by the four adjacent nodes of the grid. For the majority of nodes $\Sigma_{I,J} \cong 0$ with an accuracy up to the errors of arithmetical operations. The nodes, for which $\Sigma_{I,J} \cong \pm 2\pi$, correspond to the contours containing one or more dislocations. If $|\Sigma(I, J)| > \pi$, we considered that the

dislocation was discovered, to which the coordinates (x_d, y_d) of the contour center were attributed:

$$x_d = h_{\perp} \left(I + \frac{1}{2} - I_0 \right), y_d = h_{\perp} \left(J + \frac{1}{2} - J_0 \right) \quad (1.34)$$

Clearly, such a method does not permit detecting a pair of dislocations with different signs falling into the contour considered, but in this case they do not affect the results of solution of the propagation problem.

Let us consider the results of simulation of the precise phase conjugation. Figure 1.2 present the curves indicating the dependence of peak intensity W_{\max} and the coordinates of dislocation x_d on the time t , normalized as follows⁷:

$$t' = \frac{t}{\tau_V}, \tau_V = \frac{2a_0}{V}; W' = W \frac{2k^2 \alpha n'_T a_0^3}{\rho C_P V_{\perp} n_0}; P' = P \frac{2k^2 \alpha n'_T a_0}{\rho C_P V_{\perp} n_0}; x'_d = \frac{x_d}{a_0} \quad (1.35)$$

(later the primes of normalized values are omitted). The diagrams are given for the two values of axial intensity of the beam: $W_0 = 16$ and $W_0 = 24$. At the beam intensity $W_0 = 16$ (curve 1) the dislocations do not appear and the beam parameters become stationary. With the increase of beam intensity up to 24 we observed the intensity oscillations (curve 2) followed by periodic appearance of dislocations in the reference beam (curve 3). Dislocations appear close to the axis of the optical system and translate in the direction coinciding with the wind direction $\mathbf{V} = (V_x, 0), V_x > 0$, until they do not go out from the registration zone $x_d^2 + y_d^2 \leq (2a_0)^2$. At increase of intensity up to 32 resulted a new pair of dislocations appeared before the preceding pair had gone out from registration zone.

Figure 1.3 shows the typical intensity distribution of a corrected beam in the cross-section $z = f/32$. The two intensity gaps, traveling to the lee edge of the beam, correspond to the two dislocations in the phase of the reference beam.

To understand the mechanism of origination of oscillations, given in Fig. 1.2, the coordinate of cross-section z_{\max} was recorded, in which the peak intensity of a corrected beam is maximal, that is, the position of beam waist.

Figure 1.4 shows the dependence of position of beam waist z_{\max} and peak intensity in it on the time. At the intensity $W_0 = 16$ the beam waist is gradually shifted to the emitting aperture and its position is stabilized at the mark $z_{\max} \approx 0.85 \cdot f$. At $W_0 = 24$ the waist is shifted close to the emitting aperture and its position varies near the point $z_{\max} \approx 0.4 \cdot f$ with the amplitude of the order of $\Delta z_{\max} \approx 0.15 \cdot f$. At the same time, the intensity in the waist much exceeds the initial intensity of the beam. The period of oscillations of waist position coincides with the period of dislocation appearance. This effect can be interpreted as the manifestation of positive feedback between the adaptive system and the thermal lens. At the initial stage of heating $t \leq \tau_v$ the main contribution to distortions is introduced by defocusing. Its compensation results in an additional focusing of high-power beam and its waist shift to the source. The waist becomes narrower, and its intensity increases that leads to the medium temperature increase in the beam waist and to amplification of defocusing strength of the thermal lens. This results in subsequent shift of waist and so on.

The thermal lens shift to the emitting aperture decreases "the feedback coefficient". In the limiting case when the thermal lens intensity is concentrated close to the AOS aperture and the additional focusing, contributed by AOS, is compensated by the defocusing thermal lens, we do not observe the subsequent increase of defocusing of reference beam and focusing of high-power beam. If the distortions in the high-power beam waist achieve the value sufficient for appearance of dislocation in the reference beam, the information on the defocusing introduced by thermal lens, is erased without reaching the adaptive system, and the high-power beam focusing causing whereas its

waist to be shifted to the target. As a result, the intense thermal lens, being the cause of the occurrence of the dislocations, begins to cool off and some time later the lens is cooled to the state when dislocations disappear and the feedback is reconstructed. Then the whole cycle is repeated and the system develops into the regime of auto-oscillations typical for nonlinear systems with feedback.

At subsequent stage of work the AOS was simulated with a Hartmann-Shack sensor, consisting of 16 subapertures arranged in four rows. The fourcorner subapertures were not taken into account, and local tilts were estimated only in 12 subapertures (Fig. 1.5). The size of the sensor aperture $D = 4a_0$ corresponds to the beam diameter at the intensity level $1/e^2$. The reference beam was fed to the sensor after passing through correcting and focusing systems:

$$U(\mathbf{r}, 0, t + \Delta t) \cdot \exp\left(i \frac{kr^2}{2f} + i\Phi(\mathbf{r}, t)\right). \quad (1.36)$$

The phase correction was determined as a sum of Zernike polynomials Z_ℓ

$$\begin{aligned} \Phi(\mathbf{r}, 0) &= 0, \\ \Phi(\mathbf{r}, t + \Delta t) &= \Phi(\mathbf{r}, t) + \Delta\Phi, \\ \Delta\Phi &= \sum_{\ell=2}^{15} c_\ell(t + \Delta t) \cdot Z_\ell\left(\frac{\mathbf{r}}{2a_0}\right). \end{aligned} \quad (1.37)$$

with the weight factors c_ℓ obtained by modal estimating the phase^{25,26,27} on the circle inscribed in the sensor aperture.

Figure 1.6 shows the dynamics of peak intensity at the target for three values of initial beam intensity. In all the three cases the oscillations are lacking, i. e., the application of the Hartmann sensor with modal estimate damps the oscillations or, at least, increases the threshold of their appearance. Nevertheless, the dislocations in the reference beam

could appear. It turned out that in the focal plane of the sensor subaperture to which the dislocation comes, the two focal spots are observed, each having the diffraction size (Fig.1.7). In contrast to AOS with a precise phase conjugation the position of dislocations remained relatively stable.

Since the phase correction is now determined by the weighted sum of the Zernike polynomials it is possible to control directly the aberration spectrum of phase correction. The above considerations enable us to assume that the positive feedback between the adaptive system and the thermal lens is closed mainly by the control of quadratic aberrations. In this case such a feedback affects negatively the correction efficiency. Besides, it is known that with thermal blooming the optimal focal length is larger¹⁷ than in vacuum while the adaptive correction decreases the focal length of the system, compensating the thermal lens effect.

The first step that we can propose for decreasing the harmful influence of this effect is the complete exclusion of the focusing control:

$$\Delta\Phi = \sum_{\ell=2}^{15} (1 - \delta_{\ell,4}) c_{\ell}(t + \Delta t) \cdot Z_{\ell}\left(\frac{\mathbf{r}}{2a_0}\right), \quad \delta_{\ell m} = \begin{cases} 0, \ell \neq m \\ 1, \ell = m \end{cases}. \quad (1.38)$$

It turned out that excluding astigmatism control

$$\Delta\Phi = \sum_{\ell=2}^{15} (1 - \delta_{\ell,4}) \cdot (1 - \delta_{\ell,5}) \cdot (1 - \delta_{\ell,6}) \cdot c_{\ell} Z_{\ell}, \quad (1.39)$$

gives an additional increase of correction efficiency. Since except for quadratic aberrations the tilt and coma contribute greatly, the correction by Eq.(1.39) results in mainly beam pointing and straightening of a characteristic "sickle", owing to coma.

Figure 1.8 shows the steady values of parameters of a corrected beam as a function of the initial intensity when correcting by the formula (1.37) (curve 1) and the formula (1.39) (curve 2), that is, without control of total beam focusing and astigmatism. Curve 3

in this figure corresponds to the precise phase conjugation (the boundary condition(1.29)), and the curve 4 corresponds to the system without correction. The data for precise phase conjugation are obtained by averaging over time the corresponding instantaneous values.

It is seen that the correction efficiency by the formula (1.37) is somewhat lower than the efficiency of precise phase conjugation while the correction by the formula (1.39) (with disconnecting of control of quadratic aberrations) is more effective than the precise phase conjugation starting from the power, at which the dislocations and auto-oscillating regime take place ($W_0 \approx 20 \div 24$). Together with optimization of the beam initial intensity the correction by the formula (1.39) gives a gain in peak intensity in the focal plane more than twofold as compared with the system without correction and approximately 1.5-fold gain as compared with precise phase conjugation and the gain in power P is 3- and 1.5-fold, respectively.

The exclusion of control of quadratic aberrations will not, to be sure, give the best gain in all situations. For the beams with the non-Gaussian profile of intensity and for a vertical path or with beam scanning the results may be different. In particular, for the vertical path the small-scale instability is more typical; for suppressing the above instability one must exclude the small-scale part of the reference beam phase⁸.

1.6. Conclusion

We consider the problem of compensation of nonstationary thermal blooming by the phase conjugation method. Analysis of the numerical experiment data has shown that the appearance of continuous auto-oscillations in adaptive system is connected with the occurrence of dislocations in the reference beam.

The use of the Hartmann sensor with low spatial resolution and modal estimation of the phase results in smoothing the phase estimate and damps the AOS oscillations. Adaptive compensation of defocusing and astigmatism results in the shift of the beam waist to the source and in the appearance of strong thermal lens. Elimination of the quadratic aberrations control weakens this effect and increases the efficiency of thermal blooming correction along the homogeneous path.

This project was made possible with support from the following grants: No.1000/1300 from the International Science Foundation and No.94-02-03027a from the Russian Foundation of Fundamental Researches.

1.7. References for Chapter 1

1. D.C.Smith, "High-power laser propagation: Thermal blooming", Proc.IEEE, Vol.65, No.12, pp.1679-1714, 1977.
2. L.C. Bradley, J.Herrmann, "Phase compensation for thermal blooming", Appl.Opt., Vol.13, No.2, pp.331-334, 1974.
3. J.A. Fleck, J.R.Morris, "Equivalent thin lens model for thermal blooming compensation", Appl.Opt., Vol.17, No.16, pp.2575-2579, 1978.
4. C.A. Primmerman, D.G. Fouche, "Thermal-blooming compensation: experimental observation using a deformable mirror system", Appl.Opt., Vol.15, No.4, pp.990-995, 1976.
5. J. Herrmann, "Properties of phase conjugate adaptive optics systems", J.Opt.Soc.Am., Vol.67, No.3, pp.290-295, 1977.
6. M.A.Voronsov, "Phase conjugation method in the light field thermal defocusing compensation problem", Kvant. Electron., Vol.6, No. 10, pp. 2078-2083, 1979.
7. V.E. Zuev, P.A. Konyaev, V.P. Lukin, "Minimization of atmospheric distortions of optical waves by methods of adaptive optics" Izv. Vyssh. Uchebn. Zaved., Fiz., Vol. XXVIII, No. 11, pp. 6-29, 1985.
8. V.L. Dmitriev, A.A. Mashukova, V.P. Lukin, V.V. Sychev, "Peculiarities of correction of laser radiation self-action along atmospheric paths using 'slow' phase-conjugate adaptive system", Atmospheric Optics, Vol. 3. No. 12, pp. 1269-1272, 1990.
9. B. Johnson, C. Primmerman, "Experimental observation of thermal-blooming phase-compensation instability", Opt.Lett., Vol.14, No.12, pp.639-641, 1990.
10. T.J. Karr, "Atmospheric effects on laser propagation", Proc.SPIE, Vol.1060, pp.120-128, 1989.

11. J.F. Schonfeld, "Linearized theory of thermal-blooming phase-compensation instability with realistic adaptive-optics geometry", J.Opt.Soc.Am.B, Vol.9, No.10, pp.1803-1812, 1992.
12. P.A. Konyaev, "Thermal blooming instabilities" Atmospheric and Oceanic optics, Vol. 5, No.12, pp. 1261-1268, 1992.
13. N.B. Baranova, B.Ya. Zel'dovich, "Dislocations of wave front surfaces and amplitude zeros", Zh. Eksper. Teor. Fiz., Vol. 80, pp.1789-1797, 1981.
14. N.B. Baranova, A.V. Mamaev, N.F. Pilipetsky, V.V. Shkunov, B.Ya. Zel'dovich, "Wave-front dislocations: topological limitation for adaptive systems with phase conjugation", J.Opt.Soc.Am., Vol.73, No.5, pp.525-528, 1983.
15. D.L. Fried, J.L. Vaughn "Branch cuts in the phase function", Appl.Opt., Vol.31, No.15, pp.2865-2882, 1992.
16. J.L. Walsh, P.B. Ulrich. "Thermal blooming of the laser beam in the atmosphere", Laser Beam Propagation through the Atmosphere, Topics in Applied Physics, Vol.25, Ed. by D. Strohbehn, Springer-Verlag, New York, 1981.
17. J.A. Fleck, J.R. Morris, M.D. Feit, "Time-dependent propagation of high-energy laser beam through the atmosphere", Appl.Phys., Vol.10, No.1, pp.129-139, 1976.
18. G.I. Marchuk, Methods of Computational Mathematics, M., Nauka, 535 p., 1980.
19. D.L. Fried, "Least-square fitting a wave-front distortion estimate to an array of phase-difference measurements", J.Opt.Soc.Am., Vol.67, No.3, pp.370-375, 1977.
20. R.H. Hudgin, "Wavefront reconstruction for compensated imaging", J.Opt.Soc.Am., Vol.67, No.3, pp.375-378, 1977.
21. K. Freischlad, C.L. Koliopoulos, "Wavefront reconstruction from noisy slope or difference data using the Discrete Fourier Transform", Proc.SPIE, Vol.551, pp.74-80, 1985.

22. A.N. Bogaturov, "Solution of systems of equations for zone reconstructions of wave front in adaptive optics", *Izv. Vyssh. Uchebn. Zaved., Fiz.*, Vol. XXVIII, No. 11, pp. 86–95, 1985.
23. J. Herrmann, "Least-squares wave front errors of minimum norm", *J.Opt.Soc.Am.*, Vol.70, No.1, pp.28-35, 1980.
24. R.J. Noll, "Phase estimates from slope-type wave-front sensors", *J.Opt.Soc.Am.*, Vol.68, No.1, pp.139-140, 1978.
25. V.P. Lukin, N.N. Maier, B.V. Fortes, "Calculation of point spread function for an adaptive telescope with a Hartmann wave front sensor", *Atmospheric Optics*, Vol.5. No. 12, pp. 1241–1251, 1992.
26. R. Cubalchini, "Modal wave-front estimation from phase derivative measurements", *J.Opt.Soc.Am.*, Vol.69, No.7, pp.972-977, 1979.
27. J. Herrmann, "Cross coupling and aliasing in modal wave-front estimation", *J.Opt.Soc.Am.*, Vol.71, No.8, pp.989-992, 1981.

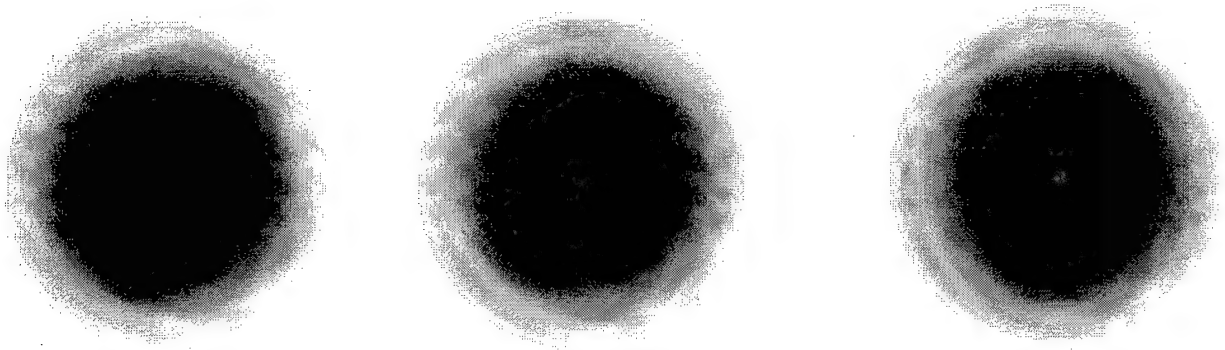


Fig. 1.1. Intensity cross sections at beam diffraction with boundary conditions (1.31) in vacuum. From left to right $z' = 0.03$, $z' = 0.06$, $z' = 0.09$.

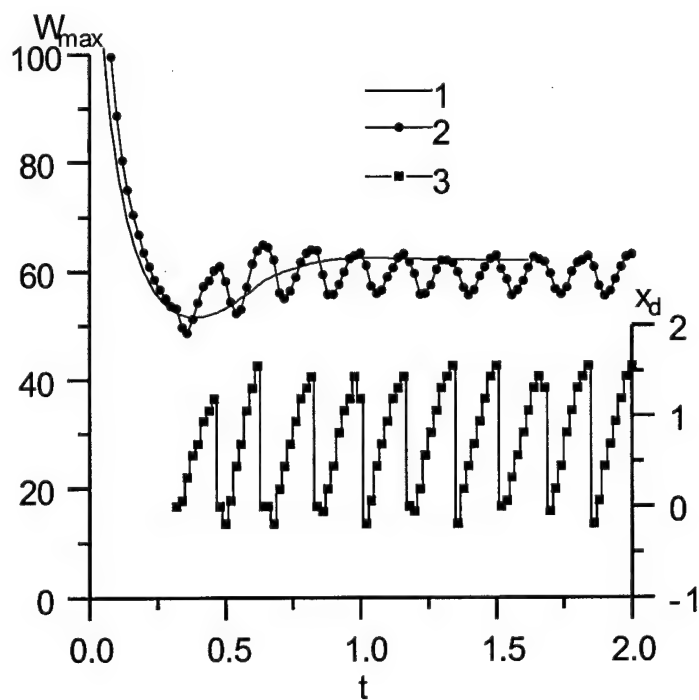


Fig. 1.2. Dynamics of peak intensity W_{\max} of a corrected beam in focal plane: 1—at the beam initial intensity, $W_0 = 16$; 2— $W_0 = 24$; 3—the coordinate of the reference beam dislocation $x_d(t)$ at $W_0 = 24$.

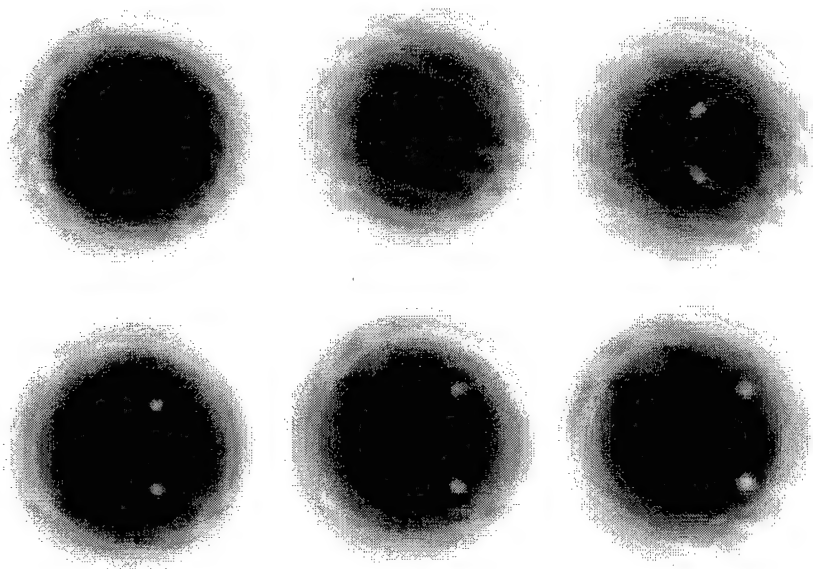


Fig. 1.3. Intensity distribution of a corrected beam in the cross section $z = f/32$ when originating the wave front dislocations in the reference beam. $W_0 = 24$. The first series: $t = 0.50; 0.52; 0.54$; the second series: $t = 0.56; 0.58; 0.60$.

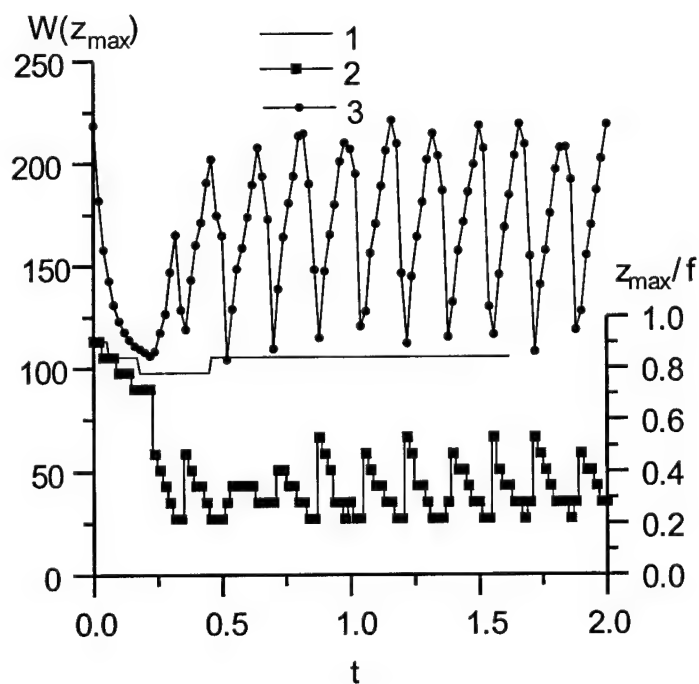


Fig. 1.4. Dynamics of beam waist position of a high-power beam $z_{\max}(t)$; 1 - $W_0 = 16$, 2 - $W_0 = 24$; 3 - peak intensity in the caustic for $W_0 = 24$.

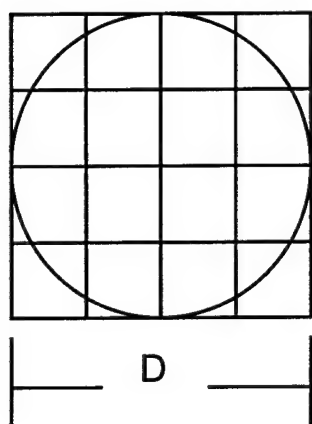


Fig. 1.5. Configuration of the wave front sensor.

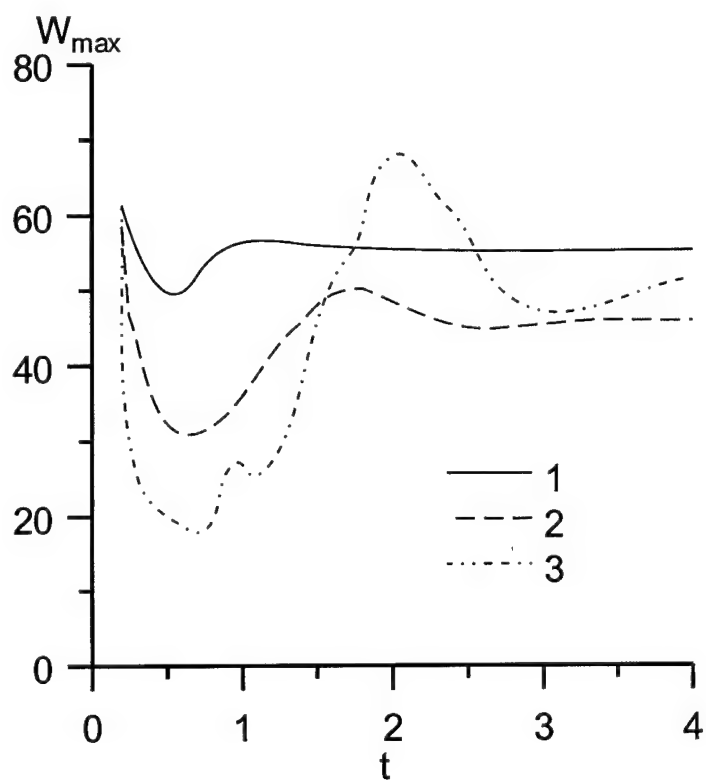


Fig. 1.6. Dynamics of peak intensity $W_{\max}(t)$ in the AOS focus with the Hartmann sensor.

1 – $W_0 = 16$; 2 – $W_0 = 32$; 3 – $W_0 = 64$

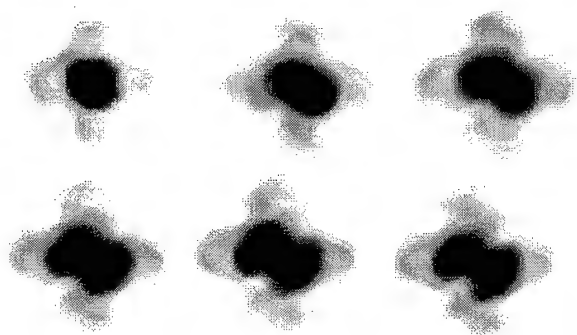


Fig. 1.7. Dynamic of intensity distribution in the subaperture focus of the Hartmann sensor at dislocation origination in the reference beam.

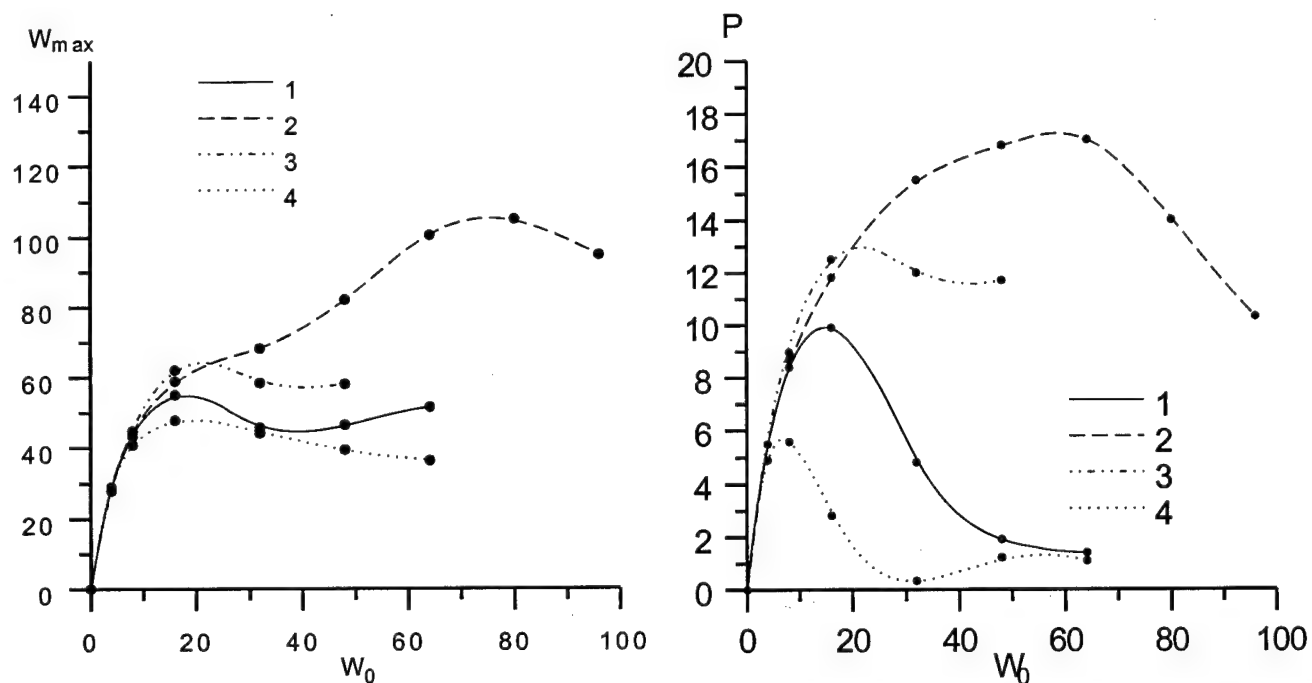


Fig. 1.8. Dependence of peak intensity W_{\max} (a) and the power at the target P (b) on the beam initial intensity W_0 for different versions of AOS. 1 – AOS with the Hartmann sensor (37); 2 – AOS with the Hartmann sensor (39); 3 – precise PC (phase conjugation); 4 – without correction.

CHAPTER 2. Adaptive Correction of Laser Beam

A laser beam propagating in the atmosphere are influenced simultaneously by thermal blooming and turbulence that results in aberrations of a focal spot. Character of thermal blooming depends not only on atmospheric conditions but also on beam power and velocity of a target. Turbulent aberrations prevail at large speed of scanning, from this point of view they are more important.

In the previous chapter it was pointed out that thermal aberrations of laser beams decrease sharply as the object velocity increases. Effectiveness of phase correction for thermal blooming increases at increase of scanning velocity, because in this case the thermal lens is placed near the transmitting aperture.

On the contrary, effectiveness of correction for turbulent aberrations decreases when the object velocity increases. Turbulent aberrations do not depend on speed of angular scanning but in the case of a moving object the requirements to the adaptive system bandwidth are higher than that for a motionless target.

The stated above is also true for the low atmosphere paths when a source is placed on the earth and an object altitude is a few kilometers. In this case the influence of thermal blooming is less comparing with turbulence because the coefficient of atmospheric absorption decreases more abruptly than intensity of turbulent aberrations. Additional factor of thermal blooming decreasing is angular scanning.

Even when the turbulent and nonlinear aberrations are of the same order, correction for thermal blooming is easier because scales of thermal aberrations are greater and frequencies lower. The only exception is a homogeneous path in the absence of scanning. In this case the strong thermal lens which appears near the beam focus may induce instability and decrease of control efficiency. For a moving object this effect can be disregarded.

2.1. Adaptive Optics Correction of Laser Beams on High Altitude Extended Paths and on Lower Atmosphere Paths with Real Beacons

Considering the problem of adaptive correction for turbulent aberrations a number of factors should be allowed for. These factors are connected with the peculiarities of aberrations and also with spatio-temporal characteristics of a system elements.

In this section the results of computations of the main parameters of adaptive optics system are presented, in the first order approximation the requirements to the system characteristics are formulated, and efficiency of correction are assessed on the given paths. The importance of such parameters as ratio of an aperture diameter to the coherence length, variance of beacon wave intensity fluctuations, and frequency bandwidth of a system are clearly shown.

The requirements to the beacon intensity are also considered as well as possibility to create a corresponding beacon.

2.1.1. Phase Fluctuations

Turbulent inhomogeneities of refraction index induce phase fluctuations of optical radiation^{1,2}. In the problem of adaptive correction such characteristic of phase aberration as ratio of an aperture diameter to the coherence length is most important. The size of sensor subapertures and choice of wave front corrector are defined by this parameter.

In the problems of compensation for turbulent aberrations considered here an adaptive optics system detects and reproduces phase aberrations of a reference wave. When beacon is formed by reflection or scattering, reference wave is generated by a number of point sources. Because of this a coherence length r_0 should be assessed using an equation for spherical wave originated in the target plane³:

$$r_0^{-5/3} = 0.423k^2 \int_0^L C_n^2(x) Q^{5/3} \quad (2.1)$$

where

$$Q = 1, \quad Q = 1 - x/L \quad (2.2)$$

for a plane and spherical wave, respectively, x - is a distance from the aperture of adaptive system. Let us consider the results of computation of coherence length performed under the conditions of average turbulence for wavelength $\lambda = 1.315 \mu\text{m}$ (Fig. 2.1). For paths in the lower atmosphere which we are interested in the coherence length is in the interval 5 - 15 cm, excluding focusing at low-altitude flying objects ($H_t = 100-500 \text{ m}$) when on paths $L > 10 \text{ km}$, r_0 decreases to 3 - 5 cm. On paths in the upper atmosphere the range of r_0 values are more wide, it extends from a few centimeters to one meter. It should be noted that coherence length depends strongly on a source height H_s . When H_s increases from 10 to 20 km, the value of r_0 increases on an order of magnitude.

As pointed out above, an important parameter characterizing an adaptive optics system is the ratio of an aperture diameter to the coherence length D/r_0 . The results of this parameter calculations on the low atmosphere paths are presented in Fig. 2.1 for $D = 0.5$ m, and on the upper atmosphere paths for $D = 1$ m.

In the first case a normalized diameter D/r_0 is not greater than 10 on paths $L < 10$ km. This means that an adaptive optics system with the size of an element $d = D/10$ can effectively compensate for turbulent aberrations. Here d is the inter-actuator spacing or/and subaperture size.

Calculations for paths in the upper atmosphere show that when source is placed on 20 km height, the correction for general tilts is sufficient⁶, because $D/r_0 < 4$. When $H_s = 10$ km in most cases spatial resolution $d = D/10$ is sufficient excluding paths directed at -2° and -3° to the horizon.

2.1.2. Amplitude Fluctuations

Rejection of information carried by the amplitude of a beacon wave imposes principal limits on the effectiveness of phase only correction. Let us assess the range of path lengths where phase conjugation yields substantial growth in intensity of a focal spot.

Let us consider a homogeneous path. For this problem we have the following initial parameters: wavelength of optical radiation λ (corresponding wave number is $k = 2\pi/\lambda$), path length L , and intensity of fluctuations C_n^2 . Using these parameters it is possible to assess magnitude of phase and amplitude fluctuations of a beam. In approximate estimations it is possible to use the following formulas for coherence length r_0 and variance of plain wave log-intensity fluctuations^{1,2} σ_x^2 :

$$r_0^{-5/3} = 0.423k^2 C_n^2 L, \quad (2.3)$$

$$\sigma_x^2 = 0.307C_n^2 k^{7/6} L^{11/6}. \quad (2.4)$$

Here we used a coherent length as defined by Fried⁵, a definition introduced by Tatarskii¹ differs by the coefficient

$$\rho_0^{-5/3} = 1.46k^2 C_n^2 L, \quad r_0 \approx 21\rho_0. \quad (2.5)$$

These parameters for spherical wave and for a beam differ by the coefficient

$$r_0^{-5/3} = 0.159k^2 C_n^2 L, \quad (2.6)$$

$$\sigma_x^2 = 0.124C_n^2 k^{7/6} L^{11/6}. \quad (2.7)$$

From the formulas presented above it follows that variance of log-intensity fluctuations are related with the ratio of path length to diffraction length calculated over the coherence length

$$\sigma_x^2 = 0.726 \left(\frac{L}{kr_0^2} \right)^{5/6}. \quad (2.8)$$

The index of scintillations β_0^2 is often used to describe intensity fluctuations. In the region of weak fluctuations the index can be defined as

$$\beta_0^2 \approx 4\sigma_x^2 = 2.9 \left(\frac{L}{kr_0^2} \right)^{5/6}. \quad (2.9)$$

Let us note that by combining initial parameters λ, L, C_n^2 another two parameters can be formed that completely determine amplitude and phase correlation characteristics

$$p_1 = k^3 C_n^2, \quad p_2 = k^{-1} L. \quad (2.10)$$

Because we are interested in determining phase correction efficiency as function of relation between phase and amplitude fluctuations it is more convenient to use such parameters as coherence length and scintillation index for a plane wave. There are the following relation between these parameters:

$$\begin{aligned} r_0^{-5/3} &= 0.423 p_1 \cdot p_2, \quad \beta_0^2 = 1.23 p_1 \cdot p_2^{11/6} \text{ (plane wave),} \\ r_0^{-5/3} &= 0.159 p_1 \cdot p_2, \quad \beta_0^2 = 0.496 p_1 \cdot p_2^{11/6} \text{ (spherical wave).} \end{aligned} \quad (2.11)$$

Although these equations hold only for weak fluctuations, they can be used as parameters of a problem with fluctuations of greater intensity.

Growth of intensity fluctuations influence efficiency of phase correction in two ways. From one hand, the loss of information carried by amplitude of the reference wave results in incomplete correction for aberration even in the case of an adaptive system with infinite spatio-temporal resolution.

From the other hand, at high enough strength of the fluctuations wave front dislocations⁷ take place. In this case phase front cannot be represented as continuous function of coordinates as required for efficient correction. It affected mainly the process of phase aberration detection, because discontinuous phase surface can be approximated by a segmented mirror.

Algorithms of phase reconstruction that use finite-difference representation of a Poisson equation⁴ are employed in a Hartmann sensor as well as in a shift

interferometer. Such procedure is equivalent to filtration of a curl component of phase which carries wave front dislocations. So the curl component is considered as noise and the potential component remaining after filtration is a continuous function of coordinates and can be reproduced by flexible or segmented mirror with precision defined by spatial resolution of a mirror. But the curl component also carries some information that are lost at filtration, and because of this, the system efficiency is lower.

Let us consider this effect taking as an example a problem of image correction. In this case the loss of information carried by an amplitude of a wave does not influence notably the efficiency of correction, deterioration of image quality are caused only by the loss of the curl component of phase fluctuations.

In such conditions the problem of image correction can be formulated in the following way. A plane wave emitted by a point source placed at infinity is incident on a layer of a randomly inhomogeneous medium. In the plane of receiving aperture phase and amplitude fluctuations are characterized by parameters r_0 and β_0^2 which are parameters of wave propagating in a randomly inhomogeneous medium. A parameter which characterizes a system of imaging is a ratio of a telescope aperture diameter D to the coherence length. The criterion of correction efficiency is Strehl ratio, that is a ratio of axial intensity of long exposure image of a point source to diffraction limited value of this parameter.

In numerical experiments it was assumed that spatial resolution of a sensor and wave front corrector is equal to the step of computational grid. Because fluctuations with scales less than the step of a grid are absent in numerical experiments, this assumption means infinite spatial resolution. To avoid decreasing of turbulent aberration intensity due to omission of small scales, the grid step was chosen from inequality $\Delta < 0.3r_0$. Algorithm of phase reconstruction was realized with the use of discrete Poisson equation.

$$4\varphi_{i,j} - \varphi_{i+1,j} - \varphi_{i-1,j} - \varphi_{i,j+1} - \varphi_{i,j-1} = \Delta_{i-1,j}^x + \Delta_{i,j-1}^y - \Delta_{i,j}^x - \Delta_{i,j}^y \quad (2.12)$$

$$i, j = 1, \dots, N$$

Differences in the right-hand part of the equation were computed using the values of complex amplitude E in nodes:

$$\Delta_{i,j}^x = \arg(E_{i+1,j}E_{i,j}^*), \quad \Delta_{i,j}^y = \arg(E_{i,j+1}E_{i,j}^*). \quad (2.13)$$

Periodic boundary conditions have been used to solve the problem.

Strehl ratio as a function of scintillation index is shown in Fig. 2.2 for different diameters of an aperture. Sharp decrease of efficiency is seen for $\beta_0^2 > 1$. At $\beta_0^2 = 3$ Strehl ratio is less than 0.1 for all $D/r_0 > 10$. Thus to achieve high efficiency of correction the condition $\beta_0^2 < 1$ should be fulfilled. Partial correction is possible at $\beta_0^2 \approx 2-3$.

Let us consider influence of amplitude fluctuations in a randomly inhomogeneous medium on quality of phase correction of spatio-limited beams. In this case decreasing of efficiency of phase-only correction at increasing of amplitude fluctuations in a reference wave induced by two factors. There are, firstly, the loss of information carried by an amplitude of a reference wave, and, secondly, the loss of information contained in curl part of wave front phase. Let us consider the influence of amplitude fluctuations on Strehl ratio assuming that phase correction is exact. In this case boundary conditions for complex amplitude of corrected beam E_0 include an argument of a reference beam complex amplitude E_r :

$$E_0(\vec{\rho}) = A(\vec{\rho}) \cdot \exp(-i \arg E_r(\vec{\rho})). \quad (2.14)$$

Strehl ratio in a focal plane of corrected beam vs. scintillation index is presented in Fig. 2.3. The scintillation index was computed for spherical wave the source of which is placed in a focus of corrected beam. In Rytov approximation the scintillation index for spherical wave can be defined as

$$\beta_0^2 = 0.496k^{7/6}C_n^2L^{11/6}. \quad (2.15)$$

In reality, a beam conjugated with diffraction-limited corrected beam is used in numerical experiments. The value of scintillation index was taken as for a spherical wave because after the waist this beam spreads like a spherical wave. It is seen from the results presented in Fig. 2.3 that high enough quality of correction can be obtained for all considered values of β_0^2 . To our surprise Strehl ratio is almost independent of normalized beam size $D/r_0 = 2a_0/r_0$. Moreover, the quality of correction increases when the ratio D/r_0 increases. Let us note that in our problem decreasing of D/r_0 causes increasing of reference beam diameter, as a consequence, a beam becomes more close to a plane wave for which scintillation index of intensity fluctuations is almost two times greater than that for a spherical wave. It can be one of possible cause of Strehl ratio decreasing at small values of D/r_0 .

Another cause of Strehl ratio decreasing can be implicitly defined inner scale of turbulence l_0 , which is equal to step of computational grid. At increasing of D/r_0 (actually, at decreasing of r_0) ratio r_0/l_0 decreases, that means taking out of consideration small scale amplitude fluctuations and increasing of correction efficiency at large D/r_0 .

In spite of the pointed out shortcomings, which are connected with peculiarities of numerical simulation, the results obtained allow one to obtain reasonable estimation of phase correction efficiency under the conditions of strong amplitude fluctuations.

Now let us consider phase correction taking into account the fact that ordinary adaptive optics system corrects only smooth component of a wave front. Phase dislocations that appears with strong intensity fluctuations are filtered in the process of phase restoration on the basis of Eq.(2.12) like a noisy component of a signal. It is an

additional factor that decreases efficiency of phase correction for turbulent aberrations. Boundary conditions used in numeric experiment can be formulated as

$$E_0(\vec{\rho}) = A(\vec{\rho}) \exp(-i \hat{F}[E_r(\vec{\rho})]), \quad (2.16)$$

where F is operator describing the method of solution for Eqs. (2.12) and (2.13).

The dependence of the described phase correction from the scintillation index is shown in Fig. 2.3. As it can be seen, the values of Strehl ratio are close to 0.1 even at $\beta_0^2 = 1.5$. So the efficient phase correction required the fulfillment of condition $\beta_0^2 < 1$.

This condition gives us the possibility to assess the feasibility of adaptive correction on the paths which we are interested in. Let us consider values of β_0^2 computed for a spherical reference wave (the results are presented in Fig. 2.4). The calculations have been performed at $\lambda = 1.315 \mu\text{m}$ using the following formula:

$$\beta_0^2 = 4 \cdot 0.563 k^{7/6} \int_0^L C_n^2(x) ((L-x)x/L)^{5/6} dx. \quad (2.17)$$

Obviously, limitations associated with amplitude fluctuations are the main factor contributing into aberrations for a system placed at altitude $H_s = 10$ km. In this case for most paths and angles condition $\beta_0^2 < 1$ is not fulfilled. At the same time for $H_s = 20$ this condition is fulfilled for most paths excluding the path directed at -3° to the horizon. It should be noted that for other paths the turbulent aberrations are not strong. Changing wave length to $3.8 \mu\text{m}$ it is possible to achieve threefold decreasing of β_0^2 that allows us to obtain higher efficiency of adaptive correction on different paths, in particular, for $H_s = 10$ and for angles greater than 0 .

For the low atmosphere paths amplitude fluctuations are also important. In many cases for such paths $\beta_0^2 > 1$ and sometimes increases up to 10. In other cases values of β_0^2 are in the interval $0.1 - 1$.

2.2. Bandwidth Consideration

In the previous part we have considered limitations induced by amplitude fluctuations in the reference wave. To make an analysis more complete we should also consider limitations associated with finite bandwidth of adaptive optics system. The bandwidth can roughly be estimated with the use of formula proposed by Greenwood³:

$$f_c^{-5/3} = 0.102 \cdot k^2 \cdot \int_0^L C_n^2(x) \cdot V^{5/3}(x) dx, \quad (2.18)$$

where V is the sum of wind velocity and the velocity of a beam travel due to scanning. The frequency defined by Eq.(2.18) corresponds to unit variance of residual phase aberrations for a system dynamic characteristics of which are described by a frequency filter:

$$H(f, f_c) = (1 + i f / f_c)^{-1}. \quad (2.19)$$

This equation is typical for resistor - capacitor electric circuits. The results of bandwidth calculations are presented in Fig. 2.5. Atmospheric wind had constant velocity 10 m/s. Let us note that when the speed of scanning is large the wind speed can be neglected.

The presented results show that quick movement of a target sets strict conditions on the bandwidth, in some cases frequency should be greater than 10 kHz. It should be emphasized that dependence of frequency f_c on the distance to the target is changed when an angle is changed from negative to positive values.

For $\alpha=+3^\circ$ at increasing of the distance to the target the frequency f_c decreases. It is due to decreasing of the velocity of scanning in the regions close to the source where the main turbulent perturbations are concentrated.

For $\alpha = -3^\circ$ increase of the distance to the target induces increase of frequency f_c because the region near the target contributes significantly to aberrations of the wave front.

At $\alpha = 0^\circ$ these effects compensate each other and frequency f_c is almost independent of the distance to the target.

Taking into account frequency characteristics of the adaptive optics system, from the results presented above one can conclude that high-altitude flying objects are more easily to shot down at long distances. Whereas probability to shot down low-altitude flying objects greater at short distances.

For the low atmosphere paths the frequency of the system must be in the interval from 1 to 10 kHz (Fig. 2.6). Only for objects moving with speed less than the speed of sound frequency less than 1 kHz is sufficient.

The formulated requirements to the frequency characteristics of the adaptive optics system are strict because of small intensity of a reference wave when beacon is formed by scattering or reflection of optical radiation.

2.3. Anisoplanatic Degradation of Correction with Real Beacon

An effect of anisoplanarity is caused by difference of aberrations on paths of the direct and reference beams. These differences are due to variances of path geometric characteristics (different angles or divergence) or due to the presence of temporal lag. In many cases the causes of these factors are similar, moreover, methods of their mathematical representations are similar too.

Let us consider the problem of compensation for turbulent aberrations in approximation of a phase screen placed on a path in some point with coordinate x . Using the approximation of δ -correlated in the direction of propagation turbulent fluctuations in that follows we perform integration over x variable.

We assume that a random screen $\varphi(\rho, x, t)$ is placed at the point x in moment t , where ρ is transverse coordinate. According to Taylor's hypothesis of frozen turbulence the parameters of a phase screen in different moments of time can be related in the following way:

$$\varphi(\vec{\rho}, x, t + \tau) = \varphi(\vec{\rho} - \vec{V}\tau, x, t + \tau) = \varphi(\vec{\rho} - \vec{V} - \vec{V}\tau, x, 0). \quad (2.20)$$

From here follows the similarity of mathematical description for angular anisoplanarity and temporal lag.

Beacon angular coordinates and direction of a system optical axis we describe by variables $\theta_B(t)$ and $\theta_A(t)$. For an object (target) moving with speed $v = M^*330\text{m/s}$ in the transverse direction the angular coordinate $\theta_T(t)$ is changed as

$$\theta_T(t) = vt/L = \omega t. \quad (2.21)$$

In the case of a beacon formed by reflection from a target $\theta_B(t) = \theta_T(t)$. Allowing for shift of an object, finite speed of light c , and lag τ_d of adaptive system Rayleigh beacon can be formed beforehand. In this case

$$\theta_B(t) = \theta_T(t) + 2\tau_c/L + \tau_d v/L = \theta_T(t) + 2v/c + \tau_d v/L, \quad \tau_c = L/c. \quad (2.22)$$

In general

$$\theta_B(t) = \theta_T(t) + \eta \cdot \{2vc + \tau_d v/L\}, \quad (2.23)$$

where $\eta > 0$ corresponds to a beacon with forestalling, $\eta = 0$ corresponds to a beacon without forestalling.

In the choice of direction of the axis of an adaptive optics system the lag associated with a finite speed of light also should be taken into account. Thus

$$\theta_A(t) = \theta_T(t) + v \cdot \tau_c/L = \theta_T(t) + v/c. \quad (2.24)$$

A line directed at angle θ crosses plane x at the point θ_x . So crossing the screen a reference wave radiated in a moment t acquires the aberrations

$$\varphi_B(\vec{\rho}) = \varphi(\vec{\rho} + \theta_B(t)x, t + (L - x)/c) = \varphi(\vec{\rho} + \theta_B(t)x - (L - x) \cdot v/c, t). \quad (2.25)$$

Here we assumed that the time of reference wave propagation to the phase screen is $(L-x)/c$.

At the time $t+L/c$ the reference wave attains the aperture of an adaptive optics system and at the moment $t+L/c+\tau_d$ correcting surface is formed with the use of the information carried by this wave.

The controlled beam arrives at the phase screen at the moment $t+L/c+\tau_d+x/c$ and acquires the following aberrations:

$$\begin{aligned} \varphi_A(\vec{\rho}) &= \varphi(\vec{\rho} + \theta_A(t + L/c + \tau_d) \cdot x, t + L/c + \tau_d + x/c) = \\ &= \varphi(\vec{\rho} + \theta_A(t + L/c + \tau_d) \cdot x - v \cdot (L/c + \tau_d + x/c), t) \end{aligned} \quad (2.26)$$

Comparing Eqs. (2.25) and (2.26) we can see that the residual error of correction is caused by relative shift of the phase screen. This shift is

$$\Delta = [\theta_A(t + L/c + \tau_d) - \theta_B(t)] \cdot x - v[\tau_d + 2x/c]. \quad (2.27)$$

Substituting into this formula Eq. (2.24) we obtain

$$\Delta = [v/L (t + \tau_d) + 2v/c - \theta_B(t)] \cdot x - V [\tau_d + 2x/c] \quad (2.28)$$

and using Eq. (2.23) we find

$$\Delta = v \cdot (\tau_d \cdot x/L + 2x/c)(1 - \eta) - V \cdot [\tau_d + 2x/c]. \quad (2.29)$$

When $\tau_d = 0$ the formula becomes more simple

$$\Delta = 2x/c (v \cdot (1 - \eta) - V). \quad (2.30)$$

The relative shift can be nullified by appropriate choice of parameter η

$$\eta_0 = 1 - V/v. \quad (2.31)$$

If wind speed V is equal to an object speed v , the optimal value of parameter η is equal zero, i.e., the beacon formed by reflection is optimal. When $v \gg V$, optimal value of η approaches unity, i.e., the forestalling Rayleigh beacon is optimal. In the case when the object moves in the direction opposite to the direction of wind, the value of η_0 is greater than unity.

At lags τ_d greater than zero the shift Δ can be nullified if

$$\eta_0 = 1 - \frac{V}{v} \frac{\tau_d + 2x/c}{\tau_d x/L + 2x/c}. \quad (2.32)$$

In the case when turbulence is concentrated near the object, i.e. $x = L$, we obtain

$$\eta_0 = 1 - \frac{V}{v}. \quad (2.33)$$

In this situation the optimal value of parameter η_0 is not influenced by the lag. In the opposite situation when x - coordinate approaches zero we obtain

$$\eta_0 \approx 1 - \frac{V}{v} \frac{1}{x} \frac{\tau_d}{\tau_d/L + 2/c}, \quad x \ll \frac{\tau_d c}{2}, \quad (2.34)$$

or

$$\eta_0 \approx 1 - \frac{L/v}{x/V}, \quad \tau_d \gg 2L/c = 2\tau_c. \quad (2.35)$$

In the region close to aperture (coordinate x is small) unity can be disregarded in this equation, so

$$\eta_0 \approx -\frac{L/v}{x/V}, \quad (2.36)$$

i.e., when the velocity of wind and the object are of the same direction, the parameter of forestalling approaches negative infinity, and positive infinity when the object moves in the direction opposite to wind.

In the general case turbulence is distributed all over the path, so we have to consider a set of phase screens. Moreover, the dependence of wind speed on the coordinate x should be allowed for, this means that phase screens should move with different speed.

In the general case optimization of a beacon forestalling angle is difficult. Moreover, the intensity of Rayleigh beacon is too small to perform phase correction. But in some situations optimization of a beacon forestalling is profitable.

To assess the efficiency of correction the variance of residual error must be computed. In the general case this variance is an integral over the path of some function dependent on the turbulence intensity distribution $C_n^2(x)$ and on the shift $\Delta(x)$.

The required equation can be obtained from the well-known formula describing angular unisoplanarity because in both cases the origin of the residual error is the same. For angular unisoplanarity variance of residual phase errors is⁸

$$\sigma_\varphi^2 = (\theta/\theta_0)^{5/3} = \theta^{5/3} \cdot 2.91k^2 \int_0^L C_n^2(x) x^{5/3} dx. \quad (2.37)$$

Because the product of θ and x is the shift of trajectories of a reference and the main beams we can obtain the following equation:

$$\sigma_{\Delta\varphi}^2 = 2.91k^2 \int_0^L C_n^2(x) (\theta x)^{5/3} dx = 2.91k^2 \int_0^L C_n^2(x) \Delta^{5/3}(x) dx. \quad (2.38)$$

Let us note that for a phase screen, i.e., for a thin turbulent layer characterized by the coherence length

$$r_0^{-5/3} = 0.423k^2 C_n^2 \delta x, \quad (2.39)$$

equation for the variance has the form

$$\sigma_{\Delta\varphi}^2 = 6.88(\Delta/r_0)^{5/3}. \quad (2.40)$$

This equation coincides with phase structure function written for coordinate difference Δ . It should be noted that variance of the residual error calculated according these formulas allows for the constant phase component (piston). Because this component does not influence the efficiency of correction, the efficiency will be underestimated.

Accuracy of Eq. (2.38) increases when the ratio Δ/D (D is the aperture diameter) decreases. Equation for variance without constant component of the phase is presented in Ref. 9. Using designations introduced in the present report this equation can be written in the form

$$\sigma_{\Delta\varphi}^2 = 2.91 \cdot k^2 \int_0^L C_n^2(x) D(x)^{5/3} f(|\Delta(x)|/D(x)) dx, \quad (2.41)$$

where

$$f(\alpha) = 0.896 \cdot \int_0^\infty u^{-8/3} du (1 - J_0(2\alpha u)) \left(1 - 4 \frac{J_1^2(u)}{u^2}\right) \quad (2.42)$$

is spatial filtering function. Function $D(x)$ is a projection of a system aperture diameter on the plane x . The character of reference beam divergence and the direct beam focusing is taken into account. For beams with large diameters and for small beacons the equation of spherical wave can be used

$$D(x) = D \cdot (1 - x/L). \quad (2.43)$$

For small values of an argument the filtering function f can be written as

$$f(\alpha) = \alpha^{5/3} \quad (2.44)$$

and Eq. (2.41) transforms into Eq. (2.38). For large values of the argument the filtering function achieves saturation and resulting values of variance of phase correction error achieve the level two times higher than that for a system without correction

$$\sigma_{\Delta\varphi}^2(\Delta/D \rightarrow \infty) = 2 \cdot 1.03(D/r_0)^{5/3}. \quad (2.45)$$

Function $f(\alpha)$ is presented in Fig. 2.7. The points signify values obtained by numeric integration. Solid line is a result of these data approximation by a polynomial fitting of ninth power. Approximation was performed in logarithm coordinates

$$\lg f(\alpha) = \sum_{n=0}^9 a_n (\lg \alpha)^n. \quad (2.46)$$

Coefficient of approximation are presented in the table below

(a) $-4 < \lg(\alpha) < 0$

$n=0$	$n=1$	$n=2$	$n=3$	$n=4$
-0.90300263	+0.5463099	-	+1.9852349	+3.0232371
	1	0.007500502		
		9		
$n=5$	$n=6$	$n=7$	$n=8$	$n=9$
+2.2959981	+1.0072076	+0.2573047	+0.0354913	+0.0020411
		7	19	442

(b) $0 < \lg(\alpha) < 4$

$n=0$	$n=1$	$n=2$	$n=3$	$n=4$
-0.90300481	+0.4697363	-0.41229668	+0.2989732	-0.15200895
	8		2	
$n=5$	$n=6$	$n=7$	$n=8$	$n=9$
+0.0428626	-	-	+5.333567E-	-
86	0.002471344	0.002011873	4	4.1574399E-
	7	8		5

Using this approximation the variance of correction error have been obtained for different paths. At the correction with the use of a reflected signal let us consider the influence of the lag arising due to finite speed of light, i.e., when $\eta=0$ and $\tau_d=0$. At increase of the object speed the residual error of correction increases. Because of this

fact there are a limit on the object speed corresponding to the given residual error. Let us assume the residual error be equal 10% from its level without correction, i.e.,

$$\sigma_{\Delta\varphi}^2 < \frac{1}{10} \sigma_{\varphi}^2 = 0.1 \cdot 1.03(D/r_0)^{5/3} = 0.103(D/r_0)^{5/3}. \quad (2.47)$$

The values of maximum speed calculated for this level of residual error are presented in Fig. 2.8. All calculations have been performed at constant wind velocity equal to 10 m/s. The direction of the object motion and the wind speed coincide. It is seen that, as a rule, the maximum speed of the object does not exceed the speed of sound. For paths directed at negative angles relatively to horizon, this value is not greater than half the speed of sound. Let us note that according to condition (2.47) high efficiency of correction can be achieved only for small values of ratio D/r_0 . For example, for $0.103(D/r_0)^{5/3} < 1$ we obtain the condition $(D/r_0) < 3.9$.

Similar results computed for the wind speed distributed according Bufton's model are presented in Fig. 2.9. This model is described by the following equation

$$V(h) = V_g + 30 \exp\left(-\left[\frac{h - 9400}{4800}\right]^2\right), \quad (2.48)$$

where V_g is a parameter of the model corresponding to the wind speed near the surface. We assumed that $V_g = 5$ m/s. More strict condition

$$\sigma_{\Delta\varphi}^2 < \frac{1}{100} \sigma_{\varphi}^2 = 0.0103(D/r_0)^{5/3} \quad (2.49)$$

was superimposed on the residual phase error. As it can be seen, on some paths error of correction exceeds this level even at zero speed of the object. Even under the most favorable conditions the maximum speed of the object should not be greater than 50 - 100 m/s. When directions of the object velocity and wind velocity is opposite the limitations are even more strict.

From the data presented above we can see that possibilities of correction with the use of the reflected beam are limited. Let us consider correction with the use of

Rayleigh beacon. In this case it is possible to minimize the error of correction by choosing the forestalling parameter η . Because the most important for us is the case when the speed of the object is much greater than wind speed, the optimal value of forestalling parameter is close to unity. As it follows from Eq. (2.29), in this case the error of correction is entirely defined by wind velocity distribution $V(x)$ and by the lag of adaptive system τ_d and does not depend on the object speed.

Let us consider the results presented in Figure 2.10 that have been obtained for Rayleigh beacon. The graphs show the variance of residual phase aberrations normalized on variance in the absence of correction. The lag of adaptive optics system was taken equal 0, 1 and 10 msec.

Zero lag corresponds to maximum efficiency for Rayleigh beacon as well as for reflected signal when the speed of the object is zero. We can see that for most paths the relative error of phase correction is not greater than 1%. For the taken model of wind speed distribution the error almost on an order less when system is placed at 20 km height. In Bufton's model the maximum of wind speed (35 m/s) is on 10 km (parameter V_g was taken equal 5 m/s).

At increase of the lag to 1 msec we obtain the value of residual error equal to a few percents, for the lag 10 msec the error increases up to 30 - 60 % at $H_s = 10$ km and up to 5 - 10 % at $H_s = 20$ km. Thus, to obtain high enough efficiency of correction the lag should be less than 1 msec, and for efficient operation in the entire interval of considered paths the lag should be less than 0.1 msec.

Similar calculations have been made for the low atmosphere paths. The results corresponding to correction with error less than 1% are presented in Fig. 2.11, where we put the values of maximum object speed computed with zero lag of adaptive system. The maximum speed of the object was less than 2 - 3 M approximately for a half of the considered examples. When the lag is 0.1 msec the maximum speed of the object is in

the interval 0.5 - 1.5 M. Thus, on these paths reflected beacon also imposes strict conditions on the speed of the object and on the rate of adaptive control.

Taking forestalling parameter equal to unity let us consider the control with Rayleigh beacon. For the beacon of such type the residual error does not depend on the speed of the object and are defined entirely by distribution of wind speed and by the lag of adaptive system. The computational results of the normalized residual error for the lag of 1 msec are presented in Fig. 2.12. It is seen that in the entire interval we have obtained the level of residual error less than 1% and the error is almost independent of the path length.

To study the dependence of residual error on the lag of adaptive system let us consider the path of ten kilometers (the same figure). It is seen that increase of the lag up to 10 ms results in almost 15% increase of residual error. So the maximum possible lag is 1 - 2 ms.

References for Chapter 2

1. V.I. Tatarskii, *Propagation of Waves in the Turbulent Atmosphere* (Nauka, Moscow, 1967), 548 pp.
2. A. Isimaru, *Wave Propagation and Scattering in Random Media, Vol. 2* (Academic Press, New York, San Francisco, London, 1978) 318 pp.
3. D.P.Greenwood, J. Opt. Soc. Am. **67**, No.3, 390-393 (1977).
4. R.J.Noll, J. Opt. Soc. Am. **68**, No. 1, 139 - 140 (1978).
5. D.L.Fried, J. Opt. Soc. Am. **55**, No.11, 1426-1435 (1965).
6. D.L.Fried, J. Opt. Soc. Am. **56**, No.10, 1372-1379 (1966).
7. D.L.Fried, J.L.Vaughn, Appl.Opt., **31**, No.15, 2865-2882 (1992).
8. D.L.Fried, J. Opt. Soc. Am., **72**, No.1, 52-61 (1982)
9. J.Stone, P.H.Hu, S.P.Mills and S.Ma, J. Opt. Soc. Am. A **11**, No.1, 347-357 (1994).
10. R.H.Hudgin, J. Opt. Soc. Am. **67**, No.3, 375-378 (1977).
11. D.L.Fried, J. Opt. Soc. Am. **67**, No.3, 370-375 (1977).
12. R.J.Noll, J. Opt. Soc. Am. **68**, No.1, 139-140 (1978).
13. J.Herrmann, J. Opt. Soc. Am. **70**, No.1, 28-35 (1980).
14. L.Goad, F.Roddier, J.Becker, and P.Eisenhardt, Proc.SPIE **628**, 305-313 (1986).
15. R.R.Parenti and R.J.Sasiela, J. Opt. Soc. Am. **A11**, No. 1, 288-309 (1994).
16. D.G.Sandler et al., J. Opt. Soc. Am. **A11**, No.2, 925-945 (1994).
17. R.M.Measures, *Laser Remote Sensing*, (A Wiley-Interscience Publication, New York, 1984)
18. B.G. Zollars, The Lincoln Laboratory Journal, **5**, No.1, 67-92 (1992).
19. R.J. Noll, J. Opt. Soc. Am. **66**, No.3, 207-211 (1976).
20. R.H.Hudgin, J. Opt. Soc. Am., **67**, No.3, 393-395 (1977).

21. V.P Lukin and B.V.Fortes, *Atm. Ocean. Opt.* 8, No.3 (1995).
22. H.T.Barclay et al., *The Lincoln Laboratory Journal*, 5, No.1, 115-130 (1992)
23. A.S.Gurvich, A.I.Kon, V.L.Mironov, and S.S.Khmelevtsov, *Laser Radiation in a Turbulent Atmosphere*, (Institute of Atmospheric Physics, Moscow, 1976)

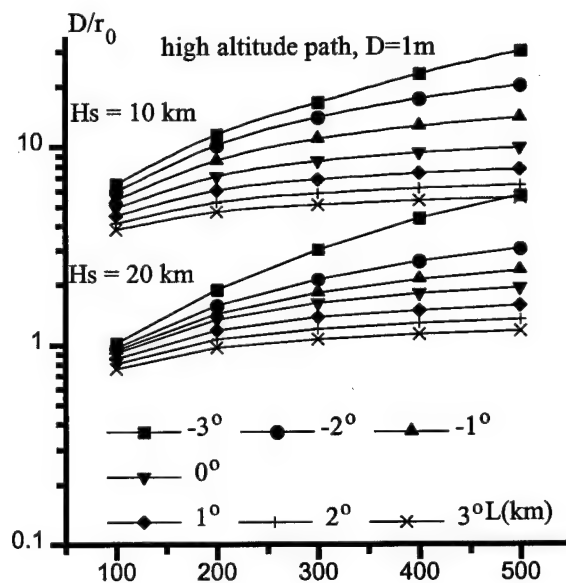
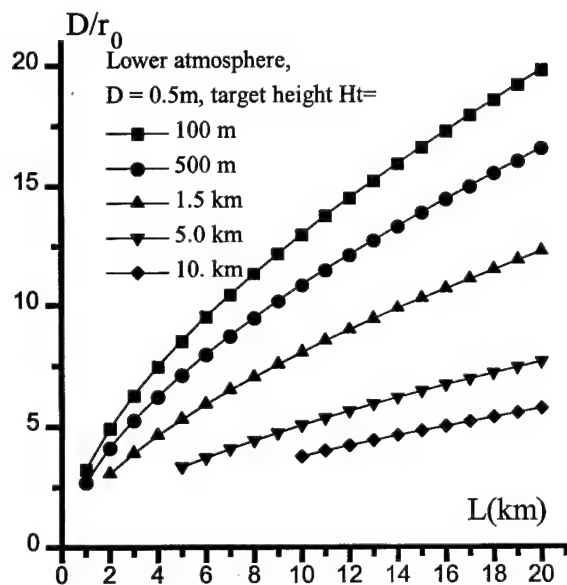
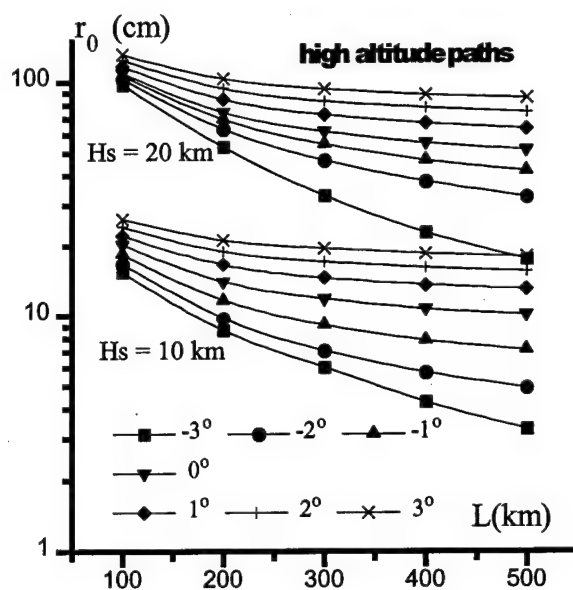
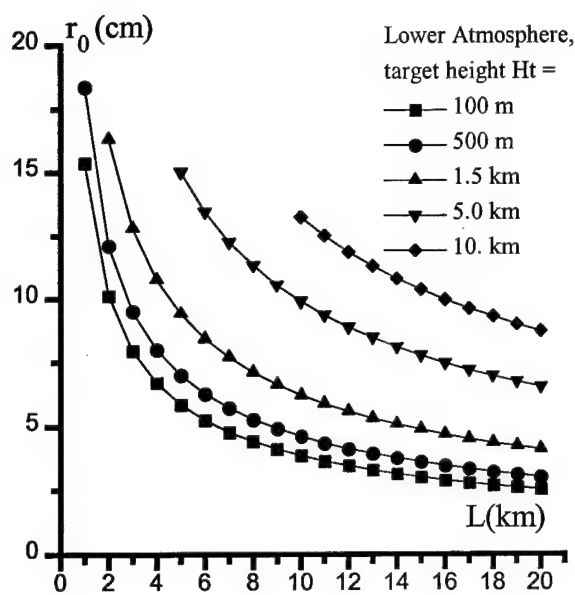


FIG.2.1. Coherence length r_0 and normalized aperture diameter D/r_0 on different paths.

Moderate intensity of turbulence, $\lambda = 1.315 \mu\text{m}$.

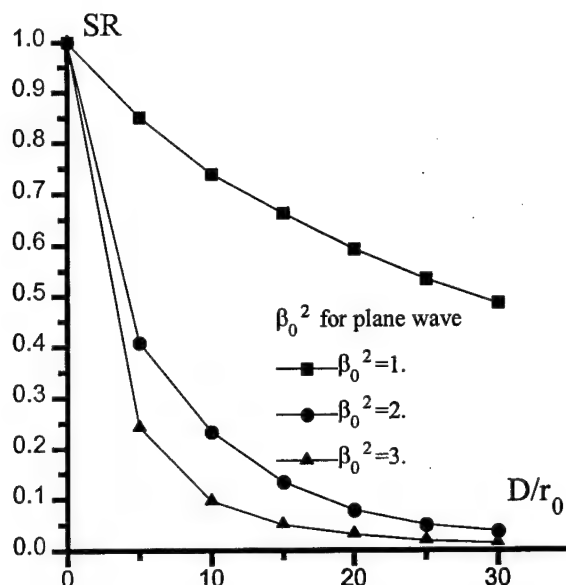


FIG.2.2. Results of correction for image aberrations. Strehl ratio vs. normalized aperture diameter for different values of scintillation index.

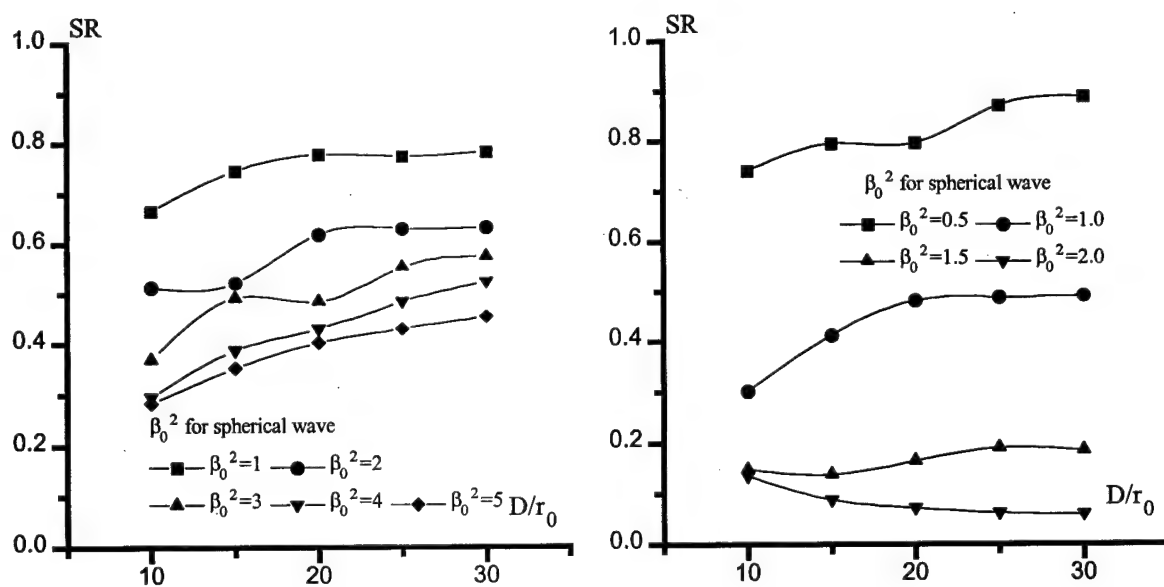


FIG.2.3. Results of correction for Gaussian beam aberrations. Strehl ratio vs. normalized aperture diameter for different values of scintillation index. The left-hand

picture corresponds to exact phase conjugation, in the right-hand picture phase dislocations have been filtered.

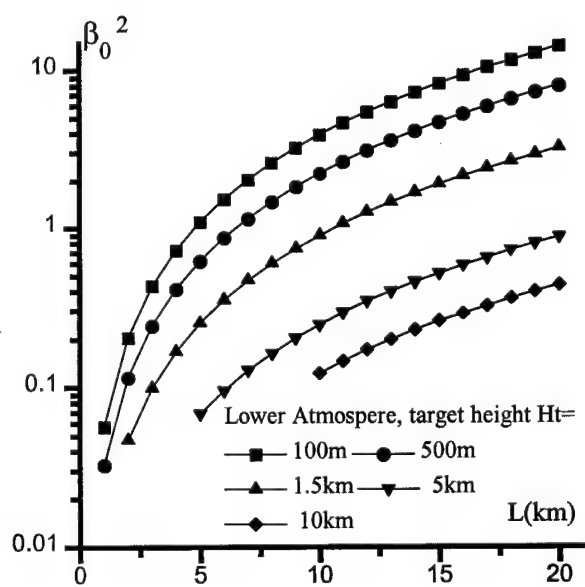
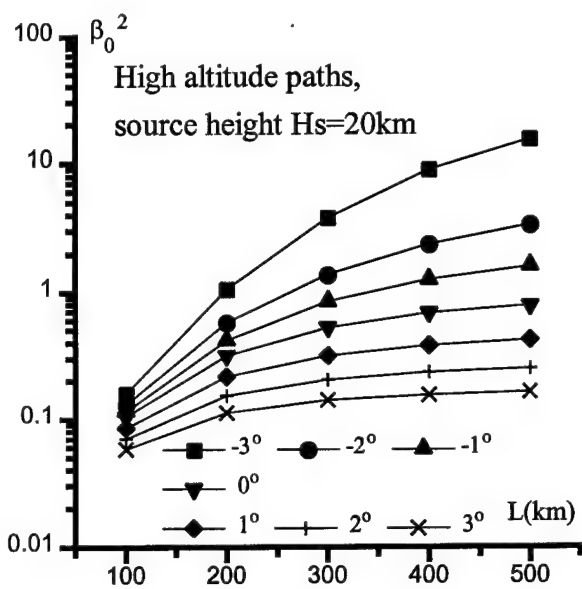
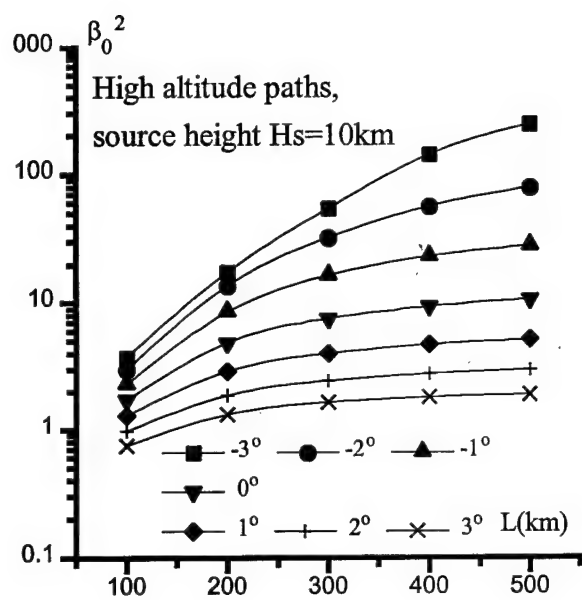


FIG.2.4. Scintillation index on different atmospheric paths. Computations have been performed in Rytov approximation for spherical wave and moderate intensity of atmospheric turbulence. $\lambda = 1.315 \mu\text{m}$.

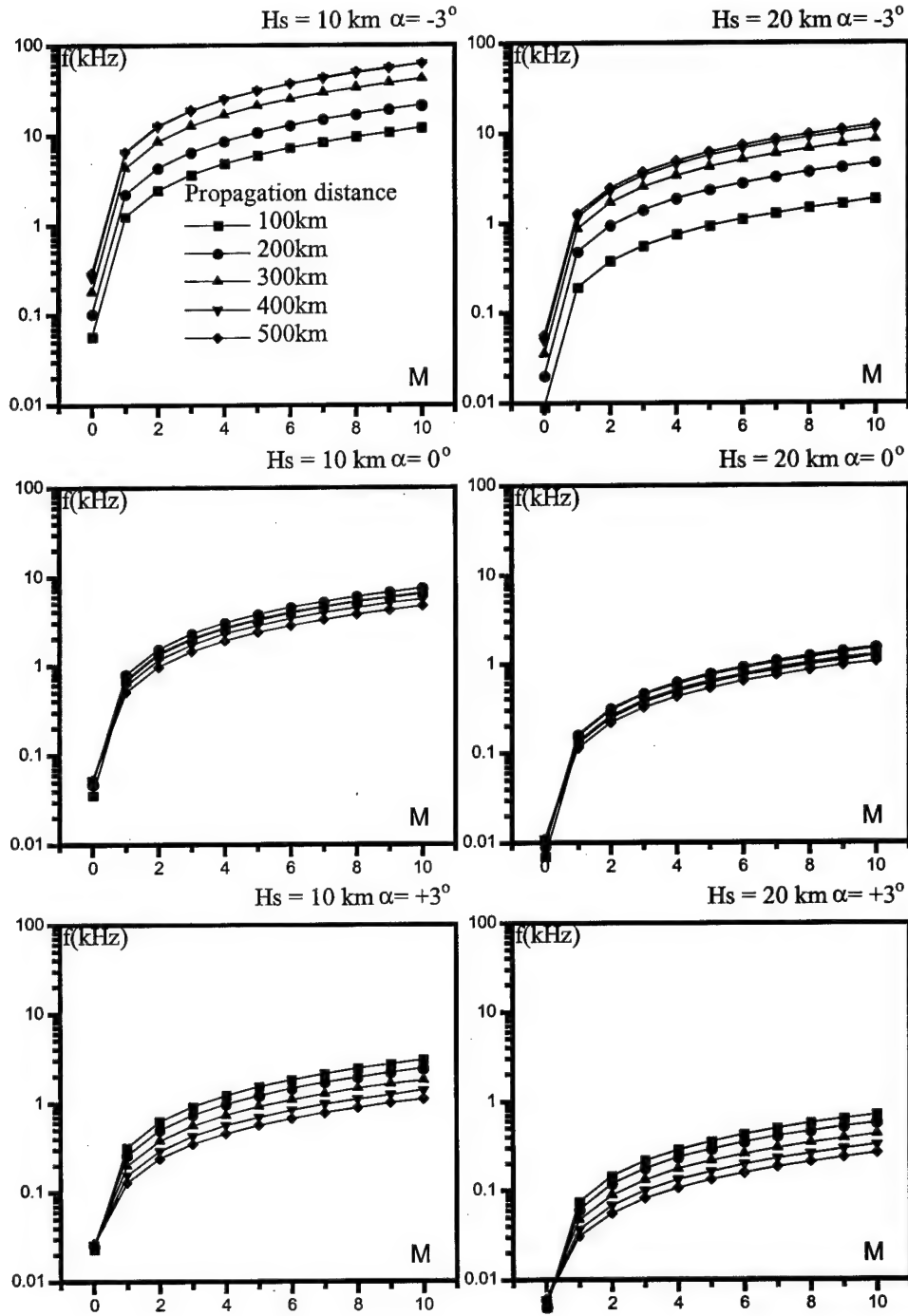


FIG.2.5. Greenwood frequency for different paths in the upper atmosphere as function of an object velocity.

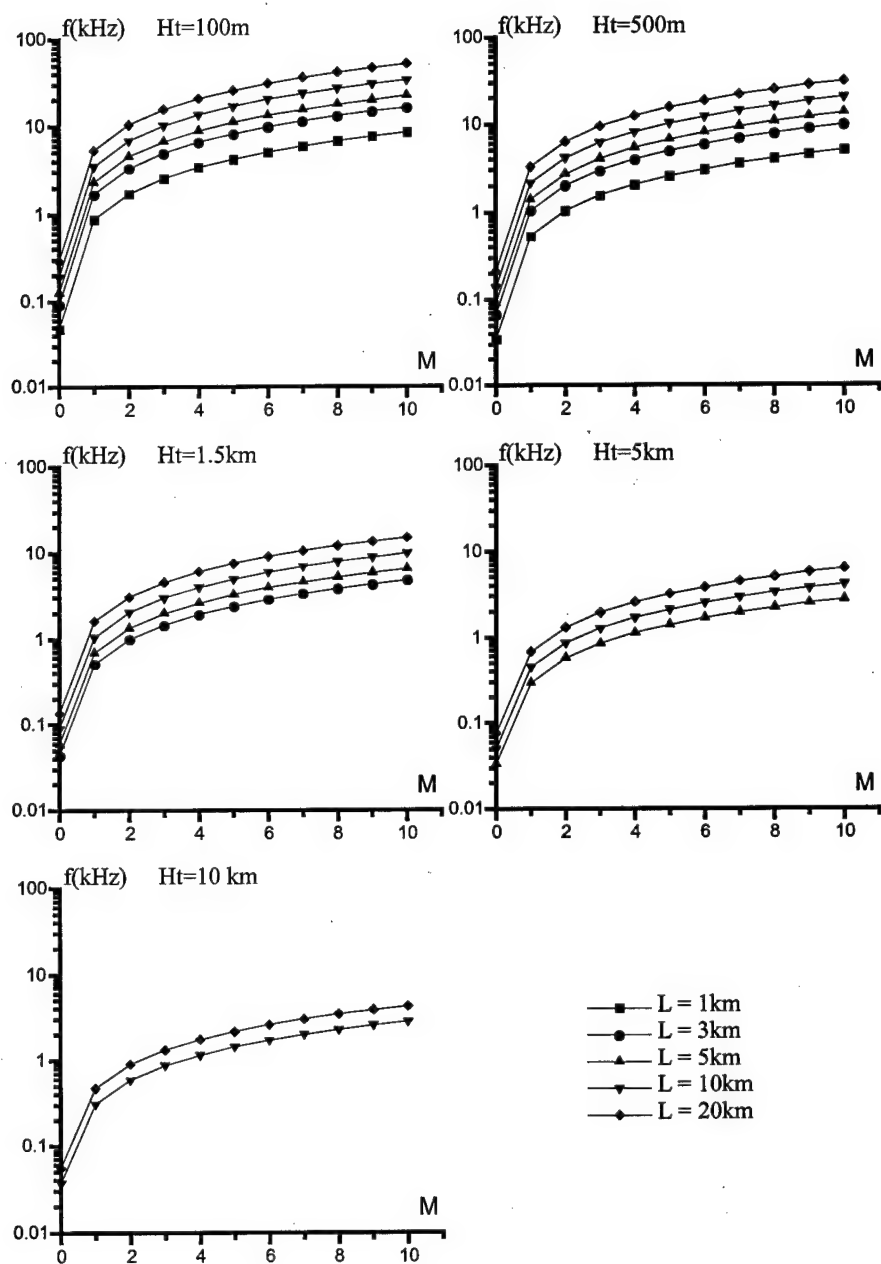


FIG.2.6. Greenwood frequency for different paths in the lower atmosphere as function of an object velocity.

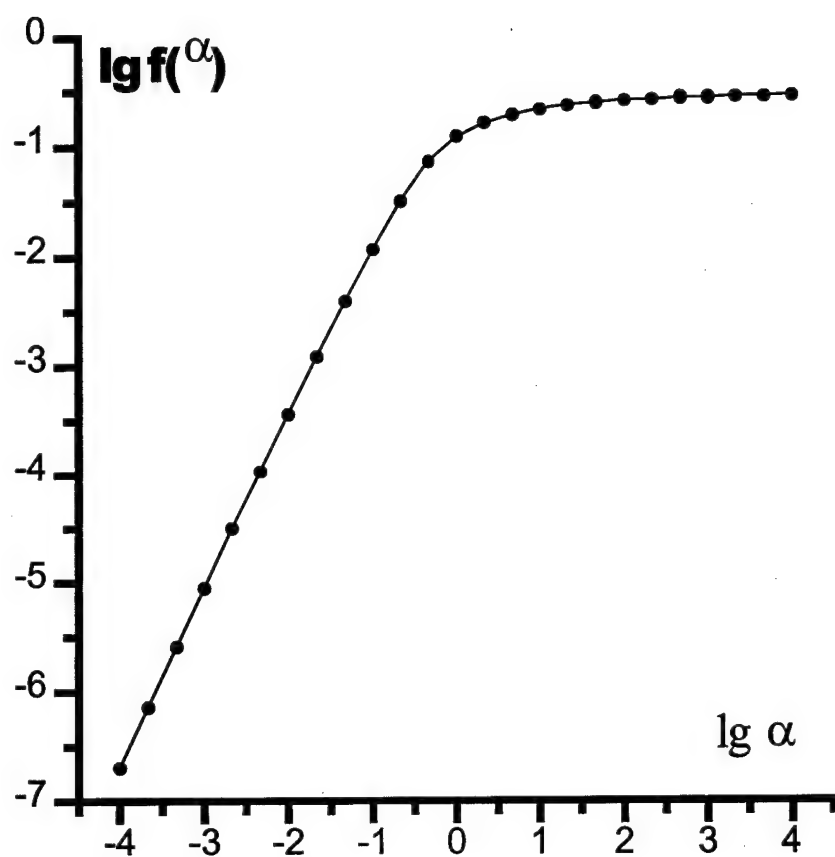


FIG.2.7. Spatial filtering function $f(\alpha)$.

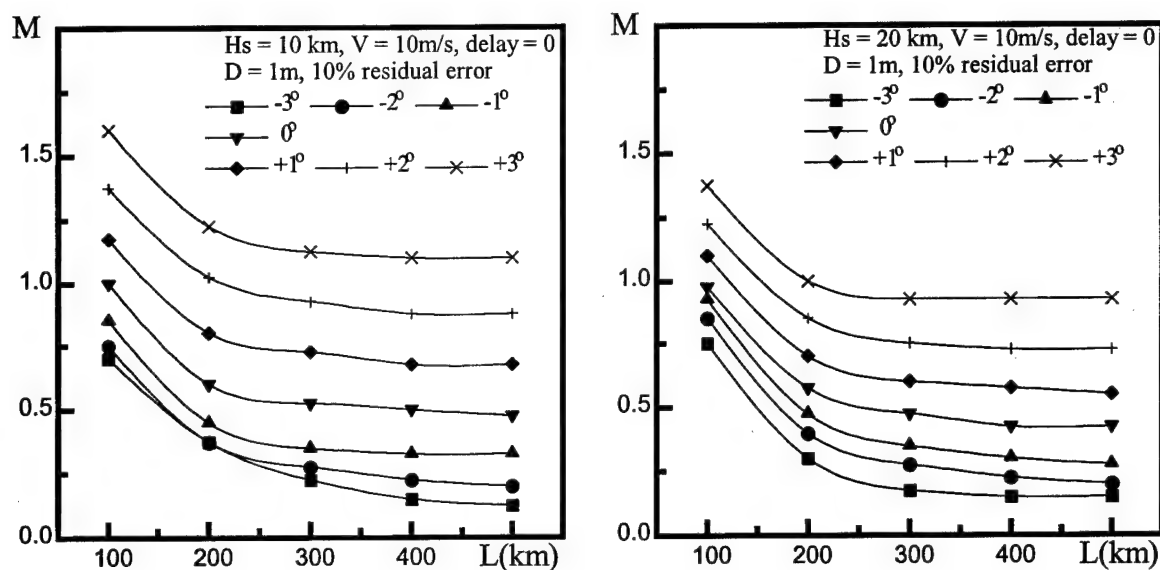


FIG.2.8. Maximum velocity of an object on the upper atmosphere paths at adaptive correction with the use of reflected signal. Wind velocity is constant (10 m/s), residual error is 10%.

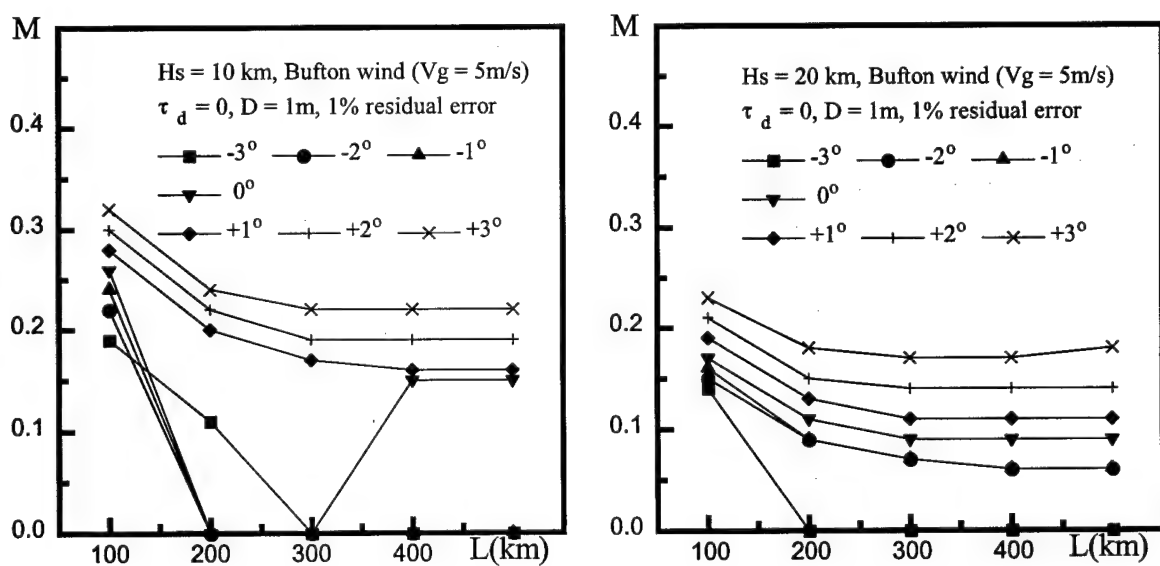
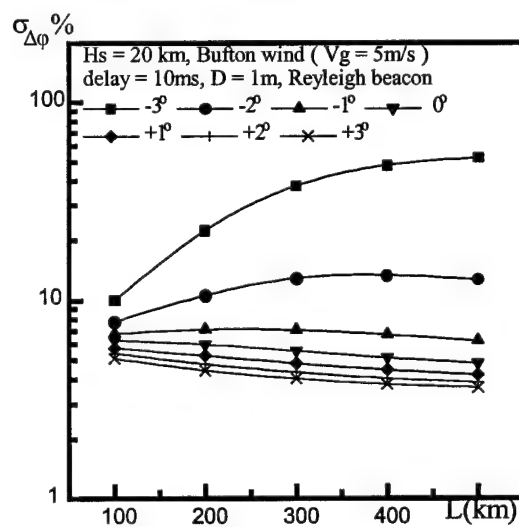
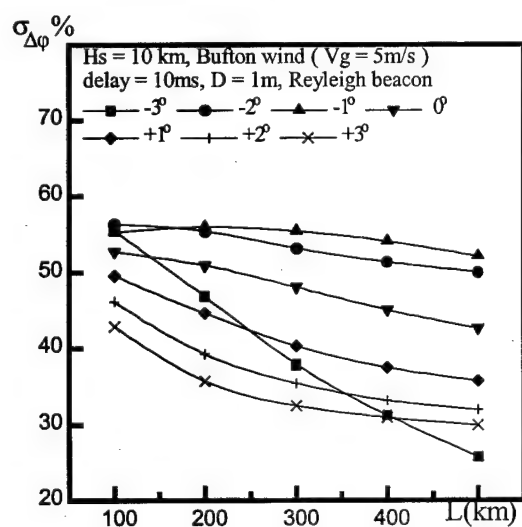
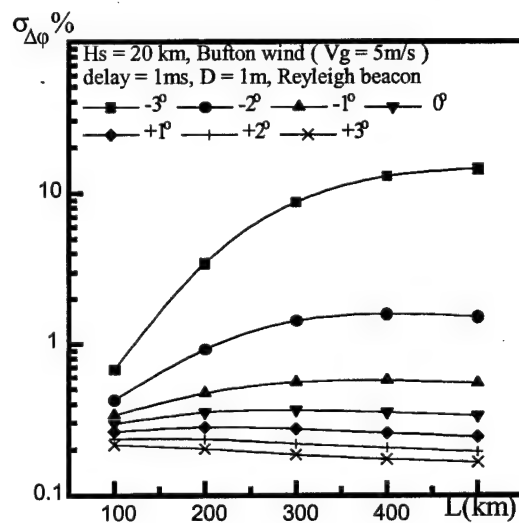
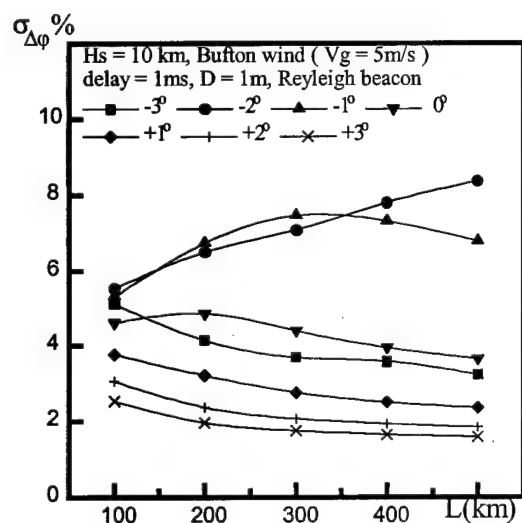
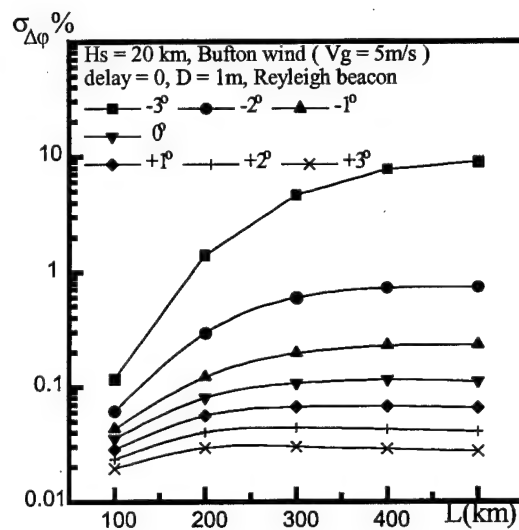
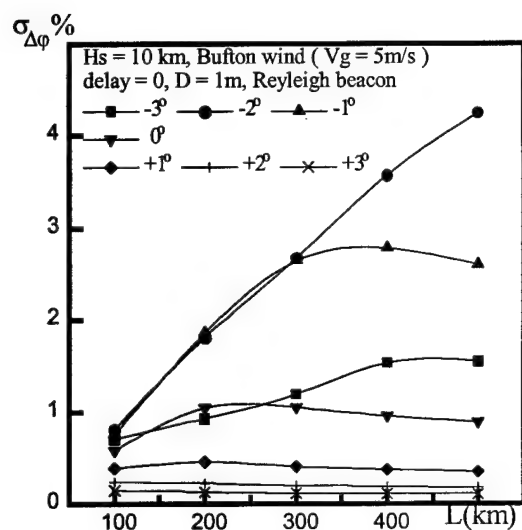


FIG.2.9. Maximum velocity of an object on the upper atmosphere paths at adaptive correction with the use of reflected signal. Calculations have been performed with the use of Bufton's model of wind, residual error was 1%.



*FIG.2.10. Normalized residual phase error at correction with a Rayleigh beacon.
Temporal lag of the system was 0, 1, and 10 msec.*

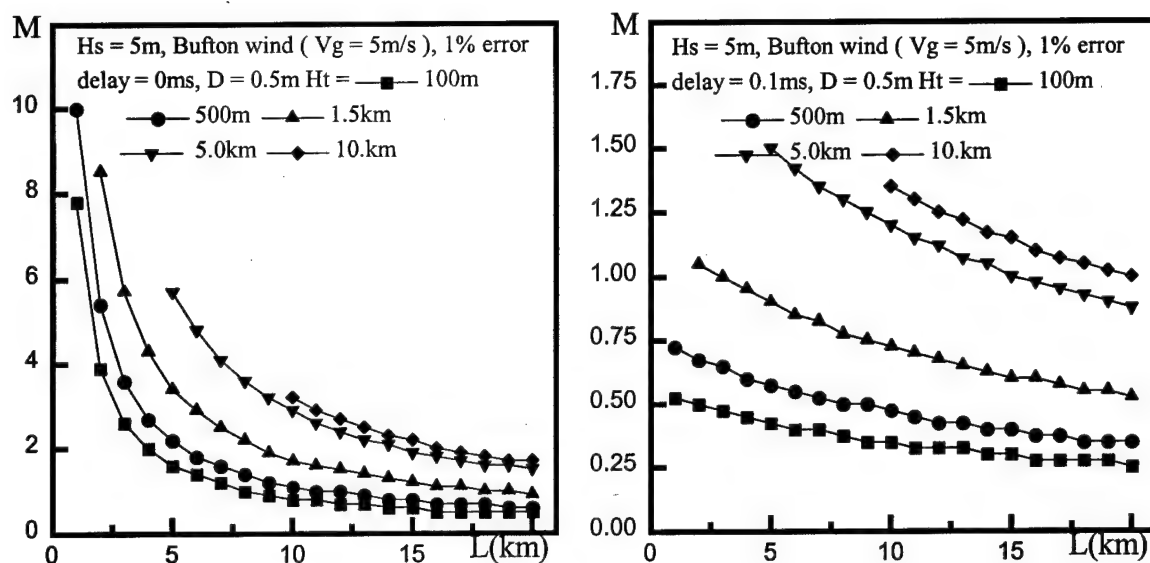


FIG.2.11. Maximum velocity of an object on the lower atmosphere paths at adaptive correction with the use of reflected signal. Residual error was 1%. Temporal lag of the system was equal zero for the left-hand picture and 1 msec for the right-hand picture.

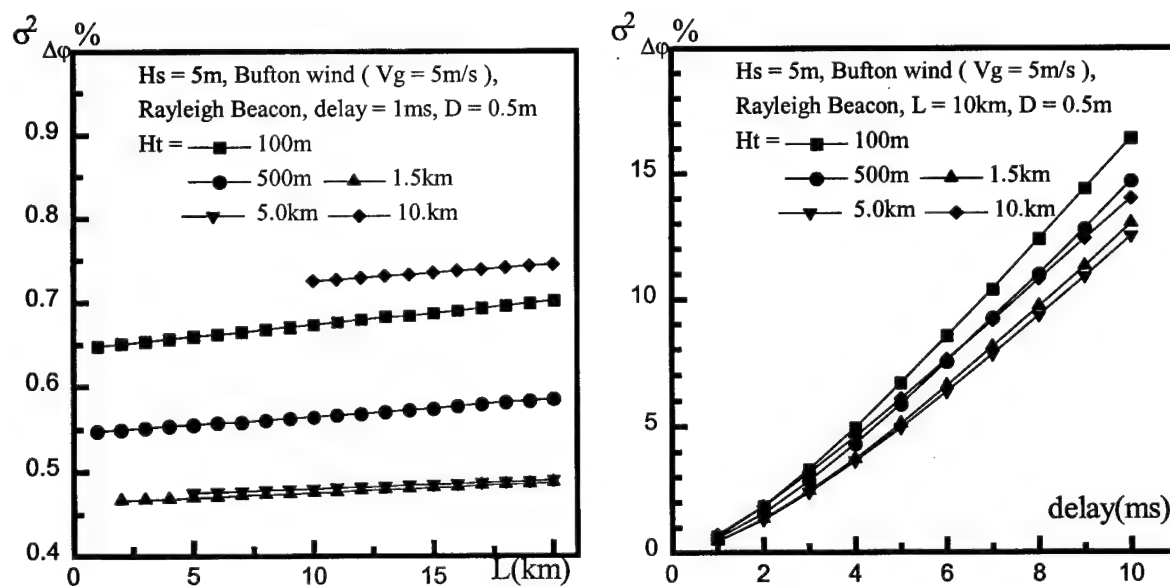


FIG.2.12. Residual error vs. path length for lag 1 msec (right-hand picture) and residual error vs. temporal lag for 10 km path (left-hand picture). In both cases Rayleigh beacon was taken as a reference source.

RUSSIAN ACADEMY OF SCIENCES
INSTITUTE OF ATMOSPHERIC OPTICS
LABORATORY OF COHERENT AND ADAPTIVE OPTICS

Report for second four month period
under contract F61775-98-WE071 (SPC98-4041)

**"Limiting possibilities for phase correction of turbulent distortions of optical
images"**

Principal Investigator
Prof. Vladimir P.Lukin

TOMSK - 1999

Contents

Abstract

Chapter1. Monostatic and bistatical schemes and optimal algorithm for tilt correction in ground-based adaptive telescopes

- 1.1. Introduction
- 1.2. The peculiarities for double-passage optical wave fluctuations
- 1.3. Correlation between instantaneous tilt for transmitted beam and reference image
- 1.4. Correction of beam direction with image of reference beacon
- 1.5. Investigation of LGS motion and full aperture angle correction
- 1.6. Correlation between natural star angle motion and auxiliary laser beam for bistatic scheme of LGS
- 1.7. «Optimal» algorithm of tip-tilt correction of natural star
- 1.8. LGS as extended source

References for Chapter1

Chapter 2. The problems of Laser Guide Stars Usage for Images Correction in the ground-based telescopes

- 2.1. Influence of temporal lag.
- 2.3. Distinction and common features of two schemes of laser guide star forming
- 2.3. References for Chapter 2.**

ABSTRACT

We have pointed out that such two terms as «an effective scattering volume» and «a laser guide star» (LGS) are scientific synonyms. The first term had been introduced earlier by specialists in atmospheric optics and laser sounding. In the report we have also represented information concerning fluctuations of waves reflected from an object and waves passed twice atmospheric inhomogeneities. Corresponding mathematical apparatus allows one to estimate correlation characteristics of a LGS. We have considered the mutual correlation function of random angular displacements of a plane wave image and the centroid displacements of a focused Gaussian laser beam. The algorithm of «optimal» correction was introduced in which *a priori* information is employed. Basing on this algorithm the variance was evaluated of residual jitters of a star image obtained with the use of LGS.

Key words: turbulence, double passage fluctuations, laser guide star, tip-tilt correction efficiency.

Chapter1. Monostatic and bistatical schemes and optimal algorithm for tilt correction in ground-based adaptive telescopes

1.1. Introduction

One of the most promising trends in the modern astronomy is a creation of ground-based adaptive telescopes which employ a signal of a laser guide star (LGS) [1]. To our mind, the most complete literature revue of the modern state of LGS was made by R.Ragazzoni [2].

The importance of investigations into the efficiency of adaptive optics systems with an artificial reference source was understood in the end of seventies. In this period were formulated the main principles upon which the modern concept of adaptive systems is based. According to this concept the reference source is the element with the use of which the information is procured concerning the distribution of fluctuations in the channel of radiation propagation. The way in which this channel is formed influences the structure of the whole system. If the principle of reciprocity is the base for an adaptive system, the most appropriate scheme is the one with an independent source of radiation generating a beam propagating in direction opposite to the corrected beam [3,4].

Aiming at the practical realization of the system, the atmosphere should be included into the loop, i.e., the backward scattering should be taken into account with radiation reflected by an object or by inhomogeneities of the atmosphere. In such a way an artificial (virtual) reference source is formed. In the early eighties in adaptive astronomy artificial reference sources were named *laser guide stars*. There are two main schemes of LGS generation: monostatic and bistatic [1, 2]. The laser used for this purposes is ground-based so the optical radiation travels two times through atmospheric inhomogeneties. First, upward, to form the LGS itself. Second, downward, in result of

backscattering (secondary emission, or elastic aerosol scattering) by atmospheric inhomogeneities. In monostatic scheme it is assumed that correlation of fluctuations for the upward and downward propagation (for direct and secondary beams) are maximum. Quite different conditions are characteristic for the bistatic scheme (in some papers the term "bistatic" means the LGS scheme formation, where there is no correlation between upward and downward propagation). In the both schemes one need to take into account peculiarities of optical parameters fluctuations of radiation passed twice through atmosphere.

1.2. The peculiarities for double-passage optical wave fluctuations

Approximately in beginning of seventies scientists working with optical systems of seeing and beam forming in the atmosphere and also with sounding systems understood that the peculiarities of fluctuations of reflected waves should be allowed for. In contradistinction to transmitting systems, in the systems of optical sounding the effect of two-fold passing of the atmosphere is always present. Sounding radiation passes through the same optical inhomogeneities two times: during the direct and reverse propagation. Scientists involved in investigations connected with atmospheric sounding introduces such terms as *effective scattering volume*, *monostatic optical scheme*, *bistatic scheme of laser sounding* and some others.

The LGS is aimed at providing a reference source bright enough for adaptive optics. This concept recently begun to be widely discussed, but in fact it is not so new. We would like to declare that two scientific terms: *effective scattering volume* and *laser guide star* are **scientific synonyms**. The first term had been introduced earlier by specialists in atmospheric optics and laser sounding. The second term - *laser guide star* - had been introduced in astronomy for application with adaptive optical image correction. In this connection the great benefit for the tasks of adaptive optics for astronomy possible to obtain with application earlier theoretical investigations which have been developed in the atmospheric optics and laser sounding. In the next part of this chapter we are going to present some results and formulae concerning fluctuations of waves reflected from an object and waves passed twice atmospheric inhomogeneities. In particular, the corresponding mathematical apparatus allows one to estimate correlation characteristics of a LGS.

The following Russian scientists were working in the field: Yu.A.Kravtsov, A.N.Malakhov, A.S.Gurvich, K.S.Gochelashvily, V.I.Shishov, A.I.Saichev, V.A.Banach, V.L.Mironov, V.U.Zavorotny, V.I.Klyatskin, A.I.Kon, V.I.Tatarskii,

Yu.N.Barabanenkov, S.S.Kashkarov, G.Ya.Patrushev, V.P.Aksenov. M.I.Charnotskii, M.L.Belov, I.G.Yakushkin, Z.I.Feizulin, A.G.Vinogradov, A.B.Krupnik, L.Apresyan. The most complete overview of the problem and Russian papers in the field were presented on the International Meeting for Wave Propagation in Random Media «Scintillation» held in USA (Seattle, August 1992) [5]. This paper presents the review of the results of the effect of atmospheric refractive index fluctuations on the propagation of optical wave when the wave traverses the same region of the atmosphere twice. Such situation is realized at reflection of laser beams from a target or at wave backscattering on atmospheric aerosol. In the case light-wave propagation properties are determined by correlations between incident and wave traversing the same inhomogeneities in a turbulent atmosphere.

Fluctuations of an image center of gravity of backscattering volume were considered in the book by M.L.Belov et al. (Ref.[6]). The image was formed through an inhomogeneous medium in a sounding system with the use of a focused laser beam. Particularly, fluctuations were investigated of the image displacements of a sounding volume. Monostatic and bistatic schemes were considered. For irradiation of the volume focused and collimated laser beams were used. Equations describing the variance of centroid fluctuations were obtained for an image in the photodetector plane without any restrictions on reflection properties of an object (pp.84 - 95 of Ref. 6). It was shown that for the case of strong dispersion on a reflection surface (Lambertian approximation) in the bistatic sounding scheme the variance of linear displacements of the image center of gravity $\vec{\rho}_{im}$ can be written as (see page 92 of Ref.6):

$$\langle \rho_{im}^2 \rangle = \frac{F^2}{\chi^2} \langle \rho_{lb}^2 \rangle + F^2 \langle (\varphi_F^s)^2 \rangle, \quad (1)$$

where $\langle \rho_{lb}^2 \rangle$ is the variance of random displacements of the beam centroid in a sounding plane (it was assumed that the beam propagates forward) and $\langle (\vec{\rho}_F^{\text{ss}})^2 \rangle$ is the variance of random angular displacements of an image of «secondary» motionless source (backward propagation). So, it was shown that for the bistatic scheme the variance of angular displacements of an image is a sum of angular displacements of the image and of the «secondary» motionless source. If a focused beam is used in strongly scattering medium the "secondary" source is, practically, a point source.

In this period calculations were performed for cases when the source can be treated as a point and also for objects with finite volumes. As an example the paper by M.A.Kalistratova and A.I.Kon (Ref.7) can be taken where jitter of image was considered for a thin irradiating string.

So we can conclude that in the USSR in early eighties scientists understood that in some conditions a volume could be considered as infinite small (a point source) and that in other problems its size should be allowed for, i.e., if an object is large enough averaging over its volume is necessary as it was performed in Refs.7, 16. At the same time the authors of Ref. 6 were not able to calculate correctly mutual correlation between fluctuations of focused beam displacements and displacements of a image of reference sources. It was performed in 1979-1980 (see Refs. 8, 9).

1.3. Correlation between instantaneous tilt for transmitted beam and reference image

In 1979-1980 V.P.Lukin was considering [8,9] the problem of stabilization direction for laser beam in turbulent atmosphere. As a method to solve this problem, the detection of an image of a reference source (including the natural star) in a focal plane of a telescope was proposed. In particular, a mutual correlation function $\langle \vec{\rho}_{lb} \vec{\rho}_F \rangle$ for a vector characterizing random shifts of the beam centroid $\vec{\rho}_{lb}$ and vector defining coordinates of image centroid of a reference signal $\vec{\rho}_F$ was computed for a turbulent atmosphere. It was assumed that as a reference signal an image of some beacon (in focal plane of telescope) can be used.

In Ref.8 have been calculated the mutual correlation between the random displacements of the center of gravity of Gaussian beam and the center of gravity of some image for infinite plane wave. The beam and plane wave propagate along the same optical path. Random displacements of the beam centroid are given by the vector [10]:

$$\rho_{lb} = \frac{1}{P_0} \int_0^X d\xi (X - \xi) \iint d^2 R I(\xi, \mathbf{R}) \nabla_R n_1(\xi, \mathbf{R}), \quad (2)$$
$$P_0 = \iint d^2 R I(0, \mathbf{R}),$$

where $n_1(\xi, \mathbf{R})$ denoted the fluctuations of the atmospheric refractive index in the point (ξ, \mathbf{R}) , $I(\xi, \mathbf{R})$ is the optical field intensity at the point (ξ, \mathbf{R}) from the laser source placed at the coordinate origin in the initial plane (for $\xi = 0$); X is the thickness of the turbulent layer.

The random displacements of the any image in the focal plane of the optical system (telescope, or equivalent to a "thin" lens with focal length F and area $\Sigma = \pi R_0^2$) are given by the expression [11]:

$$\rho_F = -\frac{F}{k\Sigma} \iint_{\Sigma} \nabla_{\rho} S(x, \rho) d^2 \rho, \quad (3)$$

where k is the wave number of the radiation, $S(x, \rho)$ are the fluctuations of the phase of the optical wave over the aperture of the optical system (in the $\xi = X$ plane) at the point ρ . The mutual correlation of the random vectors ρ_{lb} and ρ_F is given [8,9] by

$$K = \langle \rho_{lb} \rho_F \rangle / \left[\langle \rho_{lb}^2 \rangle \langle \rho_F^2 \rangle \right]^{1/2}. \quad (4)$$

Here and in any places in this report $\langle \dots \rangle$ denotes averaging over the ensemble of realizations of the random function $n_1(\xi, \mathbf{R})$ [11, 10]. In that follows we assume that functions $\langle I(\xi, \mathbf{R}) \rangle$ and $\Phi_n(\xi, \kappa)$ are isotropic and average intensity $\langle I(\xi, \mathbf{R}) \rangle$ is given for Gaussian laser beam in representation [10,11]:

$$\langle I(\xi, \mathbf{R}) \rangle = \frac{a^2}{a_{eff}^2(\xi)} \exp(-R^2 / a_{eff}^2(\xi)), \quad (5)$$

where

$$a_{eff}^2(\xi) = a^2 \left[\left(1 - \frac{X}{f} \xi \right)^2 + \Omega^{-2} + \Omega^{-2} \left(\frac{1}{2} D_s(2a) \right)^{6/5} \right],$$

$\Omega = \frac{ka^2}{X\xi}$, a and f are initial parameters of the Gaussian beam, $D_s(2a)$ is a phase structure function [10]. All in all we obtain [8]

$$\begin{aligned}
K = & \int_0^1 d\xi (1 - \xi) \int_0^\infty d\kappa \kappa^3 \Phi_n(\kappa) \exp\left(-\frac{\kappa^2(R_0^2 + a_{\text{Eff}}^2)}{4}\right) \cos\left(\frac{\kappa^2 x(1 - \xi)}{2\kappa}\right) \times \\
& \times \left(\int_0^1 d\xi (1 - \xi)^2 \int_0^\infty d\kappa \kappa^3 \Phi_n(\kappa) \exp\left(-\frac{\kappa^2 a_{\text{eff}}^2(\xi)}{2}\right) \right)^{-1/2} \times \\
& \times \left(\int_0^1 d\xi \int_0^\infty d\kappa \kappa^3 \Phi_n(\kappa) \exp\left(-\frac{\kappa^2 R_0^2}{2}\right) \cos^2\left(\frac{\kappa^2 x(1 - \xi)}{2\kappa}\right) \right)^{-1/2},
\end{aligned} \quad (6)$$

In calculations we use the following spectrum

$$\Phi_n(\xi, \kappa) = 0.033 C_n^2(\xi) (\kappa^2 + \kappa_0^2)^{-11/6}, \quad (7)$$

which accounts for deviation from a power series in a vicinity of the outer scale $L_0 = 2\pi\kappa_0^{-1}$, $C_n^2(\xi)$ is a structure parameter of turbulent atmosphere. Estimation [8] is performed for a homogeneous path (initial beam diameter equal to the diameter of the input pupil of the telescope), the parameters of the problem are the following:

$$\kappa_0^{-1} \gg (R_0, a_{\text{eff}}, \sqrt{x/k}); \quad kR_0^2 \gg x, \quad \Omega^{-2} \left(\frac{1}{2} D_s(2a) \right)^{6/5} \ll 1.$$

V.P.Lukin obtained for focused beam ($f = X$) the value of $K = 0.84$.

Thus, the high positive correlation was shown (in Ref.8, 1979) between displacements of a Gaussian beam and displacements of the plane wave image centroid assuming that beam propagation and image forming are on the same path and in the same direction. Later in [9] these results were generalized for the case of beam and image forming when propagation is realized in opposite directions. It was also assumed that forming of the image in the focal plane of a telescope performed for the following scenarios:

- plane wave, spherical wave, Gaussian beam,
- radiation reflected from a plane mirror.

For a plane wave propagating over a homogeneous path and for a broad beam it was obtained that

- $K = -0.87$ (for collimated beam), $K = -0.82$ (for focused beam).

For spherical waves and any others reference beacons the results could be obtained from the formulas presented in Ref. 9. So as early as in 1979-1980 the sign of mutual correlation was determined and its value estimated.

1.4. Correction of beam direction with image of reference beacon

Due to relatively high correlation, an algorithm of control for correction of random angular displacements of beam $\bar{\rho}_{lb}/X$ can be performed, according to the formula $\alpha(a / 2R_0)^{1/3} \bar{\rho}_F / F$, where α is coefficient of the loop which chosen to ensure the minimum of residual angular displacements of the beam

$$\min \left\langle \left(\frac{\rho_{lb}}{X} - \frac{\alpha(a / 2R_0)^{-1/3} \rho_F}{F} \right)^2 \right\rangle.$$

So, passing from linear measurements to angular it is possible to control a laser beam position using data of measurements of the reference source image. In Ref.9 (1980) Dr.V.P.Lukin have made mention of the **fundamental possibility of using radiation backscattered by the atmospheric aerosol. And he firstly presented scheme for laser guide star formation (Fig.1.1).**

Summing up we can conclude that Soviet scientists in eighties obtained all functions necessary to analyze random displacements of the image of a sounding object for bistatic as well as for monostatic schemes.

But in any cases under to solve some principal problem, the question about the model of scattering or refracting media still is always arise. The solution of this problem have been determined the model of "secondary" source. Possible as to interaction of model of similar source, as a solution of problem for backscattering.

1.5. Investigation of LGS motion and full aperture angle correction

The two techniques for measuring with a LGS is proposed in [12]. The first technique exploits a laser beam transmitting through the main telescope and two auxiliary telescope, which are separated from the transmitter, are used to measure a LGS image motion, averaging over its angular extent. In his paper [12] author mentioned that monostatic LGS can not be used for tip-tilt correction for main telescope, but bistatic scheme (without correlation between upward and downward propagation) permits to single out the tilt component corresponding to the transmitting beam which is highly correlated with the tilt for natural star. Unfortunately, author of [12] did not made adequately references [8, 9] and several formulas in this paper are with strong errors. The new approach [13] same author exploits a small beam transmitted from main telescope, and signal for tilt correction is determined by subtracting the LGS motion measured simultaneously with the main and auxiliary telescopes. There are not necessary references [6-9, 16] in paper [13] too.

1.6. Correlation between natural star angle motion and auxiliary laser beam for bistatic scheme of LGS

Following the R.Ragazzoni approach [2], let us consider as in [14, 15] the next scheme for LGS forming (Fig.1.2). LGS created with auxiliary laser beam with separate aperture. Parameters of the problem are as follows: R_0 is a telescope aperture radius, X is an altitude of (distance from) a LGS, input pupil of the telescope is placed in the plane $\xi = 0$, a is radius of transmitting aperture for laser source, $\vec{\rho}_0$ is a vector of displacement of the laser source relatively to the telescope optical axis. We presume that the tip-tilt measurements of the wave front is performed in the telescope with the use of a LGS formed at an altitude X above the input aperture exactly at the optical axis of the telescope. The telescope is pointed at the zenith and a weak natural star and the LGS are both at the telescope axis (or within the isoplanatic area out of axis). The zenith angle of the laser beam is $|\vec{\rho}_0| / X$ (in the assumption that $|\vec{\rho}_0| \ll X$).

Let us also assume that the observed star (as a science object) has a plane wave front. The vector characterizing a random tilt of this wave front due to atmospheric turbulence is (see Ref. [11]) given Eq.(3), where

$$S^{\rho}(0, \vec{\rho}) = k \int_0^{\infty} d\xi \iint d^2n(\vec{\kappa}, x - \xi) \exp(i\vec{\kappa}\vec{\rho}) \quad (8)$$

are phase fluctuations for a plane wave on the telescope aperture, and the following spectral expansion [9,10] is used for fluctuations of the atmospheric index of refraction

$$n_1(\xi, \vec{\rho}) = \iint d^2n(\vec{\kappa}, x - \xi) \exp(i\vec{\kappa}\vec{\rho}).$$

In the last equation it is also taken into account that the wave from natural star travels from infinity to down. Random angular shifts of the centroid for LGS formed with a laser source at the altitude X can be written [16] using Eq.(2) with

$$I = I(\xi, \vec{R} + \vec{\rho}_0(1 - \xi / X)). \quad (9)$$

The fact is taken into account that the laser beam (see Fig.1.2.) is shifted by the vector $\vec{\rho}_0$ and its optical axis is also tilted at the angle $|\vec{\rho}_0| / X$.

Let us to obtain a mutual correlation function between random angular shifts of the image of a natural star (function $\vec{\varphi}_F^{pl}$, Eqs.(3), (8)) formed by the telescope and shifts of the centroid of a focused beam formed by tilted laser system (function $\vec{\varphi}_{lb}(\vec{\rho}_0)$, Eqs.(2), (9)). **We are going to based only on results of such computations, which were published in Dr.V.P.Lukin's papers (Refs.8, 9, 14, 15).** Deviation of the turbulence spectrum from a power function in the domain of large scales was accounted for [17-20]:

$$\hat{O}_n(\kappa, \xi) = 0,033C_n^2(\xi)\kappa^{-11/3}\{1 - \exp(-\kappa^2 / \kappa_0^2)\}, \quad (10)$$

where $C_n^2(\xi)$ is turbulence intensity on the path of propagation and $\kappa_0^{-1}(\xi)$ is the outer scale of turbulence. If these properties are correctly allowed for, it is possible to obtain [8, 9, 14, 15] the following equation for a correlation function:

$$\begin{aligned} \langle \vec{\varphi}_{lb}(\vec{\rho}_0) \vec{\varphi}_F^{pl} \rangle &= (-2\pi^2 0,033 \tilde{A}(\frac{1}{6})) 2^{1/3} R_0^{-1/3} \int_0^X d\xi C_n^2(\xi) (1 - \xi / X) \\ &\{ [1 + b^2(1 - \xi / X)^2]^{-1/6} {}_1F_1(\frac{1}{6}, 1; -\frac{d^2(1 - \xi / X)^2}{(1 + b^2(1 - \xi / X)^2)}) - \\ &- [1 + b^2(1 - \xi / X)^2 + 4c^2]^{-1/6} {}_1F_1(\frac{1}{6}, 1; -\frac{d^2(1 - \xi / X)^2}{(1 + b^2(1 - \xi / X)^2 + 4c^2)}) \} \end{aligned} \quad (11)$$

Here the designations were used: $b = a / R_0$, $d = |\vec{\rho}_0| / R_0$, $c = \kappa_0^{-1} R_0^{-1}$ and the ${}_1F_1(\dots)$ is a confluent Gaussian hypergeometric function.

It can readily be shown that the second term in the braces is related with the outer scale of turbulence. And if the outer scale approaches infinity, this term can be omitted so the correlation function takes the form:

$$\langle \bar{\varphi}_{lb}(\bar{\rho}_0) \bar{\varphi}_F^{pl} \rangle = (-2\pi^2 0,033 \tilde{A}(\frac{1}{6})) 2^{1/3} R_0^{-1/3} \int_0^X d\xi C_n^2(\xi) (1 - \xi/X) \times \\ [1 + b^2(1 - \xi/X)^2]^{-1/6} {}_1F_1(\frac{1}{6}, 1; -\frac{d^2(1 - \xi/X)^2}{(1 + b^2(1 - \xi/X)^2)}) \quad (12)$$

Into this equations (11), (12) the value of $d = 0$ corresponds to the monostatic scheme of a LGS. For the bistatic scheme (for $d > 0$) condition $d \gg 1$ correspond to asymptotic of a hypergeometric function ${}_1F_1(\dots)$. Thus,

$$\langle \bar{\varphi}_{lb}(\bar{\rho}_0) \bar{\varphi}_F^{pl} \rangle = (-2\pi^2 0,033 \tilde{A}(\frac{1}{6})) 2^{1/3} R_0^{-1/3} \tilde{A}^{-1}(\frac{5}{6}) d^{-1/3} \times \\ \int_0^X d\xi C_n^2(\xi) (1 - \xi/X)^{2/3} \quad , \quad (13)$$

from the analysis of the last equation it is possible to conclude that correlation between the plane wave and the beam decrease down to 0.1 for $d \geq 10^3$. This value is characteristic for the bistatic scheme (where there is no any correlation for upward and downward propagation) for infinite outer scale of turbulence.

Numerous data obtained experimentally (Refs.21-24) justify the assumption that the outer scale $\kappa_0^{-1}(\xi)$ is a finite number. Moreover, in result numerical estimations performed with the use of different altitude profiles of $C_n^2(\xi)$ and $\kappa_0^{-1}(\xi)$ scientists comes to the conclusion that it is possible to introduce some characteristics (*spatial coherence outer scale* [25], or *effective outer scale of turbulence* [26]) for the whole atmospheric column description. As it was turned out, under «moderate» conditions of seeing [27], the value of this *effective outer scale* is 5 - 60 meters [26]. So for a telescope with $R_0=4\text{m}$ parameter $c = \kappa_0^{-1} R_0^{-1} < 10$.

Let us perform asymptotic analysis of the outer scale influence on the correlation function expressed by Eq.(11). As an argument of the function we take a variable d and as parameters variables b , c , and X . Simple estimations show that when parameter $d = 0$ and $c < 5$, the correlation with the finite outer scale is two-three times lower than with the infinite outer scale. With increase of d (for $d > 1$) correlation computed by Eq.(11) is not greater than 0.2. For $d > 2c$ the correlation is 17 times lower than that for the infinite outer scale. And, at last, for $d \gg c$ the sign of correlation function $\langle \vec{\varphi}_{lb}(d) \vec{\varphi}_F^{pl} \rangle$ changes for reverse and dependence on d can approximately be written as $\approx d^{-7/3}$.

To confirm this conclusion let us estimate numerically a correlation coefficient

$$K(d, b, c, X) = \frac{\langle \vec{\varphi}_{lb}(\vec{\rho}_0) \vec{\varphi}_F^{pl} \rangle}{\sqrt{\langle (\vec{\varphi}_{lb}(\vec{\rho}_0))^2 \rangle \langle (\vec{\varphi}_F^{pl})^2 \rangle}}. \quad (14)$$

The coefficient can be expressed through correlation function (11) and corresponding variances:

$$\langle (\vec{\varphi}_F^{pl})^2 \rangle = (2\pi^2 0,033 \tilde{A}(\frac{1}{6})) 2^{1/6} R_0^{-1/3} \int_0^X d\xi C_n^2(\xi) [1 - [1 + 4c^2]^{-1/6}], \quad (15)$$

$$\begin{aligned} \langle (\vec{\varphi}_{lb}(\vec{\rho}_0))^2 \rangle &= (2\pi^2 0,033 \tilde{A}(\frac{1}{6})) 2^{1/6} R_0^{-1/3} \int_0^X d\xi C_n^2(\xi) \times \\ &\{ (b^2(1 - \xi/X)^2)^{-1/6} - (b^2(1 - \xi/X)^2 + 4c^2)^{-1/6} \} \end{aligned} \quad (16)$$

Computations were performed with a model of $C_n^2(\xi)$ corresponding to «moderate» conditions of seeing [27]. The altitudes corresponding to Rayleigh and sodium artificial stars (10 and 100km) were included into initial conditions. Parameter b was chosen as follows: $b = 0.1, 0.3, 0.7, 1.0, 3.0$, and 5.0 . The values of b greater than unity are typical in situations, when a big telescope forms an artificial star for a small one. Such ratios of parameters can be realized in observatories where telescopes of different sizes are placed. For example, when in Mauna Kea observatory the ten-meter Keck telescope

used as auxiliary one for a small telescope. In the calculations values of c were the following: 1, 3, 5, 10, 100, 1000. The case when $c = 1000$ practically corresponds to the infinite outer scale.

The results obtained are shown (with omitting a sign) in Figs.1.3 and 1.4 as a fragments a, b, c, d, e, f. All need parameters are shown on Figures. It should be noted that the results obtained numerically confirm the conclusions of the above analytic analysis. Also possible to made the next conclusions:

1. With the large outer scales ($c = 100$ and 1000) the scheme for the LGS formation can be considered as bistatic (upward and downward paths are decorrelated) one, if the difference between axis of the telescope and auxiliary laser beam is $(200 - 1000)R_0$, i.e., if $d > 200$.
2. With a finite outer scale ($c < 5$) the value of differences d in two or three outer scale times means substitution of the monostatic scheme to bistatic one (where correlation upward and downward propagation is negligible).
3. Smaller values for differences d correspond to intermediate schemes (with partial correlation for upward and downward paths).
4. It should also be noted that the results of our calculations are not coincide with results reported in (Refs.13 and 29). These authors considered mutual correlation functions for two plane waves traveling from infinity with different tilts. In particular, in our computations the correlation coefficient K for $d = 0$ is not equal to unit (with the sign minus). Only with decrease of X , the coefficient K approaches unity asymptotically.
5. It is interesting to consider the behavior of K in the region of small values of c ($c = 1, 3, 5$) and relatively large values of b ($b = 3, 5$). This situation is characteristic for the case when a large telescope generates an artificial star for a small one. The results obtained (Fig.1.3 and 1.4) show that in this scheme the correlation in the region $d < c$ is practically constant (correlation is equal, correspondingly, to 0.4, 0.5, 0.7).

6. With increasing of c the characteristic scale of correlation function K increases, i.e., the correlation radius increases. This effect was noted (for two plane waves) in [13].
7. Increasing of the correlation radius is not infinite, gradual saturation of the function was observed in our numeric experiments. For small values of c (the outer scale is small) correlation function $K(d)$ decreases down to 0.1 for $d = c$. But even for $c = 100$ the correlation falls down to 0.1 if $d = c/2$. When $c = 1000$ such fall occurs for $d = c/10$. This is possible for altitude $X=10\text{km}$ as well as for $X=100\text{km}$.
8. The predicted change of the sign for correlation function made on the basis of the asymptotic analysis (the conclusion was made comparing Eqs.(11) and (12)) is due to a finite size of the outer scale of turbulence. When the outer scale is small ($c = 1, 2, 3$) and $d > (2 - 3)c$, the correlation function change its sign to opposite. For large c this effect is impossible to register. When values of the outer scale are large, coefficient K (Eq.(14)) keeps its sign.

Really, it is interesting to find a relationship between the value of radius of mutual correlation for two plane waves [29, 13] and radius of correlation for a plane wave and a slanted laser beam (the last characteristic is presented in Figs.1.3 and 1.4). If found, these data would allow one to use the results of direct astronomical observations of images of two stars seen at different angles in prognoses about the value of correlation (for tip-tilt correction) for a system «telescope-LGS» and also to make more correct conclusions concerning the mode of operation of this system. To our regret, it is impossible to make a simple comparison between Figs.1.3 and 1.4 and the data presented in Ref.13 because in algorithms of computations different models of the atmospheric turbulence were used.

Actually, based on these Figs.1.3, 1.4 (and formulas (11), (12)), it is possible to estimate the real level of correlation between natural star motion, measured in the telescope and auxiliary tilted laser beam, which formed the LGS on optical axis of

telescope, and to obtain parameters for calculation the efficiency of tip-tilt correction with any interested parameters of telescope, size of laser beam, outer scale of turbulence and distance between telescope and laser beam axes.

The calculations of the real level of correlation between natural star motion, measured in the telescope and auxiliary tilted laser beam, which formed the LGS are carried out using the model of the spectrum of atmospheric turbulence. The structure parameter and outer scale of turbulence are the parameters of the model. Thus we shall study the peculiarities of the correlation connected with the finite value of outer scale of turbulence. Moreover, since all these value depend not only on the propagation path but also on the actual altitude of telescope above the sea level, the possible variations of the model should be seriously discussed in this aspect (model parameters) depending on the aerography of the underlying surface. We are repeating that numerous data obtained experimentally (Refs.21-24) justify the assumption that the outer scale $\kappa_0^{-1}(\xi)$ is a finite number. Moreover, in result numerical estimations performed with the use of different altitude profiles of $C_n^2(\xi)$ and $\kappa_0^{-1}(\xi)$ scientists comes to the conclusion that it is possible to introduce some characteristics (*spatial coherence outer scale* [25], or *effective outer scale of turbulence* [26]) for the whole atmospheric column description.

At the same time the models of the atmospheric turbulence spectrum, taking into account the finiteness of the outer scale of turbulence, and especially, the running value of this parameter $\kappa_0^{-1}(\xi)$ for vertical paths are rarely used. For homogeneous surface paths it is shown that value κ_0^{-1} is fully finite and commensurable with the height above the underlying surface. At the same time, for astronomical observations a number of researchers consider this value κ_0^{-1} to be equal to hundreds of meters up to some kilometers. There are many observations when the results correspond to the value of the outer scale of the order of one meter.

Undoubtedly, the outer scale of the turbulence significant variations both in the surface atmospheric layer and at large altitudes. Therefore we cannot speak about the value of the outer scale as having the definite value for the entire atmosphere. We propose to consider a number of possible versions of variations of the outer scale with altitude h :

$$(A) \quad \kappa_0^{-1}(h) = 0.4h,$$

$$(B) \quad \kappa_0^{-1}(h) = \begin{cases} 0.4h & h \leq 25m \\ 2\sqrt{h}, & h > 25m \end{cases},$$

$$(C) \quad \kappa_0^{-1}(h) = \begin{cases} 0.4h, & h \leq 25m \\ 2\sqrt{h}, & 25m < h \leq 2000m \\ 89.4m, & h > 2000m \end{cases},$$

$$(D) \quad \kappa_0^{-1}(h) = \frac{5}{\left[1 + ((h - 7500) / 2000)^2\right]},$$

$$(E) \quad \kappa_0^{-1}(h) = \frac{5}{\left[1 + ((h - 7500) / 2000)^2\right]}.$$

Model (A) is recommended in [11] for the use for small altitudes, model (B) is proposed by D.Fried [17], model (C) represents the generalization of the first two models. Model (D) and (E) are obtained as a generalization of the results of direct measurements in USA, in France, and in Chili [17, 32-34]. The resembling value of this parameters were obtained for the Mauna Kea Observatory (Hawaii) [17, 34]. Some investigators have cast doubt on these models [17, 21], however, the altitude variations of the value of outer scale within wide limits have gained recognition.

Figs.1.5, 1.6 present result of calculations of the same characteristics as on Figs.1.3, 1.4 only we apply here the outer scale as models (A, B, C, D, E) instead the different values for outer scale on Figs.1.3, 1.4. The curves on Fig.1.3 and Fig.1.5 (as Fig.1.4 and Fig.1.6) are very similar, but only for models D and E the correlation

functions became having the lower level of correlation for small difference between main telescope and laser beams axis.

1.7. «Optimal» algorithm of tip-tilt correction of natural star

A laser guide star allows one to expand the domain of stable operation for an adaptive optics system. The star is formed at some finite distance, so the problem arises to correct the data of optical measurements performed with a guide star to ensure efficient compensation for aberrations of a image of a real astronomical object [4, 1]. This correction of data is possible with the use of atmospheric models [28, 14, 15]. The models of atmospheric turbulence allow one

- to estimate the level of turbulent aberrations above the reference star, i.e., to compute optimal altitude of the star generation,
- to compensate partially focal anisoplanarity in a system with a reference star placed at a finite altitude,
- to make estimations of efficiency for a «tip-tilt» correction more precise.

Doubtless, when we use the LGS formed in the atmosphere by backscattered signal in the algorithm of correction for random wandering [1, 2, 12, 13, 14, 15] of a natural star image, the problem arises of data processing optimization. Let us try to construct the algorithm of angular natural star image motion $\vec{\varphi}_F^{pl}$ correction, using data of LGS angular position measurements $\vec{\varphi}_m$, as following [14, 15]:

$$\vec{\varphi}_F^{pl} - \dot{A}\vec{\varphi}_m. \quad (17)$$

This algorithm ensures the minimum of the variance for residual angular displacements for natural star under tip-tilt correction based on data for LGS angular position measurements:

$$\langle \beta^2 \rangle = \langle (\vec{\varphi}_F^{pl} - \dot{A}\vec{\varphi}_m)^2 \rangle = \langle (\vec{\varphi}_F^{pl})^2 \rangle + \dot{A}^2 \langle (\vec{\varphi}_m)^2 \rangle - 2\dot{A} \langle \vec{\varphi}_F^{pl} \vec{\varphi}_m \rangle. \quad (18)$$

From Eq.(18) we obtain as a minimum:

$$\langle \beta^2 \rangle_{\min} = \langle (\vec{\varphi}_F^{pl})^2 \rangle - \langle \vec{\varphi}_F^{pl} \vec{\varphi}_m \rangle^2 / \langle (\vec{\varphi}_m)^2 \rangle, \quad (19)$$

when the coefficient of correlation A is expressed through a (nonrandom) determined functions as

$$\dot{A} = \langle \vec{\varphi}_F^{pl} \vec{\varphi}_m \rangle / \langle \varphi_m^2 \rangle. \quad (20)$$

The form of this coefficient allows one to conclude that the coefficient A can be calculated from data in direct optical experiments (some time before adaptive telescope operation). Unfortunately, in other side, a most real experiment we can obtain only data on $\vec{\varphi}_m$, because vector $\vec{\varphi}_F^{pl}$ characterizing angular wandering of a natural star image is impossible to detect due to insufficient intensity of light from a natural star. In similar cases we can estimate this coefficient A by formula (20), using [15] the models of atmospheric turbulence and results for calculations the correlation function (11) and the variances (15), (16).

It should also be noted that the minimum of variance (19) is impossible to obtain with traditionally used correction algorithms (Eq.(18) with $A = -1$). To confirm this let us perform intercomparison of residual variance for optimal and nonoptimal (traditional) algorithms of correction. In our designations the minimum variance of residual fluctuations of a star image angular shifts in a scheme presented in Fig.1.2 can be estimated as:

$$\langle \beta^2 \rangle_{\min} = \langle (\vec{\varphi}_F^{pl})^2 \rangle \left\{ 1 - \frac{2^{1/3} f(X, b, d, C_n^2)}{\left[1 + \hat{a}^{-1/3} - 2^{7/6} (1 + \hat{a}^2)^{-1/6} {}_1F_1\left(\frac{1}{6}, 1; -\frac{d^2}{(1 + b^2)}\right) \right]} \right\}, \quad (18)$$

where the function

$$\begin{aligned}
f(X, b, d, C_n^2) = & \left(\int_0^X d\xi C_n^2(\xi) (1 - \xi / X) \{ [1 + (1 - \xi / X)^2]^{-1/6} - \right. \\
& \left. - [1 + b^2 (1 - \xi / X)^2]^{-1/6} {}_1F_1\left(\frac{1}{6}, 1; -\frac{d^2 (1 - \xi / X)^2}{1 + b^2 (1 - \xi / X)^2}\right) \}^2 \times \right. \\
& \left. \left[\left(\int_0^X d\xi C_n^2(\xi) (1 - \xi / X)^{5/3} \int_0^\infty d\xi C_n^2(\xi) \right)^{-1} \right] \right.
\end{aligned} \tag{19}$$

depends upon parameters of the optical experiment as well as upon the used atmospheric model (the above equations are written assuming that the outer scale of turbulence is infinite, and for assumption that LGS is a point source). For traditional algorithm ($A = -1$ in (17)) the residual variance for natural star motion is determined by the formula (18).

Numerical analysis of these equations showed [14, 15] that in result of optimal correction the residual angular distortions can be less than residual distortions of traditional methods of control. To illustrate advantages of the optimal algorithm in comparison with nonoptimal (traditional) one we include in the paper Table 1.1 where the values of residual angular distortions are presented for a telescope with a bistatic reference star. In the Table we put the values of normalized (to the variance of angular natural star motion without tilt correction) residual variances

$$\langle \beta^2 \rangle / \langle (\bar{\varphi}_F^{pl})^2 \rangle = 1 + A^2 \langle (\bar{\varphi}_m)^2 \rangle / \langle (\bar{\varphi}_F^{pl})^2 \rangle - 2A \langle \bar{\varphi}_F^{pl} \bar{\varphi}_m \rangle / \langle (\bar{\varphi}_F^{pl})^2 \rangle \tag{20}$$

for optimal and traditional algorithms for natural star tip-tilt correction. In the fifth column also placed the values of correction coefficient A computed for the model of turbulence [27]. We have presented results for different sizes for auxiliary laser beam (parameter $b = 0.3, 0.5, 0.7, 1, 2, 3, 5$) and altitudes of LGS ($X = 8\text{km}, 20\text{km}, 40\text{km}, 80\text{km}$, and 100km), the model of turbulence atmosphere have been taken from [27], parameter $d > 5000$.

It is seen from the data presented in the Table that optimal correction with properly chosen coefficient A allows one to decrease the residual distortions. So the conclusion can be drawn about efficiency of optimal correction with the use of information concerning altitude profiles of turbulence. At the same time intensity of distortions can even increase in the result of nonoptimal (traditional) correction in bistatic scheme (for parameter $d > 5000$, i.e., and for the negligible level of correlation between beam and image of natural star motion), as can be seen from Figs. 1.3f, 1.4f. But even with the considerable reduction of tilt jitter using the proper choice for A still a relatively large amount of tilt residual affects the image of natural star. Must to say that this conclusion is based on assumption that LGS image is a point.

1.8. LGS as extended source

But in some bistatic scheme a LGS image has the form of an extended source [2, 12, 13]. As a consequence, the random displacements for motionless "secondary" source might be averaged out over its angular extent [2, 12, 13]. This problem have been considered early in Refs.6, 7, 16 for strong reflection surface and sources as a thin irradiating string and extended Gaussian beams.

But we would like to make an emphasis the difference and similarity between two bistatic schemes. Approach R.Ragazzoni [2] - two auxiliary tilted laser beams and single telescope and approach from papers [12, 13] - main telescope with laser beam and two auxiliary tilted telescopes. In the both schemes the variance for random displacement of LGS image are given Eq.(1). If the LGS observing extent $a_b \gg R_0$ (aperture size for main telescope, or aperture size of auxiliary telescopes) the variance [7, 16, 13] for "secondary" source is given:

$$\langle \varphi_{ss}^2 \rangle = \langle (\varphi_F^{sp})^2 \rangle (a_b / R_0)^{-1/3} \frac{\int_0^X d\xi C_n^2(\xi) (1 - \xi / X)^2 (\xi / X)^{-1/3}}{\int_0^X d\xi C_n^2(\xi) (1 - \xi / X)^{5/3}}. \quad (21)$$

On the next step let us to compare the minimal variances for residual level of natural star motion after tip-tilt correction for these two schemes with optimal correction algorithm (17). For scheme from [2] the minimum of variance is presented as following formula:

$$\langle [\bar{\varphi}_F^{pl} - A\bar{\varphi}_m]^2 \rangle / \langle (\bar{\varphi}_F^{pl})^2 \rangle = 1 - \langle \bar{\varphi}_F^{pl} \bar{\varphi}_{ss} \rangle^2 / [\langle (\bar{\varphi}_F^{pl})^2 \rangle \langle (\bar{\varphi}_m)^2 \rangle], \quad (22)$$

and for scheme from [12,13]:

$$\langle [\bar{\varphi}_F^{pl} - A\bar{\varphi}_m]^2 \rangle / \langle (\bar{\varphi}_F^{pl})^2 \rangle = 1 - \langle \bar{\varphi}_{lb} \bar{\varphi}_F^{pl} \rangle^2 / [\langle (\bar{\varphi}_F^{pl})^2 \rangle \langle (\bar{\varphi}_m)^2 \rangle]. \quad (23)$$

Last equation may to transfer into next one:

$$\langle [\bar{\varphi}_F^{pl} - A\bar{\varphi}_m]^2 \rangle / \langle (\bar{\varphi}_F^{pl})^2 \rangle = 1 - K^2(0) / [1 + \frac{\langle \varphi_{ss}^2 \rangle}{\langle \varphi_{lb}^2 \rangle}], \quad (24)$$

where coefficient of correlation K is given in (14) for parameter $d = 0$ and presented on Figs.1.3. -1.5. The second term from Eq.(23) is normalized correlation function between angular image displacements of plane wave and "secondary" source - a broad wave beam, having size of isoplanation zone in plane of LGS, and in result of calculation formula (22) turn into next:

$$\langle [\bar{\varphi}_F^{pl} - A\bar{\varphi}_m]^2 \rangle / \langle (\bar{\varphi}_F^{pl})^2 \rangle = 1 - (2b)^{1/3} \frac{\int_0^X d\xi C_n^2(\xi)(1 - \xi/X)^{3/2}(\xi/X)^{-1/6}}{\int_0^X d\xi C_n^2(\xi)(1 - \xi/X)^{5/3} \int_0^\infty d\xi C_n^2(\xi)} \quad (25)$$

Second terms in Eqs.(24), (25) are similar and, hence, it is possible to obtain approximately the equal level of correction under these approaches [2, 12, 13]. Using the models of turbulent atmosphere [17, 18, 27] and applying the formulae (24), (25) from this report, possible to estimate the level of minimum of residual tip-tilt distortions with different LGS schemes.

One remark. In scheme [12,13] need two additional auxiliary telescopes to measure LGS image motion with accuracy 0.05". Hence, the approach from [2] is cheaper, due to usage only single large-scale telescope and two small-scale laser beam directors, but in second approach [12,13] need to use main large-scale telescope with laser beam setup and two auxiliary telescopes.

As it seems, that the most promising method of correction for general tilts of a wave front is employment of LGS adaptive optics systems with hybrid schemes and algorithms for tip-tilt correction [13, 30, 31].

1.9. References for Chapter1

1. R.Fugare, "Laser beacon adaptive optics", Optics & Photonics News, 14-19, June 1993.
2. R.Ragazzoni, "Absolute tip-tilt determination with laser beacons", Astron.Astrophys. **305**, L13-L16 (1996).
3. V.P.Linnik, "On the possibility of reducing the influence of atmospheric seeing on the image quality of stars", Optics and Spectroscopy, No.4, 401-402 (1957).
4. V.P.Lukin, *Atmospheric Adaptive Optics* (Novosibirsk, Nauka, 1986).
5. Meeting Digest of "Scintillation" International Meeting for Wave Propagation in Random Media, Conference Chairs V.I. Tatarskii, A.Ishimaru, University of Washington, Seattle, USA, August 1992.
6. V.M.Orlov, I.V.Samokhvalov, G.G.Matvienko, M.L.Belov, A.N. Kozhemyakov, *The elements of theory of wave scattering and optical ranging* (Novosibirsk, Nauka, 1982).
7. M.A. Kalistratova, A.I. Kon, "Fluctuations of arrival angle of light waves from extended source in turbulent atmosphere", Izv.VUZov. Radiofizika **9**, No.6, 1100-1107 (19).
8. V.P.Lukin, "Tracking of random angular displacements of optical beams", V All-Union Symposium on Laser Beam Propagation, Tomsk, Proc. Part II, 33-36, 1979.
9. V.P.Lukin, "Correction for Random Angular Displacements of Optical Beams", Kvant. Elektron. **7**, 1270-1279 (1980) [Sov.J.Quantum Electron. **10**, 727-732 (1980)].
10. V.I Klyatskin, *Statistical description of dynamical systems with fluctuating parameters* (M., Nauka, 1975).
11. V.I.Tatarski, *Wave Propagation in a Turbulent medium* (Dover, New York, 1961).

12. M.S.Belen'kii, "Full aperture tilt measurement technique with a laser guide star", in *Atmospheric Propagation and Remote Sensing IV*, editor J.C. Dainty, Proc.SPIE **2471**, 289-296 (1995).
13. M.S.Belen'kii, "Tilt angular correlation and tilt sensing techniques with a laser guide star" in *Optics in Atmospheric Propagation, Adaptive Systems, and Lidar Technique for Remote Sensing*, editor J.C. Dainty, Proc.SPIE, **2956**, 206-217 (1996).
14. V.P.Lukin, "Laser beacon and full aperture tilt measurement", in *Adaptive Optics* Vol.13 of OSA Technical Digest Series (Optical Society of America, Washington, D.C., 1996) Addendum AMB-35, pp.1-5.
15. V.P.Lukin, B.V.Fortes, "Comparison of Limit Efficiencies for Various Schemes of Laser Reference Star Formation", *Atm.Oceanic Optics* **10**, 34-41 (1997).
16. V.L.Mironov, V.V.Nosov, B.N.Chen, "Correlation of shifting of laser source optical images in the turbulent atmosphere", *Izv.VUZov. Radiofizika* **25**, No.12, 1467-1471(1982).
17. R.E.Good, R.R.Beland, E.A.Marphy, J.H.Brown, and E.M.Dewan, "Atmospheric models of optical turbulence" in *Modeling of the Atmosphere*, Proc.SPIE, **928**, 165-186(1988).
18. V.P.Lukin, "Investigation of some peculiarities in the structure of large-scale atmospheric turbulence", *Atm.Oceanic Opt.* **5**, 834-840 (1992).
19. V.P.Lukin, "Intercomparison of Models of the Atmospheric Turbulence Spectrum", *Atm.Oceanic Opt.* **6**, 1102-1107 (1993).
20. V.V.Voitsekhovich, "Outer scale of turbulence: comparison of different models", *J.Opt.Soc.Am.A.* **12**, 1346-1354 (1995).
21. T.S.McKechnie, "Atmopsheric turbulence and the resolution limit of large ground-based telescopes", *J.Opt.Soc.Am.A.* **9**, 1937-1954 (1992).

22. Site testing for the VLT (Very Large Telescope), Editor M.Sarazin, European Southern Observatory, VLT Report No.50, (1990).
23. N.Nakato, M.Iye, I.Yamaguchi, "Atmospheric turbulence of small outer scale", editor F.Merkle, European Southern Observatory Conference and Workshop Proceeding No.48, 521-524 (1993).
24. A.Agabi, J.Borgino, F.Martin, A.V.Tokovinin, and A.Ziad, "G.M.S: A grating scale monitor for atmospheric turbulence measurements. II. First measurements of the wave front outer scale at the O.C.A", Astron.Astrophys.Suppl. Ser. **109**, 557-562(1995).
25. J.Borgino, "Estimation of the spatial coherence outer scale relevant to long baseline interferometry and imaging in optical astronomy", Applied Optics**29**, No.13, 1863-1865(1990).
26. V.P.Lukin, E.V.Nosov, B.V.Fortes, "Effective outer scale of atmospheric turbulence", Atm.Oceanic Opt. **10**, 162-171 (1997).
27. M.A. Gracheva and A.S. Gurvich, "Simple models of turbulence", Izv. Akad. Nauk SSSR, Fiz. Atmos. i Okeana **16**, 1107-1111 (1980).
28. V.P.Lukin, "Models and measurements of atmospheric turbulence characteristics and their impact on AO design", OSA Technical Digest Series "Adaptive Optics"**13**, 150-152 (1996).
29. R.J.Sasiela, J.H.Shelton, "Transverse spectral filtering and Melin transform technique applied to the effect of outer scale on tilt and tilt anisoplanatism", J.Opt.Soc.Am.A. **10**, 646-660 (1993).
30. Yearly Status Report *Adaptive Optics at the Telescopio Nazionale Galileo*, edited by R.Ragazoni, August 1996.
31. V.P.Lukin, "Hybrid scheme of formation of laser reference star", Atm.Oceanic Opt. **10**, 975-979 (1997).

32. Coulman C.E., Vernin J., Coquegniot Y., and Caccia J.L., Outer scale of turbulence appropriate to modeling refractive-index structure profiles, Applied Optics, 1988, V.27, pp.155-160.
33. Site Testing for the VLT. Data Analysis Part I, 1987, European Southern Observatory, VLT Report No.55.
34. Site Testing for the VLT. Data Analysis Part II, 1990, European Southern Observatory, VLT Report No.60.

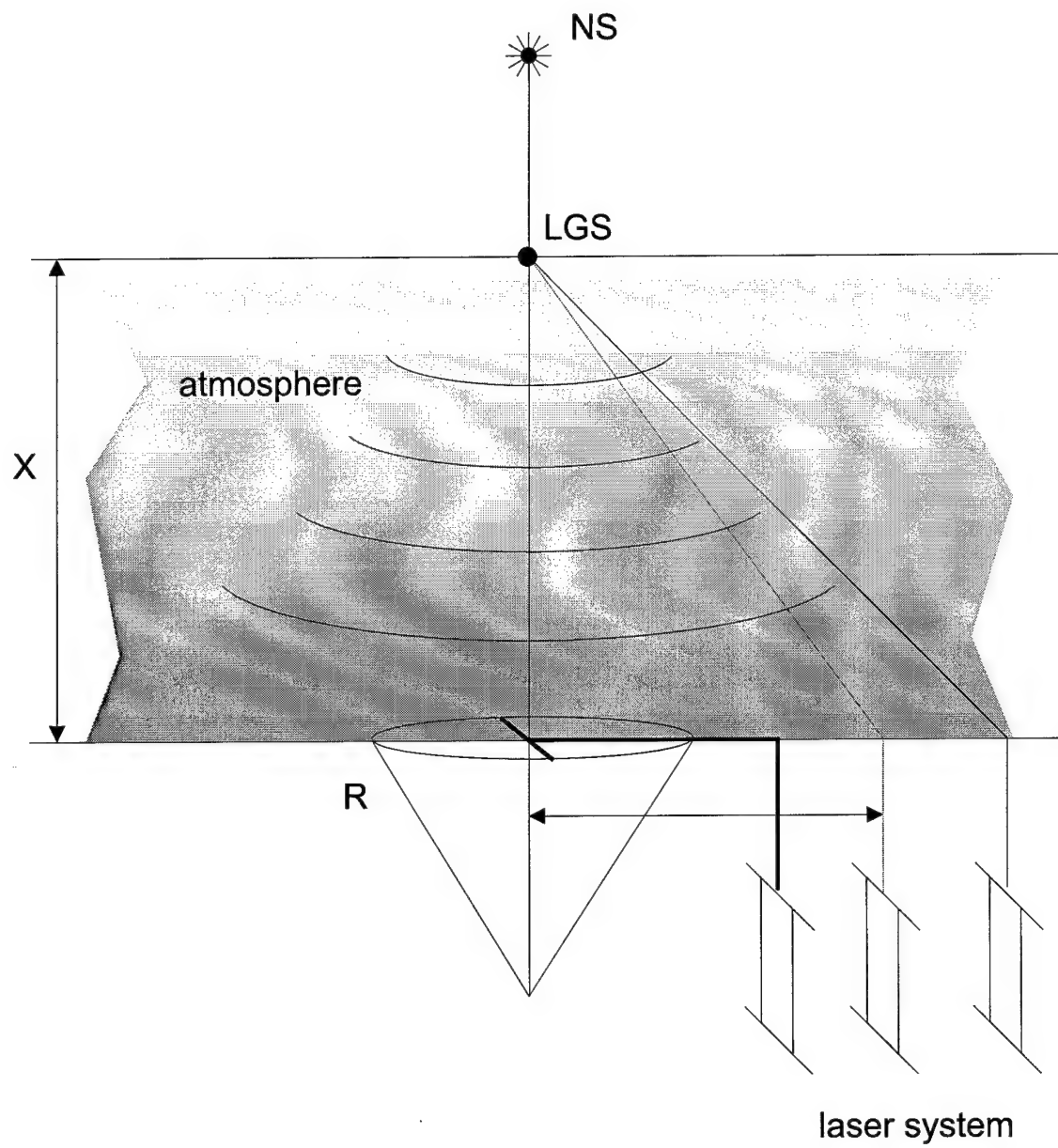


Fig.1.1. Laser guide star schemes formation.

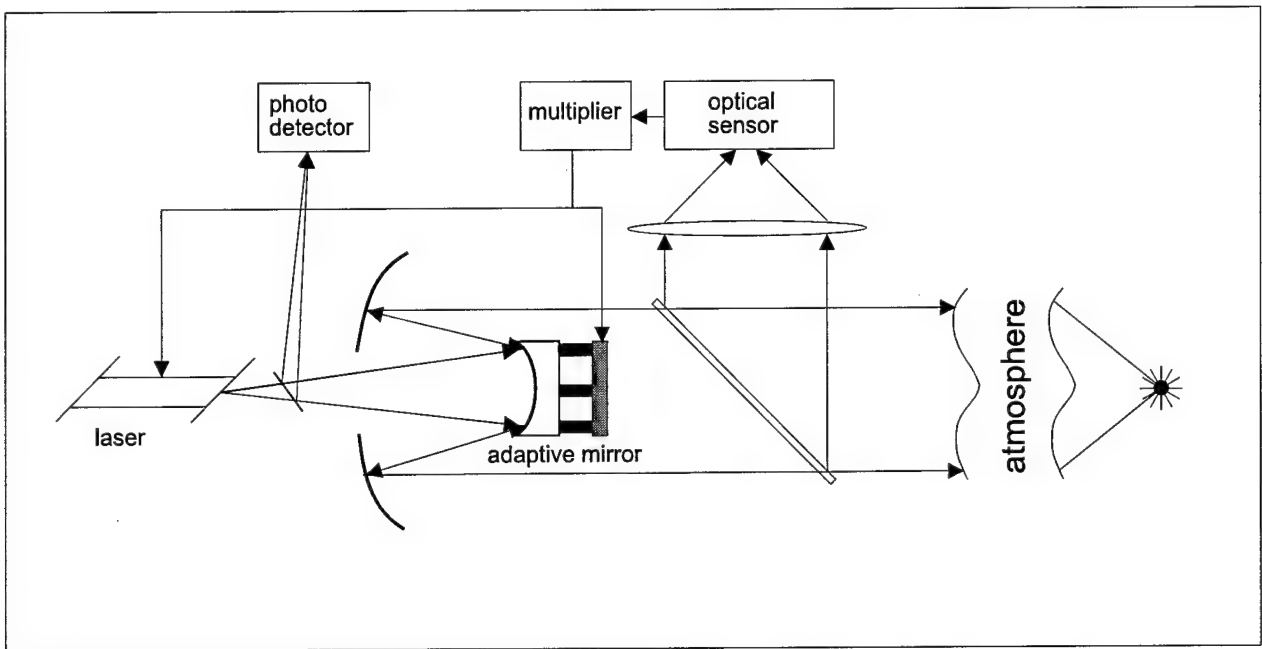


Fig.1.2. First approach for laser guide star formation through the atmosphere (1980). The elements of optical train are laser, adaptive mirror with main telescope mirror, additional lens, wave front sensor - optical measurer, electric multiplier for adaptive mirror control, photodetector.

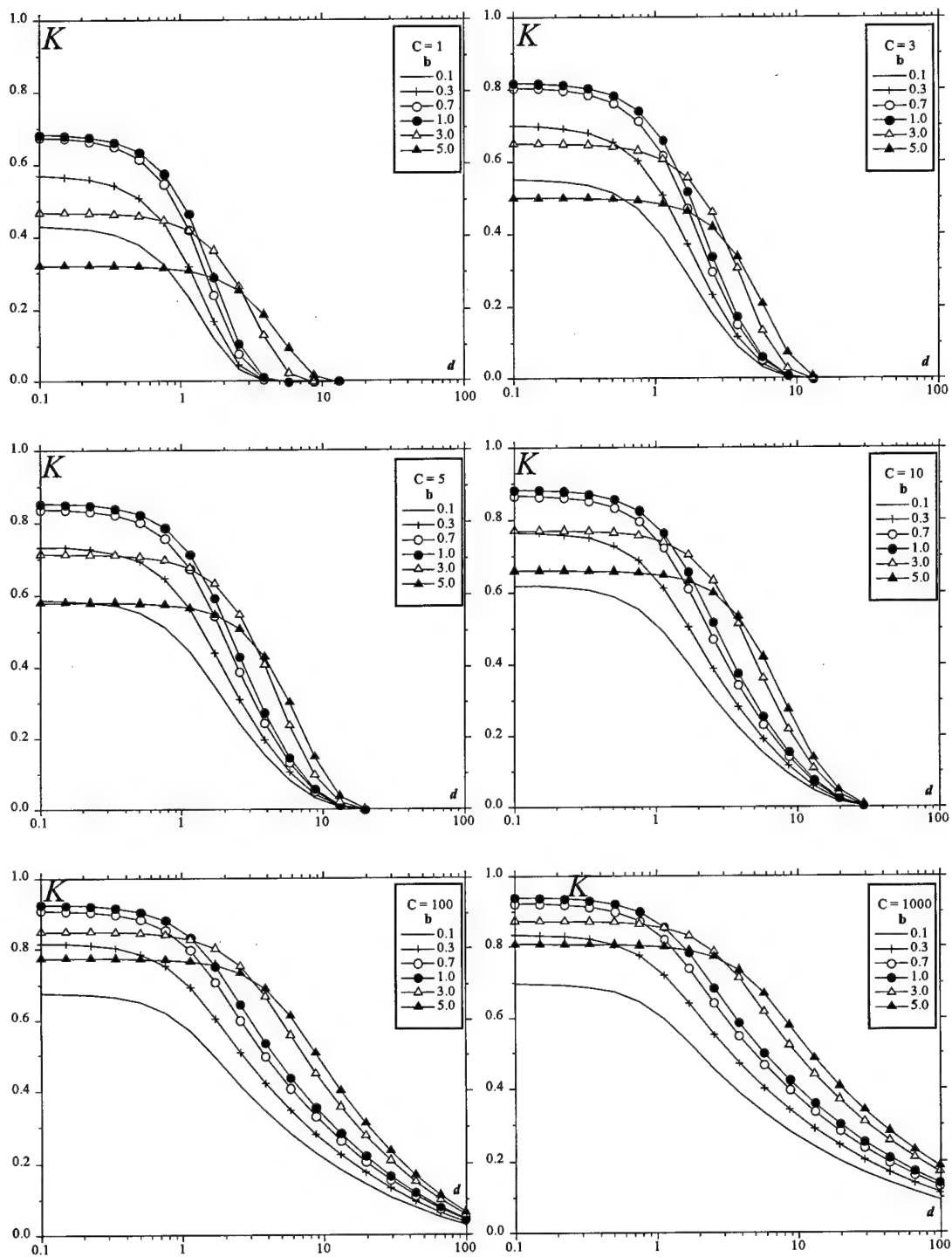


Fig.1.3. Correlation functions K from Eq.(1.14) for different sizes of outer scale of turbulence (parameter c), laser system aperture sizes (parameter b), and beacon altitude $X=10$ km.

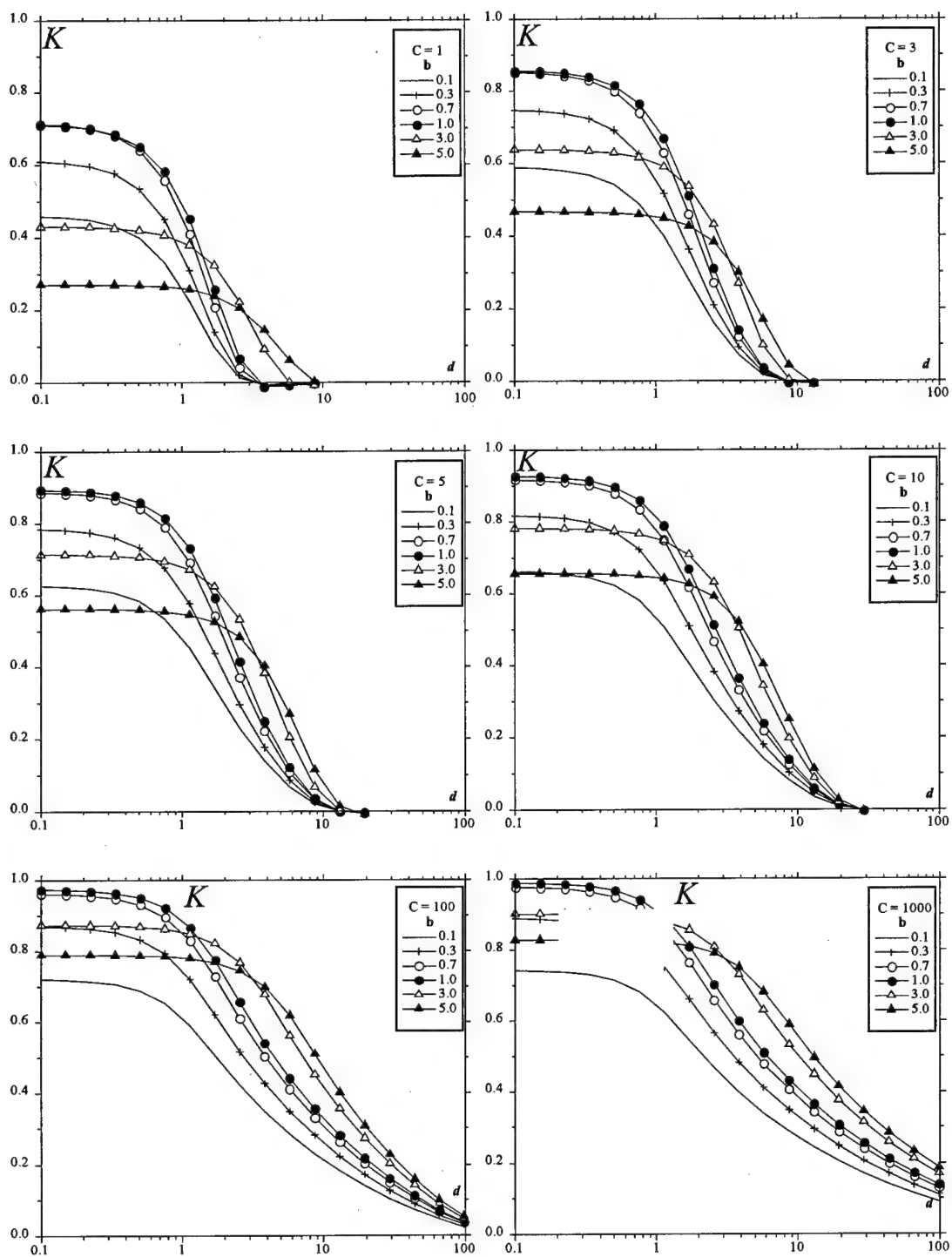


Fig.1.4. Correlation functions K from Eq.(1.14) for different sizes of outer scale of turbulence (parameter c), laser system aperture sizes (parameter b), and beacon altitude $X=100$ km.

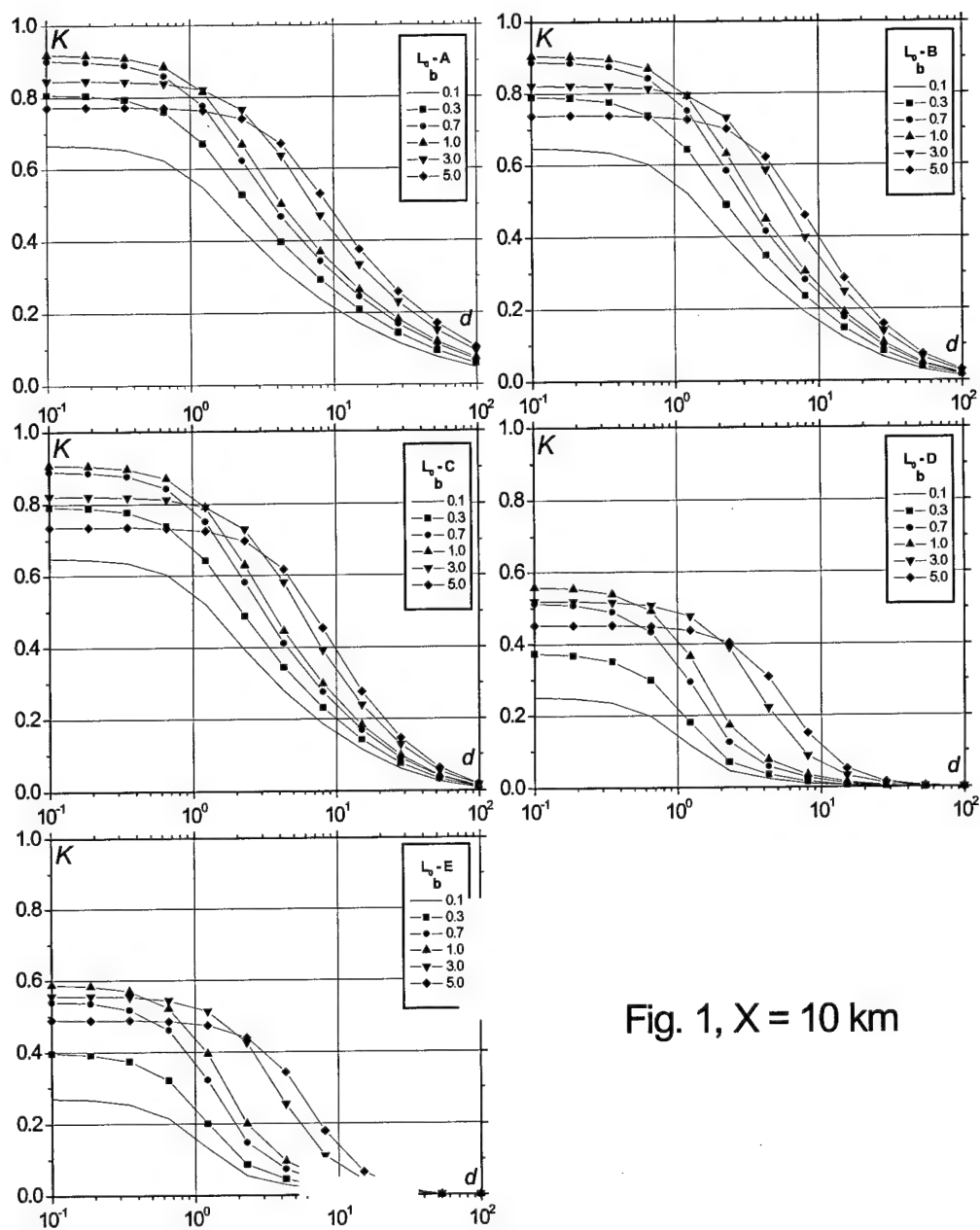


Fig. 1, $X = 10$ km

Fig.1.5. Correlation functions K from Eq.(1.14) for different models (models A, B, C, D, E) of outer scale of turbulence, laser system aperture sizes (parameter b), and beacon altitude $X=10$ km.

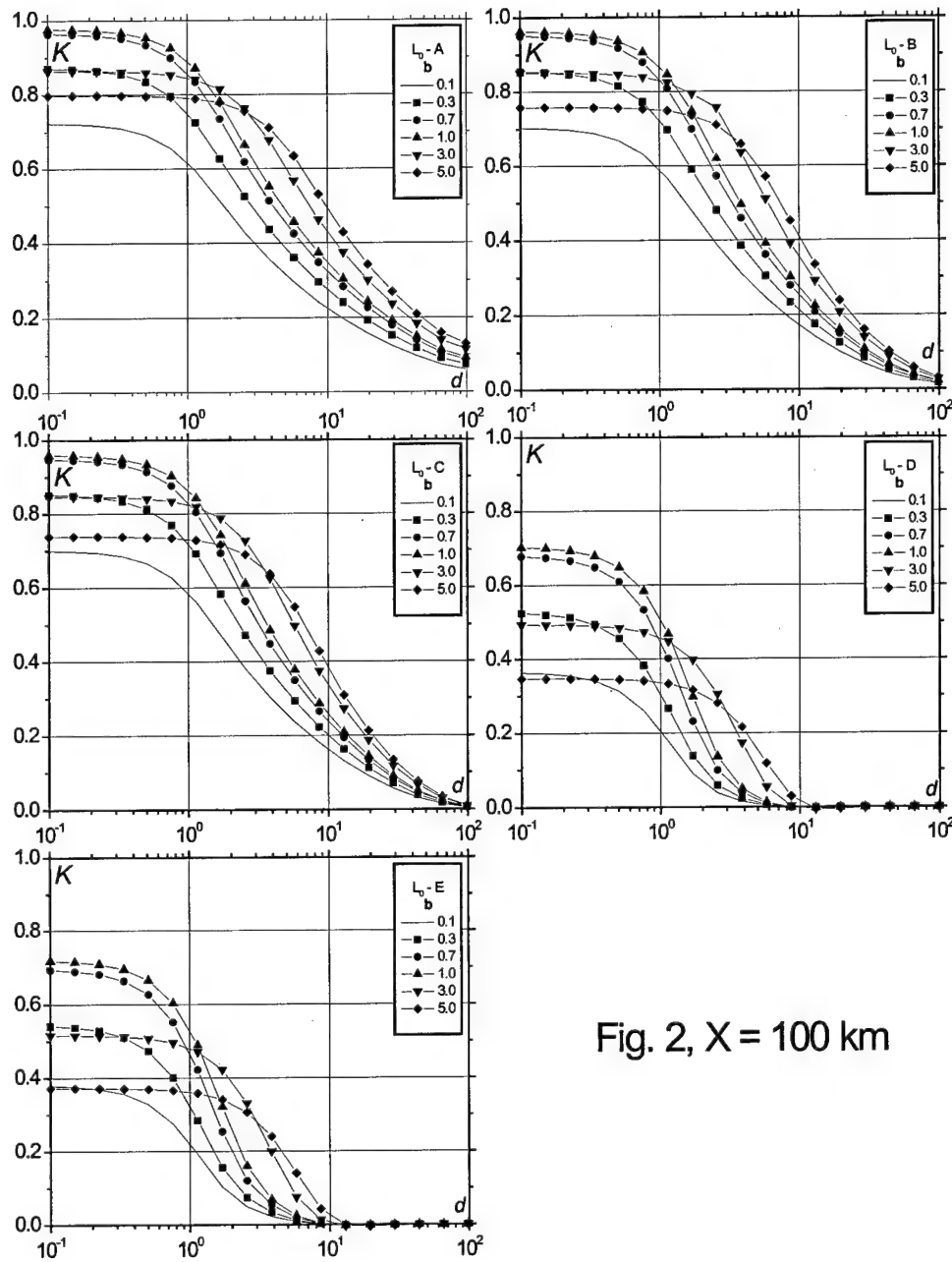


Fig. 2, $X = 100$ km

Fig.1.6. Correlation functions K from Eq.(1.14) for different models (models A, B, C, D, E) of outer scale of turbulence, laser system aperture sizes (parameter b), and beacon altitude $X=100$ km.

Table 1.1. Comparison of efficiency "optimal" and "traditional" algorithms of tilt correction for bistatical scheme.

X, km	b	Residual level of aberrations		A
		Optimal Algorithm	Traditional Algorithm	
8	0.3	0.640	1.291	-0.43
	0.5	0.603	1.105	-0.47
	0.7	0.578	0.999	-0.50
	1	0.552	0.899	-0.53
	2	0.500	0.736	-0.59
	3	0.471	0.656	-0.63
	5	0.434	0.570	-0.67
20	0.3	0.612	1.354	-0.42
	0.5	0.572	1.148	-0.46
	0.7	0.545	1.030	-0.49
	1	0.516	0.918	-0.52
	2	0.461	0.736	-0.58
	3	0.429	0.647	-0.62
	5	0.390	0.551	-0.66
40	0.3	0.602	1.406	-0.41
	0.5	0.561	1.187	-0.46
	0.7	0.533	1.062	-0.48
	1	0.504	0.944	-0.52
	2	0.447	0.751	-0.57
	3	0.414	0.657	-0.61
	5	0.374	0.556	-0.65
80	0.3	0.600	1.446	-0.41
	0.5	0.558	1.220	-0.45
	0.7	0.531	1.091	-0.48
	1	0.501	0.969	-0.51
	2	0.443	0.769	-0.57
	3	0.410	0.672	-0.60
	5	0.370	0.567	-0.64
100	0.3	0.599	1.455	-0.41
	0.5	0.588	1.227	-0.45
	0.7	0.530	1.097	-0.48
	1	0.500	0.974	-0.51
	2	0.443	0.774	-0.56
	3	0.410	0.676	-0.60
	5	0.370	0.570	-0.64

Chapter 2. New approaches for laser guide stars formation

2.1. Influence of temporal lag

Interesting possibility to correct for the general tilt of the wave front was put forward by R. Ragazzoni [1]. He proposed to take into account the fact that turbulent inhomogeneities are concentrated near the Earth's surface and the guide star is formed at altitude $h \gg h^*$, where h^* is the effective thickness of a turbulent atmosphere. So the vector characterizing a current angular position of a laser guide star at moment t is calculated as the follows

$$\vec{\varphi}_m(t) = \vec{\varphi}_c(t - \tau) + \vec{\varphi}_F^{sp}(t).$$

Here $\varphi_c(t)$ is a vector of a laser beam which is defined by atmospheric turbulence in the range of altitudes $h \ll c\tau/2$, where c is the velocity of light. If we disregard the temporal lag τ , in the monostatic scheme the laser guide star is motionless

$$\vec{\varphi}_m(t) = \vec{\varphi}_c(t) + \vec{\varphi}_F^{sp}(t) \equiv 0.$$

But if the temporal lag τ between the direct and reverse propagation exists, some angular oscillations of the guide star are present

$$\Delta\vec{\varphi}_m(t) = \vec{\varphi}_c(t) - \vec{\varphi}_c(t - \tau) = \vec{\varphi}_F^{bl3}(t - \tau) - \vec{\varphi}_F^{bl3}(t) \approx \tau \frac{\partial \vec{\varphi}_F^{bl3}(t)}{\partial t}.$$

Assuming the possibility to detect these small oscillations (in reality $\tau \approx 1\text{ms}$) we can expect that they are important for correction of temporal evolution of a natural star which is characterized by variation

$$\Delta\vec{\varphi}_F^{pl}(t) = \vec{\varphi}_F^{pl}(t - \tau) - \vec{\varphi}_F^{pl}(t).$$

The hypothesis of frozen turbulence is valid for small temporal scale t

$$\vec{\varphi}_F^{sp}(\vec{\rho}, t) = \vec{\varphi}_F^{sp}(\vec{\rho} + \mathbf{v}t, 0),$$

so

$$\frac{\partial \bar{\varphi}_F^{sp}}{\partial t} = \frac{\partial \bar{\varphi}_F^{sp}}{\partial \bar{\rho}} \frac{\partial \bar{\rho}}{\partial t} = \bar{v} \frac{\partial \bar{\varphi}_F^{sp}}{\partial \bar{\rho}},$$

where \bar{v} is a vector of effective wind velocity. As a result of this manipulations the standard deviation of temporal increments of angular spectrum of the guide star is

$$\langle (\Delta \bar{\varphi}_m)^2 \rangle = v^2 \tau^2 \langle \left(\frac{\partial \bar{\varphi}_F^{sp}}{\partial \bar{\rho}} \right)^2 \rangle.$$

Writing angular position of a point source in the turbulent atmosphere at the altitude x as

$$\bar{\varphi}_F^{sp} = -\frac{i}{\Sigma} \int_0^x d\xi \left(\frac{\xi}{x} \right) \iint d^2 n(\bar{\kappa}, \xi) \bar{\kappa} \iint_{\Sigma} d^2 \rho \exp(i \bar{\kappa} \bar{\rho} \left(\frac{\xi}{x} \right)),$$

we can calculate the standard deviation of these increments in time interval τ :

$$\langle (\Delta \varphi_m)^2 \rangle = (4\pi^2 0,033 \Gamma(\frac{1}{6})) 2^{1/6} R_0^{-1/3} \left\{ 1 - {}_1F_1\left(\frac{1}{6}, 1; -\frac{v^2 \tau^2}{2R_0^2}\right) \right\} \times \\ \int_0^x d\xi C_n^2(\xi) (1 - \xi/x)^{5/3}$$

Let us normalizing the obtained results by the standard deviation of a natural star oscillations

$$\langle (\varphi_F^{nm})^2 \rangle = (2\pi^2 0,033 \Gamma(\frac{1}{6})) 2^{1/6} R_0^{-1/3} \int_0^\infty d\xi C_n^2(\xi).$$

The ratio of these two variables is

$$\delta = \frac{\langle (\Delta \bar{\varphi}_m)^2 \rangle}{\langle (\bar{\varphi}_F^{pl})^2 \rangle} = \frac{2 \left\{ 1 - {}_1F_1\left(\frac{1}{6}, 1; -\frac{v^2 \tau^2}{2R_0^2}\right) \right\}}{\int_0^\infty d\xi C_n^2(\xi)} \int_0^x d\xi C_n^2(\xi) (1 - \xi/x)^{5/3} \approx \\ \approx \frac{1}{6} \frac{v^2 \tau^2}{R_0^2} \frac{\int_0^x d\xi C_n^2(\xi) (1 - \xi/x)^{5/3}}{\int_0^\infty d\xi C_n^2(\xi)}$$

Because $v\tau \ll R_0$ (for $\tau \approx 10^{-3}c$, $v = 10$ m/c, $R_0 = 4$ m, $\frac{v\tau}{R_0} \approx 10^{-2}$) the amplitude of angular oscillations for the guide star is hundred times less than the amplitude of a natural star image oscillations (corresponding angle is 1 - 2"). So to correct effectively for temporal shifts of a real star we need to have the possibility to measure small (about 0.01") angular shifts of the guide star image in short temporal intervals ($t < \tau \approx 10^{-3}c$)

It is also interesting to calculate correlation between temporal displacements of the real ($\Delta\phi_F^{pl}$) and artificial ($\Delta\phi_m^r$) stars in time interval τ . It can be shown that for $v\tau \ll R_0$ this correlation is equal to

$$\frac{\langle \Delta\phi_F^{pl} \Delta\phi_m^r \rangle}{\sqrt{\langle (\Delta\phi_F^{pl})^2 \rangle} \sqrt{\langle (\Delta\phi_m^r)^2 \rangle}} \approx \frac{\int_0^x d\xi C_n^2(\xi)(1 - \xi/x)^2(1 + (1 - \xi/x)^2)^{-7/6}}{\sqrt{\int_0^x d\xi C_n^2(\xi)(1 - \xi/x)^{5/3}} \sqrt{\int_0^\infty d\xi C_n^2(\xi)}}.$$

The correlation depends on the altitude of the beacon and on the altitude profile of turbulence intensity. With decreasing of x this correlation approaches unity.

So with the considered scheme which allows for temporal evolution of oscillations the angular displacements of the natural star are possible to correct for, but to realize this scheme one needs the efficient wave front detector.

2.2. DISTINCTIONS AND COMMON FEATURES OF TWO SCHEMES OF A LASER GUIDE STAR FORMING

Application of adaptive correction in a ground based telescope to improve image quality is possible if a laser guide star is formed in the atmosphere. But it is difficult to correct general tilt of a wavefront using a signal from a laser star because the required information could not be obtained directly from measurements of a star dither.

Roberto Ragazzoni made an attempt to consider systematically various approaches to the problem of a wavefront general tilt detection in adaptive optics system operating with the use of the signal from an artificial star (Refs.2-5). Some methods to solve this problem can be found in scientific publications but all of them increase complexity of the system technical realization. The following methods can be listed as examples: simultaneous measurements of general angular dither of a bright natural star and a guide star [4, 5], employment of two-color laser guide stars [6], usage of auxiliary telescopes [7, 8], and laser sources [9-11]. In the second two cases a laser star could not be considered as a point source.

Optical schemes with auxiliary telescopes or laser sources are simple enough. Roberto Ragazzoni describes two schemes of this type in Ref.6. In this report they are presented in Figs.2.1a and 2.1b.

In Ref.5 Ragazzoni even used term «symmetry» to underline the equivalence of efficiency of these two schemes from the point of view of local tilt correction. In the present part of report we will show that the exact equivalence («symmetry») is absent.

The detected informative signal determines an angular position of a laser guide star image in a focal plane of the telescope-sensor. This signal in a scheme (a) is described by the following equation

$$\vec{\varphi}_a = \vec{\varphi}_{lb}(\vec{\rho}_0) + \vec{\varphi}_F^{\infty}(0),$$

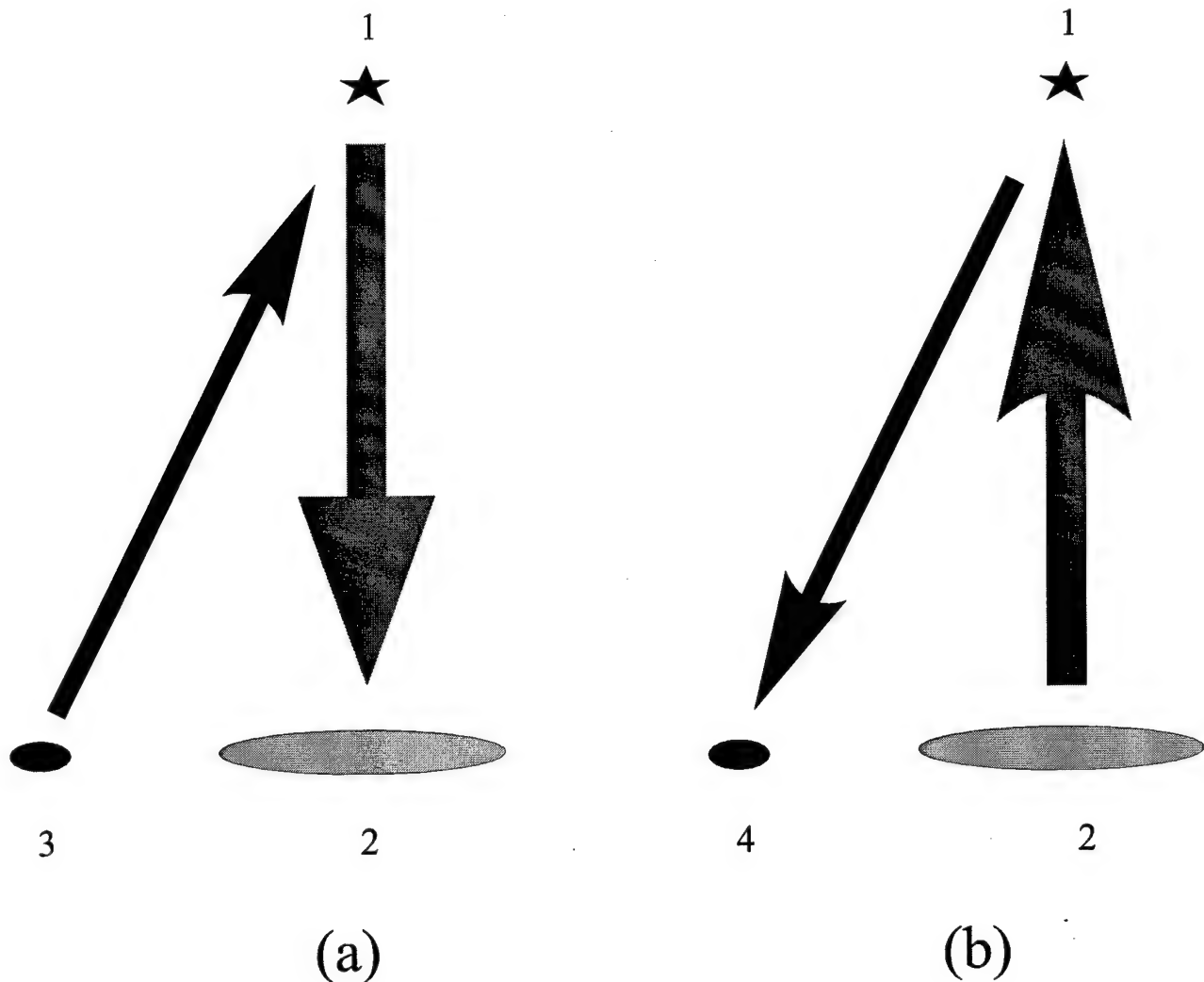


Fig. 2.1. Two schemes of a laser guide star forming: with the use of auxiliary laser illuminator (a), and with the use of auxiliary telescope (b). The following objects are drawn here: a laser guide star generated in the atmosphere (1), an aperture of the main telescope (2), an aperture of auxiliary laser illuminator (3), an aperture of auxiliary telescope (4). Axes of the main and auxiliary telescopes are placed on some distance from each other.

In scheme (b) slightly different equation is used:

$$\bar{\varphi}_b = \bar{\varphi}_{lb}(0) + \bar{\varphi}_F^{\text{ss}}(\bar{\rho}_0).$$

Here $\bar{\varphi}_{lb}(\bar{\rho}_0)$ are random angular displacements of the energy centroid for a laser beam focused on altitude X. The beam is formed by an auxiliary laser generator with the optical axis shifted from the origin on vector $\bar{\rho}_0$ and slanted from the zenith on angle - $\bar{\rho}_0 / X$, $\bar{\varphi}_{lb}(0)$ are random angular displacements of the energy centroid for a laser beam focused on altitude X. The beam is formed by the main telescope the optical axis of which is pointed exactly at the zenith, $\bar{\varphi}_F^{\text{ss}}(\bar{\rho}_0)$ is a vector characterizing random tilts of the wavefront in observations of the secondary source dither in the focal plane of the main telescope. The secondary source is formed at altitude X and its image oscillates in the focal plane due to light refraction on atmospheric inhomogeneities.

Let us assume that apertures of the main and auxiliary telescopes are placed so that correlation functions $\langle \bar{\varphi}_{lb}(\bar{\rho}_0) \bar{\varphi}_F^{\text{ss}} \rangle$ and $\langle \bar{\varphi}_{lb}(0) \bar{\varphi}_F^{\text{ss}}(\bar{\rho}_0) \rangle$ are equal to zero (Refs.10, 11, 20).

These schemes are intended to solve the problem of correction of random tilts of wavefront for a natural star, presuming that a natural star and artificial one have the same zenith distance and the same azimuth angle, i.e., to correct a random function $\varphi_F^{\text{pl}}(0)$. It is known that a natural star forms a plane wavefront in a focal plane of a telescope.

In this report we will use an algorithm of optimal correction [10, 11, 20] insuring the lowest possible level of residual errors. For the two schemes of artificial star forming let us evaluate the ratio of this level to the variance of uncorrected dither of a natural star image. The variance for the scheme (a) is represented by the formula (optimal algorithm of correction [15-20]):

$$\langle \beta^2 \rangle_a = \langle (\bar{\varphi}_F^{\text{pl}} - \bar{\varphi}_a)^2 \rangle / \langle (\bar{\varphi}_F^{\text{pl}})^2 \rangle = 1 - \frac{\langle \bar{\varphi}_F^{\text{pl}} \bar{\varphi}_a \rangle^2}{\langle (\bar{\varphi}_F^{\text{pl}})^2 \rangle \langle (\bar{\varphi}_a)^2 \rangle}$$

here

$$\langle (\bar{\varphi}_a)^2 \rangle = \langle \varphi_{lb}^2 \rangle + \langle (\varphi_F^{\text{ss}})^2 \rangle, \quad \langle \bar{\varphi}_F^{\text{pl}}(0) \bar{\varphi}_a \rangle = \langle \bar{\varphi}_F^{\text{pl}}(0) \varphi_F^{\text{ss}}(0) \rangle.$$

And for the scheme (b)

$$\langle \beta^2 \rangle_b = \langle (\bar{\varphi}_F^{pl} - \bar{\varphi}_b)^2 \rangle / \langle (\bar{\varphi}_F^{pl})^2 \rangle = 1 - \frac{\langle \bar{\varphi}_F^{pl} \bar{\varphi}_b \rangle^2}{\langle (\bar{\varphi}_F^{pl})^2 \rangle \langle (\bar{\varphi}_b)^2 \rangle},$$

where

$$\langle (\bar{\varphi}_b)^2 \rangle = \langle \varphi_{lb}^2 \rangle + \langle (\varphi_F^{ss})^2 \rangle,$$

$$\langle \bar{\varphi}_F^{pl}(0) \bar{\varphi}_b \rangle = \langle \bar{\varphi}_F^{pl}(0) \bar{\varphi}_{lb}(0) \rangle.$$

All in all, relative efficiency of correction (schemes (a) and (b))

$$\langle \beta^2 \rangle_a = 1 - \frac{\langle \bar{\varphi}_F^{pl}(0) \bar{\varphi}_F^{ss}(0) \rangle^2}{\langle (\bar{\varphi}_F^{pl})^2 \rangle [\langle \varphi_{lb}^2 \rangle + \langle (\varphi_F^{ss})^2 \rangle]}, \quad (2.1)$$

$$\langle \beta^2 \rangle_b = 1 - \frac{\langle \bar{\varphi}_F^{pl}(0) \bar{\varphi}_{lb}(0) \rangle^2}{\langle (\bar{\varphi}_F^{pl})^2 \rangle [\langle \varphi_{lb}^2 \rangle + \langle (\varphi_F^{ss})^2 \rangle]}. \quad (2.2)$$

Only numerators $\langle \bar{\varphi}_F^{pl}(0) \bar{\varphi}_F^{ss}(0) \rangle^2$ and $\langle \bar{\varphi}_F^{pl} \bar{\varphi}_{lb} \rangle^2$ of these two formulas are different and, consequently, the variances are different of residual angular fluctuations. With the use of the following representation

$$\langle \bar{\varphi}_F^{pl}(0) \bar{\varphi}_{lb}(0) \rangle = K(0) \sqrt{\langle \varphi_{lb}^2 \rangle \langle (\bar{\varphi}_F^{pl})^2 \rangle}$$

Eq.2.2 can be simplified. As a result we obtain

$$\langle \beta^2 \rangle_b = 1 - \frac{K^2(0)}{[1 + \langle (\varphi_F^{ss})^2 \rangle / \langle \varphi_{lb}^2 \rangle]}. \quad (2.3)$$

here $K(0)$ is mutual correlation in the focal plane of a telescope between angular displacements of the focused beam centroid and that for a plane wave (see Figs.1.3 -1.6). The results of function $K(0)$ calculations were presented in Ref.20. Other quantities entering Eq.2.3 were also calculated earlier (Refs.15 - 19). For example

$$\begin{aligned} \langle \varphi_{LB}^2 \rangle = & (2\pi^2 0,033 \tilde{A}(\frac{1}{6})) 2^{1/6} R_0^{-1/3} \int_0^X d\xi C_n^2(\xi) \{ [b^2(1 - \xi/X)^2]^{-1/6} - \\ & - [b^2(1 - \xi/X)^2 + 4c^2]^{-1/6} \} \end{aligned} \quad (2.4)$$

here R_0 is the radius of the main telescope aperture, X is altitude of a laser guide star forming, $C_n^2(\xi)$ is altitude distribution of the structure function of the turbulent atmosphere index of refraction, $b = a_0 / R_0$, a_0 is a size of a laser beam focused on distance X , $c = \kappa_0^{-1} R_0^{-1}$, $\kappa_0^{-1}(\xi)$ is the outer scale of turbulence on a current altitude ξ ,

$$\langle (\varphi_F^{\text{ss}})^2 \rangle = \langle (\varphi_F^{\text{sp}})^2 \rangle \left(\frac{a_{\text{igs}}}{R_0} \right)^{-1/3} \frac{\int_0^X d\xi C_n^2(\xi) (1 - \xi/X)^2 (\xi/X)^{-1/3}}{\int_0^X d\xi C_n^2(\xi) (1 - \xi/X)^{5/3}}. \quad (2.5)$$

These equation is obtained by summarizing the results of Refs.10 and 20 and published in Ref.21.

In Eq.2.5 the variance of the secondary source dither $\langle (\varphi_F^{\text{ss}})^2 \rangle$ is the product of the variance $\langle (\varphi_F^{\text{sp}})^2 \rangle$ of dither of a point reference source image located on altitude X , averaging coefficient $(a_{\text{igs}} / R_0)^{-1/3}$, where a_{igs} is a visible size of a reference star, and a ratio of two integrals

$$\frac{\int_0^X d\xi C_n^2(\xi) (1 - \xi/X)^2 (\xi/X)^{-1/3}}{\int_0^X d\xi C_n^2(\xi) (1 - \xi/X)^{5/3}}. \quad (2.6)$$

It should be noted that the effect of the last two factors in Eq.2.5 on the result is quite opposite. The factor $(a_{\text{igs}} / R_0)^{-1/3}$ lessens the variance $\langle (\varphi_F^{\text{sp}})^2 \rangle$, while the ratio of the two integrals increases with increase of altitude. There are a linear relation between such quantities as a visible size of a reference star a_{igs} and the altitude of a reference star forming X . The notation $l(X)$ is introduced for the ratio of two integrals (2.6):

$$\frac{\int_0^X d\xi C_n^2(\xi)(1 - \xi/X)^2(\xi/X)^{-1/3}}{\int_0^X d\xi C_n^2(\xi)(1 - \xi/X)^{5/3}} = 1(X). \quad (2.7)$$

The dependence of $1(X)$ on the altitude is represented in Table 2.1 for a model of $C_n^2(\xi)$ borrowed from Ref.22. Table 2.1 consists of three parts corresponding to «the worst», «the best», and «medium» characteristics of atmospheric turbulence. From these data the simple formula can be drawn describing residual dither of a natural star image

$$\langle \beta^2 \rangle_b = 1 - \frac{K^2(0)}{1 + \frac{R_0^{-1/3}}{a_0^{-1/3}} \left(\frac{a_{lgs}}{R_0} \right)^{-1/3} 1(X)} = 1 - \frac{K^2(0)}{1 + (a_{lgs}/a_0)^{-1/3} 1(X)}. \quad (2.8)$$

The value of $1(X)$ was obtained equal to 0.7 and correlation coefficient $K(0)=0.9$ in estimations of function $\langle \beta^2 \rangle_b$ performed with the following set of parameters $a_{lgs} = 10^3$ m, $a = 10^0$ m, $R_0 = 10$ m, and $c = \kappa_0^{-1} R_0^{-1} = 5-10$ and with the reference star located on the altitude of 90-100 km. So

$$\langle \beta^2 \rangle_b = 1 - 0.81/[1+0.7]=0.52,$$

that means the two-times decrease of the variance of a natural star dither for correction performed according the scheme (b).

In the case of the scheme (a) employment the variance of the residual angular dither is expressed by the equation

$$\langle \beta^2 \rangle_a = 1 - \frac{\langle \vec{\varphi}_F^{pl} \vec{\varphi}_F^{ss} \rangle^2}{\langle (\vec{\varphi}_F^{pl})^2 \rangle [\langle \varphi_{lb}^2 \rangle + \langle (\vec{\varphi}_F^{ss})^2 \rangle]}.$$

Performing the same mathematical manipulation as with Eqs.(2.7) and (2.8) let us write the function of mutual correlation in the form

$$\langle \vec{\varphi}_F^{pl} \vec{\varphi}_F^{ss} \rangle = K_1(0) \sqrt{\langle (\vec{\varphi}_F^{pl})^2 \rangle \langle (\vec{\varphi}_F^{ss})^2 \rangle}. \quad (2.9)$$

After that we obtain

$$\langle \beta^2 \rangle_a = 1 - \frac{K_1^2(0)}{[1 + \langle \varphi_{lb}^2 \rangle / \langle (\bar{\varphi}_F^{ss})^2 \rangle]} \quad (2.10)$$

Here the correlation coefficient expressed as

$$K_1(0) = \langle \bar{\varphi}_F^{pl} \bar{\varphi}_F^{ss} \rangle / \sqrt{\langle (\bar{\varphi}_F^{pl})^2 \rangle \langle (\bar{\varphi}_F^{ss})^2 \rangle} \quad (2.11)$$

More through analysis of mutual correlation function (2.9) is needed. As a result of calculations of this function analogous with calculations of $K(0)$ we obtain

$$\langle \bar{\varphi}_F^{pl} \bar{\varphi}_F^{ss} \rangle = \langle \bar{\varphi}_F^{pl} \bar{\varphi}_F^{sp} \rangle (a_{lgs} / R_0)^{-1/6} 2(X).$$

The function $2(X)$ is represented in the third column of Table 2.1. All in all, for the scheme (a)

$$\langle \beta^2 \rangle_a = 1 - \frac{K_1^2(0)(a_{lgs} / R_0)^{-1/3} 2(X)}{b^{-1/3} + (a_{lgs} / R_0)^{-1/3} 1(X)} \quad (2.12)$$

With the same parameters as were used in calculations of $\langle \beta^2 \rangle_b$ (Eq.2.8). For the altitude $X = 90 - 100$ km of a laser guide star forming we obtain $X(2) = 6$. In this problem the main telescope was used with the aperture radius $R = 8$ m and an auxiliary telescope-illuminator with size $a = 1$ m, so $b = 1/8$, and a visible size of a reference star a_{lgs} was assumed to be equal to 1 km.

So the level of residual angular distortions of a star image dither is the following

$$\langle \beta^2 \rangle_a = 1 - 0.793(6/7) / [0.5 + 0.7] = 0.43.$$

We can conclude that the scheme (a) insures lower level of residual distortions as compared with the scheme (b), so this scheme is more promising. From the other hand, technical realization of the scheme (b) is more simple. In the scheme (a) behind the main telescope one or two auxiliary telescopes should be used, while in (b) only a laser illuminator is needed and this device is more cheap.

Summing the result we should point out that the symmetry is absent in the two considered schemes (Refs.5, 7-9, and 11) of the laser guide star forming. The objective of these two projects was the generation of a guide star with finite dimensions rather than a point source. But according to the estimations presented in Ref.23 considerable decrease of angular fluctuations and an image dither was not achieved in the both schemes.

Table 2.1.

 $\frac{2}{n}(\xi)$ is «the mean»

$X, \text{ km}$	$1(X)$	$2(X)$
1	2.260	0.863
10	3.671	2.650
20	4.329	3.469
30	4.826	4.024
40	5.240	4.455
50	5.602	4.815
60	5.921	5.134
70	6.211	5.415
80	6.472	5.666
90	6.720	5.897
100	6.947	6.112

 $\frac{2}{n}(\xi)$ is «the best»

$X, \text{ km}$	$1(X)$	$2(X)$
1	2.107	0.915
10	3.661	2.884
20	4.452	3.740
30	5.000	4.319
40	5.444	4.780
50	5.826	5.161
60	6.167	5.493
70	6.468	5.793

80	6.747	6.062
90	7.005	6.310
100	7.242	6.537

$\frac{2}{n}(\xi)$ is «the worst»

$X, \text{ km}$	$1(X)$	$2(X)$
1	2.411	0.618
10	3.292	1.999
20	3.692	2.717
30	4.073	3.194
40	4.406	3.561
50	4.697	3.865
60	4.957	4.133
70	5.194	4.367
80	5.410	4.578
90	5.615	4.771
100	5.802	4.949

References to Chapter 2

1. Roberto Ragazzoni, Propagation delay of a laser beacon as a tool to retrieve absolute tilt measurements. //The Astronomical Journal, **465**, L73-L75, 1996.
2. S.Esposito and R.Ragazzoni, «Techniques for LGS tilt retrieval: a numerical comparison», in the book «Adaptive Optics at the Telescopio Nazionale Galileo», ed. by R.Ragazzoni, pp.1 - 20, December 1997.
3. S.Esposito and R.Ragazzoni, «Non conventional techniques for LGS tilt retrieval: an update», in the book «Adaptive Optics at the Telescopio Nazionale Galileo», ed. by R. Raggazoni, December 1997.
4. R.Raggazoni, «Robust tilt determination from Laser Guide Star using a combination of different techniques». //Astronomy and Astrophysics, 319, L9 - L12 (1997).
5. R.Raggazoni, «Laser guide star advanced concept: tilt problem», in the book «Adaptive Optics at the Telescopio Nazionale Galileo», ed. by R. Raggazoni, December 1997.
6. R.Foy, A.Migus, et al., «The polychromatic artificial sodium star: a new concept for correction the atmospheric tilt». //Astronomy and Astrophysics, 111, pp. 569 - 578 (1995).
7. R.Raggazoni, S.Esposito, and E.Marchetti, «Auxiliary telescopes for the absolute tilt-tip determination of a laser guide star». //Mon. Not. R. Astron. Soc. 1995. Vol.276, pp.L76 - L78.
8. M.Belen'kii, «Full aperture tilt measurement technique with a laser guide star»./Proc. SPIE. 1995. Vol.2471, pp.289 - 296.
9. M.Belen'kii, «Tilt angular correlation and tilt sensing technique with a laser guide star». //Proc. SPIE. 1996. Vol.2956, pp.206 - 217.
10. R.Raggazoni, «Absolute tilt-tip determination with laser beacons» //Astron. Astrophys. 1996. Vol.305, p.L13 - L16.

11. V.Lukin and V.Matyukhin, «Adaptive correction of an image». //Kv. Electron. 1983. Vol.10, pp.2465 - 2473.
12. V.Lukin, «Atmospheric Adaptive Optics», Nauka Publishers, Novosibirsk, 1986, 286 pp.
13. V.Lukin, «Limited resolution of adaptive telescope with the use of an artificial star». //Proc. ICO - 16, «Active and Adaptive Optics», 1993. P.521 - 524.
14. V.Lukin and B.Fortes, «Efficiency of adaptive correction of images in a telescope using an artificial star». //OSA Tech. Digest. 1995. Vol.23, pp.192 - 193.
15. V.Lukin, «Laser beacon and full aperture tilt measurements». //Adaptive Optics Techn. Digest Series, 1996, Vol.13, pp.351 - 355.
16. V.Lukin, «Adaptive forming of beams and images in the atmosphere». //Atmos. Ocean. Opt. 1995. Vol.8, pp.301 - 341.
17. V.Lukin and B.Fortes «Limits and possibilities of application for various methods of laser guide star forming». //Atmos. Ocean. Opt. 1997. Vol.10, pp.34 - 41.
18. V.Lukin «Hybrid scheme of a laser guide star forming». //Atmos. Ocean. Opt. 1997. Vol.10, pp.975 - 979.
19. V.Lukin, «Monostatic and bistatic schemes and optimal algorithms for tilt correction in ground-based adaptive telescope». //Appl. Opt., 20 July, 1998.
20. M.Kallistartova and A.Kon, «Fluctuations of an incidence angle for light waves from a finite-size source in a turbulent atmosphere». //Izv. Vyssh. Uchebn. Zaved. SSSR, Ser. Radiofiz. 1996. Vol.9, No.6, pp.1100-1107.
21. M.Gracheva and A.Gurvich «A simple model of turbulence». //Izv. Akad. Nauk SSSR, Fiz. Atmos. Okeana. 1980. Vol.16, pp.1107 - 1111.
22. V.Lukin «Problems of laser guide star forming». //Atmos. Oceanic Ops. 1998. Vol.11, No.5, pp.1 - 13.

CHAPTER 3. PHASE CORRECTION OF AN IMAGE TURBULENT BROADENING UNDER CONDITIONS OF STRONG INTENSITY FLUCTUATIONS

3.1. Introduction

Atmospheric turbulence induces phase distortions of an optical wave which transform into amplitude distortions in the wave cross sections [1]. On a long path intensity fluctuations become so strong that points appear with zero intensity. In such points wavefront distortions are of a spiral structure. Singularities of this type are called wavefront dislocations [2]. Development of wavefront dislocations was considered theoretically by the authors of Ref.3. Considerable loss in efficiency of an adaptive optics system (AOS) employing a continuous surface mirror and Hartmann-Shack sensor was also registered experimentally in the region of strong fluctuations [4]. These results confirm conclusions of numeric experiments [5]. Problems of adaptive system development intended for compensation of turbulent distortions are discussed frequently in modern scientific literature. But it is not clear yet how the principal characteristics of an adaptive optics system such as the minimum size of an element and allowed temporal lag of correction are influenced by intensity fluctuations. Many questions concerning a wavefront sensor design and phase reconstruction algorithm are still without answers.

In the present report these problems are considered in the case of a plane wave propagating in a randomly inhomogeneous medium with Kolmogorov spectrum of fluctuations. Such simplifications allow one to «purify» the problem. In reality, the performance of an adaptive optics system is influenced by many other factors [6].

The results of numeric experiments presented in this report show that requirements to the element size and speed of adaptive control remain the same in the region of strong fluctuations as in the presence of the weak ones. Particularly, the size of an element of

segmented mirror corresponds to the Fried's radius r_0 and minimum lag in a loop of adaptive control is equal to convection time r_0/V where V is speed of turbulent inhomogeneities transportation. Under these conditions the Strehl number S is not less than 0.5.

The efficiency of a local tilt sensor in the region of strong fluctuations is also estimated in the present report. We applied an algorithm according to which the wavefront with spiral singularities is reconstructed using phase differences and discrepancy of phase approximation due to errors of measurements is minimized [12, 13]. Moreover, the precision of computation of phase differences with the use of local tilts is considered. So the principal requirements to such sensors of local tilts as a shearing interferometer or Hartmann-Shack sensor is formulated.

3.2. The setting of the problem for numeric simulation

The problem of propagation of optical radiation in a turbulent medium is considered in the following setting. A plane wave travels through a homogeneous turbulent layer with thickness L (Fig. 3.1). The layer is characterized by intensity of turbulent fluctuations C_n^2 of the index of refraction n . The wave length is designated here as λ , and the wave number as $k = 2\pi/\lambda$. An adaptive optics system and a thin convergent lens is placed at the far end of the layer. The diameter of the system aperture is D . These parameters determine two scales of the problem, namely, a transverse scale, i.e., Tatarskii's coherence radius r_0 or Fried radius r_0

$$r_0 = (0.489k^2C_n^2L)^{-3/5}, \quad \rho_0 = (1.46k^2C_n^2L)^{-3/5}, \quad r_0/\rho_0 = (1.46/0.489)^{3/5} \approx 1.93 \quad (3.1)$$

and a scale in the direction of the wave propagation $L_d = kr_0^2$ (turbulent length of diffraction). Normalized aperture diameter D/r_0 and path length $q = L/L_d$ are two

dimensionless parameters of the problem. The path length q is related with the scintillation index b_0^2 by

$$\beta_0^2 = 1.24 C_n^2 k^{7/6} L^{11/6} = \frac{1.24}{1.46} \left(\frac{L}{k \rho_0^2} \right)^{5/6} = \frac{1.24}{0.489} \left(\frac{L}{k r_0^2} \right)^{5/6} = 2.54 q^{5/6}, \quad (3.2)$$

written in Rytov approximation.

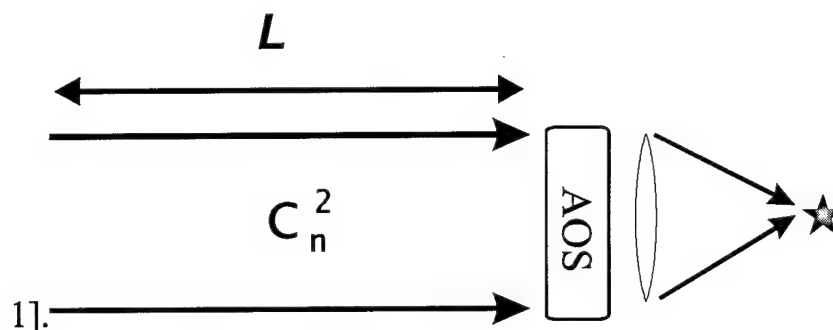


Fig. 3.1. Schematics of a wave propagation.

It should be noted that the turbulent length of diffraction is expressed here through Fried coherence length r_0 . To express it through Tatarskii's radius one should employ Eqs. 3.1 and 3.2.

Propagation of the plane wave is described by the parabolic equation

$$2ik \frac{\partial U}{\partial z} = \left(\frac{\partial^2}{\partial x^2} + \frac{\partial^2}{\partial y^2} + 2k^2(n-1) \right) U. \quad (3.3)$$

The complex amplitude U entering this equation is related with the scalar intensity of the field by the following equation $E(x,y,z) = U(x,y,z) \exp\{ikz - i\omega t\}$. Here $n-1 \ll 1$ are random fluctuations of the index of refraction $n(x,y,z)$, ω is a frequency of electromagnetic oscillations. The equation is supplemented with boundary conditions for a plane wave propagating along OZ-axis

$$(x, y, z = 0) = 1 \quad (3.4)$$

and solved numerically according the splitting algorithm [7,8] with the use of symmetric scheme. Random phase screens are generated by the method described in Refs.9 and 10. The complex amplitude and phase screens were prescribed on 128x128 uniform grid. An aperture of convergent lens was placed in the center of the grid and occupied the region with dimensions 64x64 points. For a ratio $D/r_0 = 10$ the distance between knot is 6.4 times less than a coherence length. A random medium was represented by six phase screens, and averaging of intensity distribution in a focal plane was performed over ensemble of 50 independent random realizations.

3.3. Adaptive system with a constant temporal lag

Let us consider the effect of temporal lag on the efficiency of adaptive optics system with an ideal wavefront sensor and phase corrector. In this case a phase profile is an argument of complex amplitude:

$$\varphi(\vec{\rho}, t) = \arg(U(\vec{\rho}, t - \tau)), \quad \vec{\rho} = (x, y), \quad (3.5)$$

where U is a field complex amplitude at the far end of a turbulent medium, i.e., in the plane $z = L$, t is temporal lag of the system, t is current time, \arg is a main quantity of a complex variable argument. In a region of weak intensity fluctuations ($tV \ll D$) the variance of residual phase distortions is equal to phase structure function D_j :

$$\sigma^2 \approx D_\varphi(\tau V) = 6.88(\tau V/r_0)^{5/3} \quad (3.6)$$

and Strehl ratio can be estimated approximately as

$$S \approx \exp(-\sigma^2) = \exp\left(-6.88(\tau V/r_0)^{5/3}\right). \quad (3.7)$$

Evidently, the decrease of AOS efficiency characterized by lessening of Strehl ratio depends on a phase variation during time t . Assuming that turbulence is frozen (Tailor's hypothesis), and wind velocity V does not depend upon Z coordinate, the phase

difference acquired in time t corresponds to phase difference between points placed on distance $Dr = tV$ from each other.

In a vicinity of wavefront dislocations the phase changes sharply, so it is possible to presume that efficiency of AOS in a region of strong fluctuation decrease more quickly with increase of temporal lag t . But numeric experiments do not confirm this assumption. Three curves representing dependence of S on ratio tV/r_0 are represented in Fig.3.2. One curve corresponds to calculations according Eq.3.7, the two others obtained in numeric experiments for the case of weak ($q = 0.1$) and strong ($q = 1.0$) fluctuations are practically identical. The difference between results of numerical computations and calculations with the use of Eq.3.7 can be attributed to excessively large value of residual aberration variance estimated according to Eq.3.6 and also to the fact that in phase screens employed for simulations the inhomogeneities are absent with scales greater than the size of the grid ($2D$).

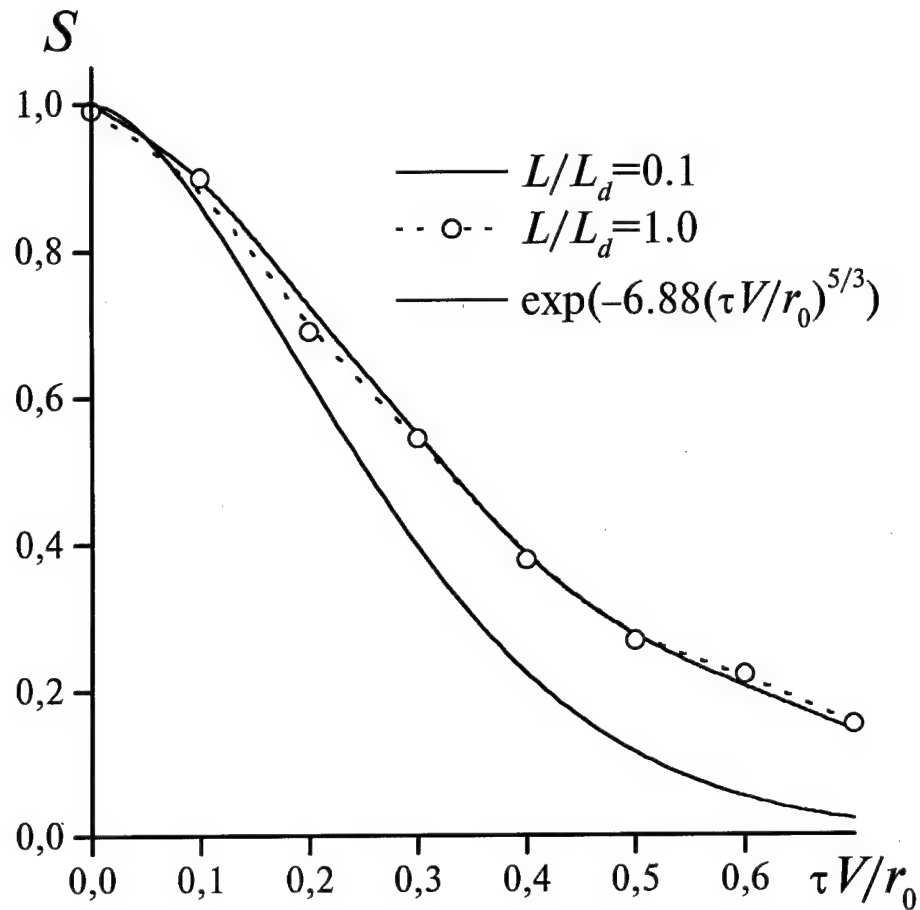


Fig. 3.2. Strehl ratio vs. normalized lag of AOS.

Regions close to dislocation points characterized by sharp variations of wavefront are relatively small and their contribution to focal spot intensity is negligible so the explicit dependence is absent of AOS efficiency on variance of intensity fluctuations.

3.4. Adaptive system with a segmented mirror

Continuous surface mirrors are inconvenient for correction of waves with broken continuity of phase surface. Seemingly, in this case segmented mirrors are more promising. Positions of mirror segments are independent and the surface prescribed by

such mirror can be broken. The dislocation of a wave front can also be represented by a mirror with continuous surface but the required number of elements in this case is much too large.

To design AOS with required efficiency one needs to know the size of corrector segment. In the region of weak fluctuations for calculations of residual phase distortion variance s^2 the following formulae are commonly used

$$\sigma^2 = 1.03(d/r_0)^{5/3}. \quad (3.8)$$

The results obtained in this way correspond to variance of phase fluctuations in a circle with diameter d after subtraction of the average phase [11]. When the mean phase and local tilts are corrected on each of the mirror segments the variance of residual phase distortions is equal

$$\sigma^2 = 0.134(d/r_0)^{5/3}. \quad (3.9)$$

Strehl ratio calculated as $S = \exp(-s^2)$ with $d = r_0$ is equal to 0.36 when the system corrects mean phase profile and to 0.87 when the mean phase and tilt are corrected.

If dislocations are present the precise detection of the wavefront is impossible. So control of a segment by tilt and piston is senseless if the wavefront and its gradient is determined by phase averaging over the aperture. To examine the dependence of segment size on efficiency of correction in the region of strong intensity fluctuations let us calculate correcting phase over an area d as

$$\varphi + k\tilde{S}\vec{\rho}, \quad (3.10)$$

where j , S_x , and S_y are correcting profiles of the mean phase and local tilts, correspondingly. They are determined through the complex amplitude averaged over the subaperture:

$$\varphi = \arg(\bar{U}); \quad \bar{U} = \frac{1}{d^2} \int_d d^2\rho U(\vec{\rho}), \quad (3.11)$$

and weight-averaged phase gradient

$$\bar{S} = \frac{1}{kP} \int d^2\rho I(\vec{\rho}) \vec{\nabla} \varphi(\vec{\rho}) = \frac{1}{kP} \int (\text{Re} U \vec{\nabla} \text{Im} U - \text{Im} U \vec{\nabla} \text{Re} U) d^2\rho. \quad (3.12)$$

Here integration is performed over an area of a size d corresponding to a segment of the corrector, $I(x, y) = UU^*$ is intensity of the incident radiation, k is a wave number, P is the energy in a subaperture

$$P = \int_d d^2\rho I(\vec{\rho}). \quad (3.13)$$

These equations allow one to calculate controlling signals without determination of the phase surface. Only the complex amplitude U (the parameter easily determined numerically) is needed.

In Fig.3.3 the dependence is represented of Strehl ratio over the normalized path length $q = L/L_d$. The results obtained are in good agreement with estimations performed with the use of Eq.3.8 and 3.9 under conditions of weak intensity fluctuations.

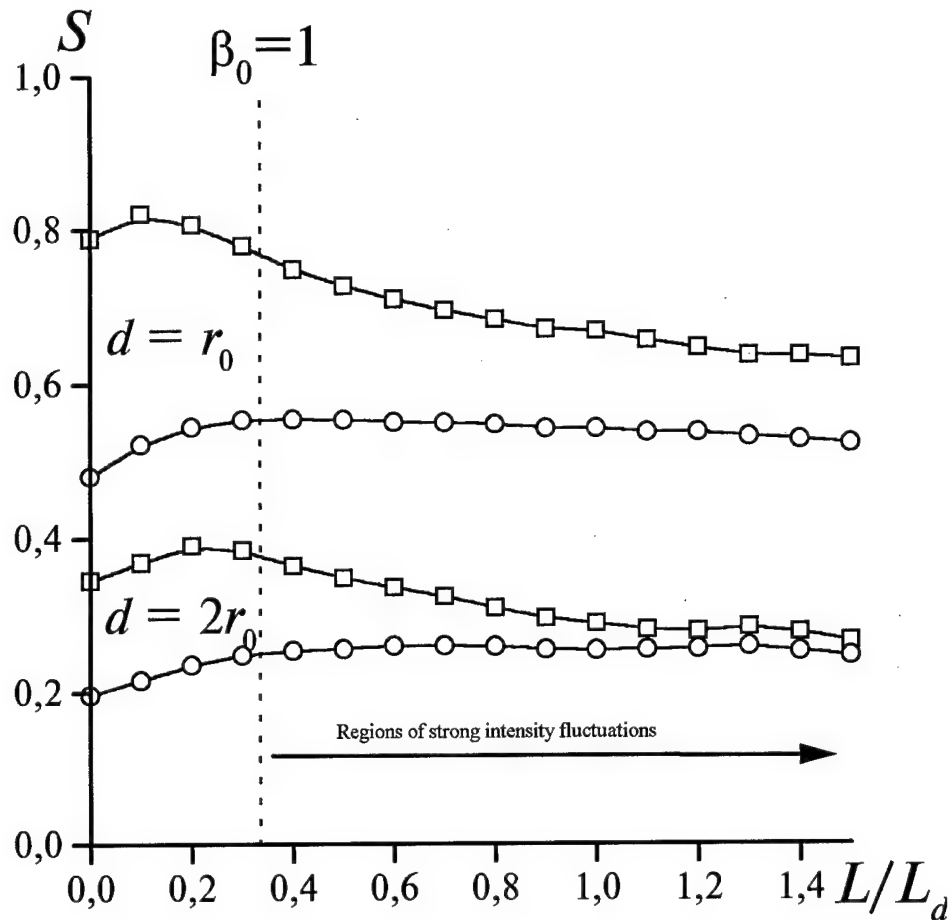


Fig. 3.3. Strehl ratio vs. normalized path length $L/(kr_0^2)$ for an adaptive system with a segmented mirror. Circles correspond to control of pistons, rectangles to control of pistons and tilts.

The data represented here show that the dependence is unpronounced of correction efficiency on normalized path length characterizing intensity fluctuations. In the case of correction for mean phase profile (without control of tilts) the dependence is practically absent. Even small increase of Strehl ratio is observed in interval $0 < L/L_d < 0.4$ which can be attributed to transformation of small-scale part of phase fluctuations into

amplitude aberrations due to diffraction and corresponding lessening of residual phase aberrations.

Efficiency of simultaneous correction for mean phase and local tilts decreases but remains higher than efficiency of correction for tilts only. The difference observed is less than 10%.

So we can conclude that high efficiency of correction can be obtained in a regions of strong and weak fluctuations if a segment of the adaptive system mirror is less in size than or equal to the coherence length. Obtained Strehl ratio is not less than 0.5-0.8 depending on the number of degrees of freedom for each segment and fluctuation intensity. There are not any additional requirements to the speed of correction so the main difficulty is creation of appropriate wavefront sensor.

3.5. An algorithm of a wavefront matrix reconstruction

Let us consider the problem of wavefront reconstruction with the use of given phase differences between a mirror subapertures. As a phase over a subaperture we use a phase prescribed to each subaperture, for example, a phase of a mean complex amplitude.

The problem of wavefront matrix reconstruction was considered by many scientists (see, for example, Refs.14, 15, 16, and 17). The common algorithm employed is based on minimization of errors by the least squares method. It was supposed that if the errors are absent, the sum of phase differences calculated over a closed contour is equal to zero.

Evidently, such supposition is not valid in the present of wavefront dislocations. If a singularity falls in this contour, the sum of phase differences is equal to 2π and errors appear in the common methods even if the phase is detected correctly. So the application of corresponding algorithms of phase reconstruction is possible only in the region of weak intensity fluctuations.

This restriction was avoided by the authors of Ref.12. They proposed to modify the initial array of phase differences by adding $2pN$ (N is an integer number) to its elements. So the sum of phase differences in the absence of errors would be equal to zero over each contour and would not exceed p if errors are present. Solution to the problem can easily be found numerically with the use of fast Fourier transform [13] on the square grid with dimensions $N \times N$. In accordance to common terminology [12, 13] let us use the term «normal equation» (NE) for a method of phase reconstruction based on the least squares algorithm. Modification of this method proposed by the authors of Refs.12 and 13 will be referred to as the modified normal equation (MNE).

These two algorithms were realized numerically and two arrays of phase differences D^x_{ij} and D^y_{ij} with dimensions $N^{1/2}(N-1)$ were used to compute the sought for phase matrix j_{ij} , $i, j = 1, 2, \dots, N$. To evaluate the fidelity of the algorithm and the code by means of which the algorithm was realized the precise phase differences computed through the complex amplitude were substituted into arrays D^x_{ij} and D^y_{ij} . Strehl ratio obtained in these numeric experiments coincided with a ratio obtained with the use of a segmented mirror (the results are presented in the previous section).

3.6. Measurements of phase differences

The modern real-time wavefront sensors working in a turbulent atmosphere are sensors of local tilts. Hartmann-Shack sensors and shear interferometers are typical examples of such devices. In both cases the output signal from every element of a sensor is proportional to the weight-averaged phase gradient over a subaperture, the intensity of an incident wave is taken as a weighting coefficient

$$\bar{g} = \frac{1}{P} \int d^2\rho I(\vec{\rho}) \vec{\nabla} \varphi(\vec{\rho}). \quad (3.15)$$

In a shear interferometer some characteristic function is added [18]. The phase

difference between in boundaries of subaperture is calculated as a product of output signal on subaperture size.

$$\Delta^x = g_x d, \Delta^y = g_y d. \quad (3.16)$$

If along with Hartmann-Shack sensor a corrector is used with the same configuration of segments, employment of the second sensor of this type allows one to lessen errors of measurements. Elements of arrays D^x_{ij} and D^y_{ij} correspond to signals of sensors. In our numeric experiments the results of which are presented below three types of local tilts sensors were used:

- The first, to fill in the array D^x_{ij} with dimensions $(N-1)N$ shifted along X -coordinate on a distance $d/2$ relatively to corrector elements.
- The second, to fill in the array D^y_{ij} with dimensions $(N-1)N$ shifted along Y -coordinate on a distance $d/2$ relatively to corrector elements.
- The third, to control the tilts of a segmented mirror. This sensor is not shifted and its dimensions are $N \times N$.

The values of j_{ij} obtained with the use of the first and second sensors are employ to control pistons and values g_{ij} from the third sensor to control tilts of the segments. We assume this configuration to be optimal or very close to it.

3.7. AOS with a sensor of local tilts. Simulation results

The adaptive optics system including three sensors of local tilts was used in numeric experiments. The results of these experiments are presented below. Local tilts were computed according the equations

$$g_x = \frac{1}{P} \int_d \left(\text{Re}U \frac{\partial \text{Im}U}{\partial x} - \text{Im}U \frac{\partial \text{Re}U}{\partial x} \right) d^2\rho,$$

$$g_y = \frac{1}{P} \int_d \left(\text{Re}U \frac{\partial \text{Im}U}{\partial y} - \text{Im}U \frac{\partial \text{Re}U}{\partial y} \right) d^2\rho.$$

Integration was performed over a subaperture with diameter d . Derivatives along X and Y coordinates were calculated numerically multiplying Fourier transforms of real and imagine parts of the complex amplitude by corresponding filtering function.

Phase correction on segment i, j of the corrector was prescribed as

$$\varphi_{i,j} + g_x x + g_y y, \quad (3.17)$$

where g_x and g_y are local tilts measured by third sensor, and j_{ij} is phase matrix obtained by solving of MNE formed from the array of phase differences obtained with thirist and second sensors.

The calculation were performed with $D/r_0 = 10$ and with $D/d = 10$. So the size of subapertire for corrector and sensor was taken equal to Freid coherence length r_0 .

In Fig.3.4 the dependence is presented of Strehl ratio on normalized path length. Computations were performed for the following variants:

- solution of NE for $d \rightarrow 0$ (a);
- solution of NE for $d = r_0$ (b);
- solution of MNE for $d = r_0$ (c).

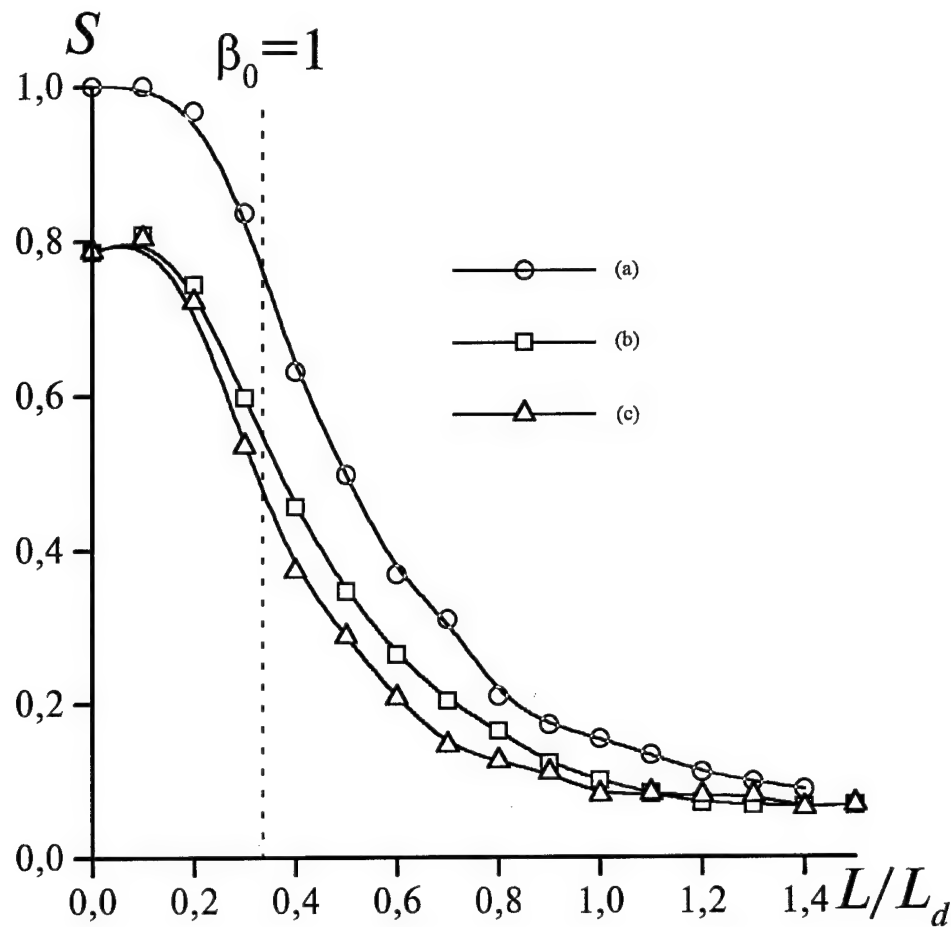


Fig.3.4. Strehl ratio vs. normalized path length $L/(kr_0^2)$ for different variants sensors.

Approaching d to zero means that the size of a segment is equal to a distances between nodes in the computational grid and phase differences are determined without calculation of local tilts, only the values of the complex amplitude are used.

Analysis of dependencies of S on (L/L_d) shows that if NE is used the correction efficiency decreases sharply when we hit the region of strong fluctuations ($b_0 > 1$). But with the use of MNE efficiency decreases even more quickly. Lessening of an element size d does not result in increase of Strehl ratio so we should conclude that an adaptive optics system with a sensor of local tilts is ineffective in the region of strong intensity

fluctuations even if an algorithm of phase reconstruction is used specially written for a phase matrix reconstruction in the presence of screw dislocations.

To understand due to what factors this failure occurs, the dependence was considered of variance of phase estimation errors on normalized path length. The error over the sensor subaperture i, j was calculated in the following way

$$\varepsilon_{i,j} = \left(\arg \overline{U}_{i+1,j} - \arg \overline{U}_{i,j}^* \right) - g_{x i,j} \cdot d. \quad (3.18)$$

Notation $\left(\overline{U}_{i+1,j} \right)$ used here means averaging over the third sensor subaperture coinciding with the corresponding element of the segmented mirror, and g_x is weight-averaged phase gradient over corresponding subaperture of the first sensor. The error ε_{ij} was recalculated to the interval $(-p, p]$. The variance of errors was determined by averaging over the whole set of subapertures and over ten random realizations.

Increase in the variance of errors of estimations of phase differences with the use of local tilts as a function of the ratio L/L_d , characterizing the variance of intensity fluctuations is illustrated in Fig.3.5. Analyzing the data presented we can conclude that the decrease of AOS efficiency is induced by sharp increase of the variance of errors.

To obtain some gain from MNE employment a sensor should be used measuring precisely the phase differences in the region of strong intensity fluctuations.

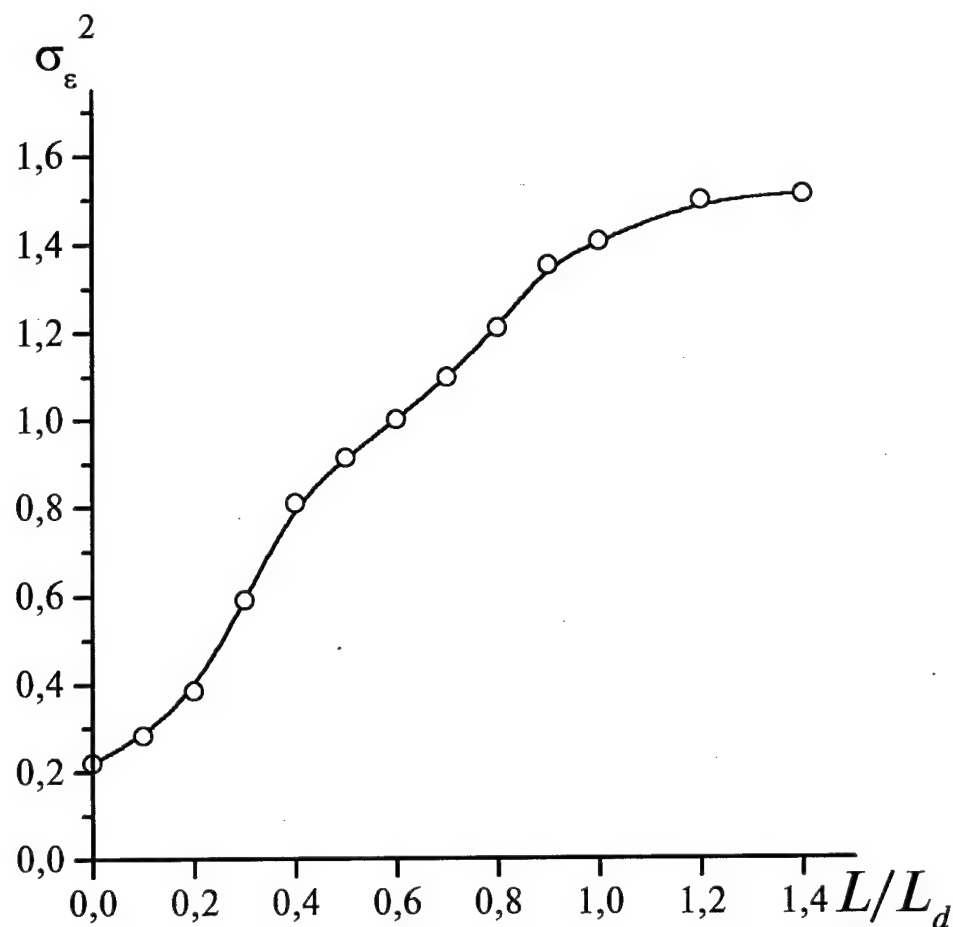


Fig.3.5. Dependence of the variance of phase difference estimations through local tilts on normalized path length.

Principally, the difference between phases can be calculated using the coordinates of an interferometer fringe obtained as a result of interference between fields of adjacent subapertures, but realization of real-time measurement of this kind in a turbulent atmosphere could be very difficult.

Let us make some notions concerning normalized aperture diameter D/r_0 . The results presented in the report were obtained with a ratio D/r_0 taken to be constant and equal to 10. The preliminary estimations for $D/r_0 > 10$ show that Strehl ratio decreases

more quickly than efficiency of AOS and approaches its value obtained in the absence of correction. In its turn, the value of Strehl ratio for a wave without correction decreases with increase of normalized diameter D/r_0 .

2.8. Conclusions

The efficiency of phase correction for turbulent distortions which induce broadening of images was analyzed in the region of strong intensity fluctuations. Results of numerical experiments allow us to conclude that the crucial element of an adaptive optics system is a wavefront sensor. Concerning the segmented mirror it is possible to say that efficiency of its application is approximately the same in regions of strong and weak fluctuations ($S \cong 0,5$ with $d = r_0$) providing that only an average phase is corrected. If local tilts are corrected along with the average phase, efficiency of AOS decreases with increase of fluctuation intensity, but remains higher as compared with the case when only the average phase is corrected. On long paths these two variants ensure approximately the same efficiency. So under condition of strong intensity fluctuations the effect of local tilt correction on efficiency is negligible, and we can exclude the control over tilts and simplify the design of the system.

The situation is almost the same with a wavefront sensor. Here detection of local tilts becomes inefficient in the region of strong fluctuations due to decrease of correlation between local tilts and phase differences. To employ the system under such conditions the wavefront sensor should be based on direct measurements of phase differences and the modified normal equation is used in the problem of phase reconstruction.

Dynamics of AOS was considered only for a system with a constant temporal lag in the control loop, other factors were not allowed for. As was shown in numerical experiments the influence of constant lag on efficiency does not depend on fluctuation

intensity. It is possible to assume that varying the lag along with other factors one may obtain more complex scenarios of a wave propagation.

Spectral characteristics of adaptive correction remain beyond the boundaries of this investigation. More likely than not, in the region of strong fluctuations the AOS is very sensitive to the difference of wavelengths between a source beam and a direct one, because scaling of phase correction from one wave to another is difficult when the phase profiles are not continuous.

References to Chapter 3

1. Tatarskii V.I. Wave propagation in a turbulent atmosphere. M. Nauka, 1967, 548 pp.
2. Baranov N.B. and Zeldovich B.Ya. //Zh. Eksp. Teor. Fiz. 1981. V.80. P.1789.
3. Fried D.L. and Vaught J.L. //Appl. Opt. 1992. Vol.31, No.15. P.2865 - 2882.
4. Primmerman C.A., Price T.R., Humphreys R.A., Zollars B.G., Barclay H.T., Herrmann J. //Appl. Opt. 1995, Vol.34, ¹12. P.2081-2089.
5. Lukin V.P. and Fortes B.V. //III Symposium on Atmospheric and Oceanic Optics, Tomsk, 1996. P.28-29.
6. Lukin V.P. Atmospheric Adaptive Optics. Novosibirsk, Nauka, 1986, 286 pp.
7. Fleck J.A., Morris J.R., and Feit M.D. //Appl. Phys. 1976. Vol.10. ¹1, P.129-139.
8. Konyaev V.A. //VII All-Union Symposium on Laser Radiation Propagation in the Atmosphere, Tomsk, 1983, p.104-106.
9. Lukin V.P., Fortes B.V., and Mayer N.N. //Atmospheric Optics. 1991. Vol.4. No.12. P.1298-1302.
10. Fortes B.V. and Lukin V.P. //Proc. SPIE. 1992. Vol.1668. P.477-488.
11. Noll R.J. //J. Opt. Soc. Am. 1976. Vol.66, ¹3. P.207-211.
12. Hiroaki Takajo and Tohru Takahashi //J. Opt. Soc. Am. A. 1988. Vol.5. ¹3. P.416-425.
13. Hiroaki Takajo and Tohru Takahashi //J. Opt. Soc. Am. A. 1988. Vol.5. ¹11. P.1818-

1827.

14. Fried D.L. //J.Opt.Soc.Am. 1977. Vol.67. 13. P.370-375.
15. Hudgin R.H. //J.Opt.Soc.Am. Vol.67, P.375-378 (1977).
16. Hunt B.R. //J.Opt.Soc.Am Vol.69, P.393-399 (1979).
17. Herrmann J. //J.Opt.Soc.Am Vol.70, P.28-35 (1980).
18. Goad L., Roddier F., and Becker J., Eisenhardt P. //Proc. SPIE 1986 Vol. 628 P.305-313.

Chapter 4. Conclusions

As a result of executed by us last years of researches, including, and in with the task under the given project, it is possible to formulate the following conclusions.

A. The application of lasers for tasks of formation of artificial guide stars can increase limiting opportunities of ground-based telescopes, and also systems of construction of the image for objects formed in conditions of turbulent atmosphere.

B. The theoretical aspects of a problem of account of efficiency of application of laser guide stars potentially were incorporated in works of the Soviet scientist studying a problems of propagation of optical waves in randomly non-uniform media:

- 1. V.P.Lukin, Atmospheric Adaptive Optics (Novosibirsk, Nauka, 1986).**
- 2. Meeting Digest of "Scintillation" International Meeting for Wave Propagation in Random Media, Conference Chairs V.I. Tatarskii, A.Ishimaru, University of Washington, Seattle, USA, August 1992.**
- 3. V.M.Orlov, I.V.Samokhvalov, G.G.Matvienko, M.L.Belov, A.N. Kozhemyakov, The elements of theory of wave scattering and optical ranging (Novosibirsk,Nauka, 1982).**
- 4. M.A. Kalistratova, A.I. Kon, "Fluctuations of arrival angle of light waves from extended source in turbulent atmosphere", Izv.VUZov. Radiofizika, 1966, V.9, No.6, 1100-1107.**
- 5. V.L.Mironov, V.V.Nosov, B.N.Chen, "Correlation of shifting of laser source optical images in the turbulent atmosphere", Izv.VUZov. Radiofizika, V.25, No.12, 1467-1471, 1982.**

C. Is particular, the calculations of a signal with use of a laser guide star for adaptive systems of phase correction were executed firstly in USSR about 20 years back.

D. History of a question of the first works under the theory of application of laser guide stars in article

**Robert Q.Fugate, Walter J.Wild, " Untwinkling the Stars - Part I ",
Sky and Telescope, May 1994, pp.2-9.**

practically ignores all aspects of development of this question in USSR. Really in the early eighties in adaptive astronomy artificial reference sources were named laser guide stars. In this work the following stages of development of a problem are stated:

- a) Summer 1982 - conference in La Jolle, CA, first calculation of Dr. D.Fried.
- b) Dr.Will Happer made a new approach - sodium artificial beacon.
- c) Air Force Phillips Lab - experiment at SOR (1983).
- d) Report on classified conference in Febr.1984.
- e) Lincoln Lab - experiment at WSMR (1984-1985).
- f) Renaud Foy and Antoine Labeyrie published in Astronomy & Astrophysics laser-beacon concept, 1985.
- g) Laird Thompson, C.Gardner - experiment on Mauna Kea, 1987.

E. It would be necessary once again to emphasize, that in USSR about 20 years the following accounts back were executed. So during 1979-1980 years in works:

**1. V.P.Lukin, "Tracking of random angular displacements of optical beams", V
All-Union Symposium on Laser Beam Propagation, Tomsk, Proc. Part II, 33-36,
1979.**

2. V.P.Lukin, "Correction for Random Angular Displacements of Optical Beams", Kvant. Elektron. V.7, pp.1270-1279, 1980 [Sov.J.Quantum Electron. 10, 727-732 (1980)].

Dr.Vladimir P.Lukin was first, who have made **mention of the fundamental possibility of using radiation backscattered by the atmospheric aerosol for adaptive phase of correction.**

F. As far as we know the first works on use of the laser for formation reflected from of an atmosphere of a signal for active management with correction of the image were executed in USSR in 1978-1983 years. One of pioneers of such works has become Dr.Vadim G.Vugon, working then in SPA "Astrophysics". The first experiments under his management were executed in area in territory Special Astrophysical Observatory of Academy of Sciences USSR (Northern Caucasus).

G. In work of the **Dr R.Fugate, "Laser beacon adaptive optics", Optics and Photonics News, 14-19, June 1993** for the first time was shown, that in the classical approach the monostatic scheme of formation of a laser guide star is not effective from the point of view of correction of general inclinations of wave front.

H. In works

1. V.P.Lukin, "Correction for Random Angular Displacements of Optical Beams", Kvant. Elektron. 7, 1270-1279 (1980) [Sov. J.Quantum Electron. 10, 727-732 (1980)].

2. V.Lukin and B.Fortes "Efficiency of adaptive correction of images in a telescope using an artificial star". OSA Tech. Digest. 1995. Vol.23, pp.192 - 193.

3. V.P.Lukin, "Laser beacon and full aperture tilt measurement", in Adaptive Optics Vol.13 of OSA Technical Digest Series (Optical Society of America, Washington, D.C., 1996) Addendum AMB-35, pp.1-5.

the algorithm of "optimum" correction of an inclination of wave front was offered and the efficiency of this algorithm was shown. Unfortunately this algorithm nor gives to effective correction of a general inclination of wave front for the traditional monostatic scheme of a laser guide star.

I. During 1993-1996 years it was offered a number of the various schemes, including, and of the schemes, which on a plan of the authors should give the decision of a problem of correction of a general inclination of wave front. It is necessary to specify the following works:

1. R.Foy, A.Migus, et al., " The polychromatic artificial sodium star: a new concept for correction the atmospheric tilt ", Astronomy and Astrophysics, 111, pp. 569 - 578 (1995).

2. R.Ragazzoni, S.Esposito, and E.Marchetti, "Auxiliary telescopes for the absolute tilt-tip determination of a laser guide star" Mon. Not. R.Astron. Soc. 1995. Vol.276, pp.L76 - L78.

3. R.Ragazzoni, "Absolute tip-tilt determination with laser beacons", Astron.Astrophys. 305, L13-L16 (1996).

4. M.S.Belen'kii, "Full aperture tilt measurement technique with a laser guide star", in Atmospheric Propagation and Remote Sensing IV, editor J.C. Dainty, Proc.SPIE 2471, 289-296 (1995).

5. M.S.Belen'kii, "Tilt angular correlation and tilt sensing techniques with a laser guide star" in Optics in Atmospheric Propagation, Adaptive Systems, and Lidar Technique for Remote Sensing, editor J.C. Dainty, Proc.SPIE, 2956, 206-217 (1996).

6. **Yearly Status Report Adaptive Optics at the Telescopio Nazionale Galileo**, edited by R.Ragazoni, August 1996.
7. **Roberto Ragazzoni**, Propagation delay of a laser beacon as a tool to retrieve absolute tilt measurements, *The Astronomical Journal*, 465, L73-L75, 1996.
8. **R.Ragazzoni**, "Absolute tilt-tip determination with laser beacons" *Astron. Astrophys*, 1996, Vol.305, p.L13 - L16.
9. **S.Esposito and R.Ragazzoni**, "Techniques for LGS tilt retrieval: a numerical comparison", in the book "Adaptive Optics at the Telescopio Nazionale Galileo", ed. by R.Ragazoni, pp.1 - 20, December 1997.
10. **S.Esposito and R.Ragazzoni**, "Non conventional techniques for LGS tilt retrieval: an update", in the book "Adaptive Optics at the Telescopio Nazionale Galileo", ed. by R. Ragazzoni, December 1997.
11. **R.Ragazzoni**, "Robust tilt determination from Laser Guide Star using a combination of different techniques", *Astronomy and Astrophysics*, 319, L9 - L12 (1997).
12. **R.Ragazzoni**, "Laser guide star advanced concept: tilt problem", in the book "Adaptive Optics at the Telescopio Nazionale Galileo", ed. by R. Ragazzoni, December 1997.

K. At the same time more careful analysis of a backscattering signal (as a signal describing a random angular position of a laser guide star) for use for correction of a general inclination executed in following works:

1. **V.Lukin**, "Limited resolution of adaptive telescope with the use of an artificial star", *Proc. ICO - 16. "Active and Adaptive Optics"*, 1993. P.521 - 524.
2. **V.Lukin** "Adaptive forming of beams and images in the atmosphere". *Atmos. Ocean. Opt.*, 1995. V.8, pp.301 - 341.

3. V.P.Lukin, "Models and measurements of atmospheric turbulence characteristics and their impact on AO design", OSA Technical Digest Series "Adaptive Optics", 1996, V.13, pp.150-152.
4. V.P.Lukin, B.V.Fortes, "Comparison of Limit Efficiencies for Various Schemes of Laser Reference Star Formation", Atm.Oceanic Optics, 1997 V.10, pp.34-41.
5. V.P.Lukin, "Hybrid scheme of formation of laser reference star", Atm.Oceanic Opt., 1997, V.10, pp.975-979.
6. V.Lukin, "Monostatic and bistatic schemes and optimal algorithms for tilt correction in ground-based adaptive telescope" Appl. Opt., 20 July, 1998.
7. V.Lukin "Problems of laser guide star forming" Atmos. Oceanic Ops., 1998, V.11, No.5, pp.1 - 13.
8. V.P.Lukin, "Two Schemes of Laser Guide Star Formation"//Atm.Oceanic Opt., 1998, V.11, pp.1253-1257

shows, that

- the bistatic scheme cannot give (even provided that the laser guide star is not a point source and probably to carry out averaging on its seen size) rather effective signal for complete correction of a general inclination of wave front,
- offered a number of the authors the hybrid schemes by simultaneous use of signals for monostatic and bistatic guide stars, nor give of appreciable improvement of correction.

L. As show estimations a residual level of random angular jitter of the image of a natural star (after correction with use of a laser guide star) makes approximately 40% from a level of this signal without correction. If to consider, that the jitter of the image makes approximately 80-85 % for all of a variance of phase fluctuations, after correction on the basis of use of a laser guide star the residual level phase will make approximately 30%

from initial. That is in a limit use only of signal from a laser guide star can reduce a level phase fluctuations approximately in 3 times.

M. Simultaneous use of a signal of a natural star and laser guide star can give an opportunity to reduce a residual level of the phase fluctuations 10-20 time.

N. With formation of the image of object through a layer of an atmosphere (for unastronomical objects) most effective can be use, alongside with a signal from a laser guide star measurement of an instant position of the image of the object. This signal can effective be used for correction general jitter of the image of object.

O. Use of several laser guide stars hardly can give serious improvement of a situation with correction of a general inclination of wave front of the formed image.

Report for third four month period under contract SPC98-4041

**Limiting possibilities for phase correction of turbulent distortions of optical images
and beams**

**Principle Investigator
Prof.Vladimir P.Lukin**

TOMSK - 1999

Contents

Abstract

Chapter 1. Some problems in the use of laser guide stars

1.2. "Optimal" algorithm of tip-tilt correction for natural star

1.3. Bistatic schemes LGS

1.4. Distinction and similarity of two schemes of formation Laser Guide Star

1.5. Hybrid scheme LGS

References for Chapter 1

Chapter 2. Adaptive correction of the focused beam in conditions strong fluctuations of intensity

2.1. Introduction

2.2. Comparison cases for plane wave and gaussian beam

2.3. Two-colour adaptive system

References for Chapter 2

Abstract

In the first chapter of report we have considered to limiting possibilities of adaptive correction of images in astronomical telescopes which operated with laser guide stars forming. Some problems, connected with development of ground-based adaptive telescope, particularly, with its fitting additional optical system for laser guide star formation, are treated in the paper. The point of the work is determination of the type of the laser guide star being formed. Here, the calculated results are presented for scheme for laser guide star formation, when arbitrary magnitudes of the correlation between random angular displacements of the image of scattering volume stipulated by the laser beam fluctuations over direct and back paths can be obtained. Expressions for the monostatic and bistatic schemes are obtained as limiting cases.

In the second chapter of this report we deal with laser beams turbulent distortions correction under strong fluctuations of its intensities.

This material is based upon work partially supported by the European Office of Aerospace Research and Development, Air Force Office of Scientific Research, Air Force Research Laboratory, under contract SPC 98-4041.

Keywords: turbulence, tilt correction, adaptive telescope, laser guide star, bistatic and hybrid schemes, strong fluctuations, plane wave, laser beam, wave-front sensor.

Chapter 1. Some problems in the use of laser guide stars

1.1. Introduction

It is known [1-7], that the application of engineering of laser guide stars (LGS) can considerably expand a range of effective work of adaptive optical systems for astronomical ground-based telescopes. At the same time there are rather serious problems on a way of real application LGS in astronomy.

One of such problems is the practical impossibility of correction of a general inclination of wave front of a real star $\bar{\varphi}_F^{pl}$, using only data of measurements jitter of the image of a laser guide star in focal plane of a telescope [7-11]. Was shown earlier [7, 10, 11], that the monostatic scheme of formation LGS does not give an opportunity effectively to correct fluctuations of a general inclination of wave front. The attempts to improve this situation, using algorithm "optimum" corrections, have appeared nor too are effective [12-15], in view of low effective of the given measurements of an angular position of LGS for the monostatic scheme of formation.

1.2. "Optimal" algorithm of tip-tilt correction for natural star

Algorithm of "optimum" correction [13, 16, 17], ensuring a minimum of the following functional, describing a level residual fluctuations

$$\langle (\bar{\varphi}_F^{pl} - A \bar{\varphi}_m)^2 \rangle_{\min} = \langle (\bar{\varphi}_F^{pl})^2 \rangle > \left\{ 1 - \frac{\langle \bar{\varphi}_F^{pl} \bar{\varphi}_m \rangle^2}{\langle (\bar{\varphi}_F^{pl})^2 \rangle \langle (\bar{\varphi}_m)^2 \rangle} \right\}, \quad (1)$$

is achieved by scaling the given optical measurements $\bar{\varphi}_m$ on an adjusting multiplier

$$A = \frac{\langle \bar{\varphi}_F^{pl} \bar{\varphi}_m \rangle}{\langle (\bar{\varphi}_m)^2 \rangle}. \quad (2)$$

Here $\langle \dots \rangle$ is the brackets designate averaging on fluctuations, connected with action atmospheric turbulence, $\bar{\varphi}_F^{pl}(R_0)$ - angular fluctuations of random displacement of the image of a real star (fluctuations of a general inclination of wave front of the plane optical wave which has come on the aperture of a telescope R_0), $\bar{\varphi}_m$ - measured angular fluctuations of random displacement of the image LGS, caused by action atmospheric turbulence, $\langle (\bar{\varphi}_F^{pl})^2 \rangle$ - variance of fluctuations of a general inclination of wave front for a natural star. It is necessary to note, that adjusting factor A can be determined experimentally during operation of adaptive system on a telescope. For it is necessary to have an opportunity of realization of measurements of mutual correlation and variance of jitters of the images LGS and bright natural star. Probably also to do the preliminary calculation of adjusting factor A till the formula (2), using the models of vertical distribution of parameters of atmospheric turbulence.

If to consider, that formed in an atmosphere LGS it is not restored by the reception aperture of a telescope, then

$$\bar{\varphi}_m = \bar{\varphi}_{lb} + \bar{\varphi}_F^{sp}, \quad (3)$$

where $\bar{\varphi}_{lb}$ is the random angular displacement of a laser beam forming LGS, $\bar{\varphi}_F^{sp}$ is random angular displacement of the image of a dot source in focal plane of a telescope. If to characterize quality of correction, as ratio of the variance of residual fluctuations (1) to the value of the initial variance $\langle (\bar{\varphi}_F^{pl})^2 \rangle$

$$\beta = \langle (\bar{\varphi}_F^{pl} - A \bar{\varphi}_m)^2 \rangle_{\min} / \langle (\bar{\varphi}_F^{pl})^2 \rangle = \left\{ 1 - \frac{\langle \bar{\varphi}_F^{pl} \bar{\varphi}_m \rangle^2}{\langle (\bar{\varphi}_F^{pl})^2 \rangle \langle (\bar{\varphi}_m)^2 \rangle} \right\}, \quad (4)$$

then, as shown in [15], the quality of correction for the monostatic scheme is given

$$\beta = 1 - \frac{2^{1/3} \left(\int_0^X d\xi C_n^2(\xi) (1 - \xi/X) \left\{ \left[1 + b^2 (1 - \xi/X)^2 \right]^{-1/6} - \left[1 + (1 - \xi/X)^2 \right]^{-1/6} \right\} \right)^2}{\left[1 + b^{-1/3} - 2^{7/6} (1 + b^2)^{-1/6} \right] \int_0^X d\xi C_n^2(\xi) (1 - \xi/X)^{5/3} \int_0^\infty d\xi C_n^2(\xi)} \quad (5)$$

Here X is a height of formation LGS, $b = a_0 / R_0$, a_0 is initial size of a laser beam, C_n^2 is a vertical structure of intensity of turbulence, $\langle \bar{\varphi}_m^2 \rangle$ is variance fluctuations of an angular position of the image of LGS.

1.3. Bistatic schemes LGS

The transition from monostatic scheme to the limiting bistatic scheme gives a really appreciable benefit [8-12]. Limiting bistatic scheme is realized provided that fluctuations of optical radiation on direct (from ground up to a guide star) and return (from a guide star down to the aperture of a telescope) paths completely noncorrelated. One of variants of such bistatic scheme has offered R.Ragazzoni [8, 9]. In his scheme the guide star forms with use additional laser illuminator, displaced of a rather optical axis of a telescope on two orthogonal directions. In the assumption, that LGS represents a dot source, the level residual fluctuations [12, 18] is given

$$\beta = 1 - \frac{2^{1/3} \left(\int_0^X d\xi C_n^2(\xi) (1 - \xi/X) \left[1 + (1 - \xi/X)^2 \right]^{-1/6} \right)^2}{\left[1 + b^{-1/3} \right] \int_0^X d\xi C_n^2(\xi) (1 - \xi/X)^{5/3} \int_0^\infty d\xi C_n^2(\xi)} \quad (6)$$

Other variant of the bistatic scheme is possible [10, 11], when the laser star is formed on an axis of the main telescope, and the measurements of LGS jitter carry out two additional removed telescopes, for which formed scheme of LGS is limiting bistatic one. In this case with "optimum" correction (for dot LGS) the value β (level residual fluctuations) is given [12, 18] by

$$\beta = 1 - \frac{2^{1/3} \left(\int_0^X d\xi C_n^2(\xi) (1 - \xi/X) \left[1 + b^2 (1 - \xi/X)^2 \right]^{-1/6} \right)^2}{\left[1 + b^{-1/3} \right] \int_0^X d\xi C_n^2(\xi) (1 - \xi/X)^{5/3} \int_0^\infty d\xi C_n^2(\xi)} \quad (7)$$

As shows the numerical analysis, for $b = a_0 / R_0 \leq 1$ the expressions (6) and (7) practically coincide. It even has entitled R.Ragazzoni to talk about "symmetry" of these two schemes.

1.4. Distinction and similarity of two schemes of formation laser guide star

It is necessary once again to emphasize, that the expressions (6) and (7) are received under condition that the LGS is "visible" in the aperture of a telescope as a dot source. In too time it is known [8 - 11], that bistatic scheme of formation LGS enables to create undot, but extended guide source. Then for the scheme of formation LGS with two additional illuminators (scheme of R.Ragazzoni [8, 9]), laser star giving the image, as a luminous string, the quality of correction of a general inclination of wave front $\bar{\varphi}_F^{pl}(R_0)$ is given

$$\beta = 1 - \frac{\langle \bar{\varphi}_F^{pl} \bar{\varphi}_F^{ss} \rangle^2}{\langle (\bar{\varphi}_F^{pl})^2 \rangle \left\{ \langle \bar{\varphi}_{lb}^2 \rangle + \langle (\bar{\varphi}_F^{ss})^2 \rangle \right\}}, \quad (8)$$

where $\bar{\varphi}_m = \bar{\varphi}_{lb} + \bar{\varphi}_F^{ss}$, $\bar{\varphi}_F^{ss}$ is vector describing random angular displacement of the image of an extended "secondary" source.

For the scheme of formation LGS [10, 11], using laser illuminator and main telescope, working on same axis, and two additional telescopes, which "see" a guide star as a luminous piece of a direct line, we receive [12, 18 - 20

$$\beta = 1 - \frac{\langle \bar{\varphi}_F^{pl} \bar{\varphi}_{lb} \rangle^2}{\langle (\bar{\varphi}_F^{pl})^2 \rangle \left\{ \langle \bar{\varphi}_{lb}^2 \rangle + \langle (\bar{\varphi}_F^{ss})^2 \rangle \right\}}. \quad (9)$$

For realization of a comparative estimation of efficiency of the various schemes we shall take advantage of results of the paper [18]. In it the factor of correlation of random displacement of a center of gravity of the focused optical beam $\bar{\varphi}_{lb}$ and angular displacement of the image of a plane wave $\bar{\varphi}_F^{pl}(R_0)$ in focal plane of a telescope caused atmospheric turbulence was calculated with a displacement $\bar{\rho}_0$ axes of an optical beam and telescope

$$K(d) = \frac{\langle \bar{\varphi}_{lb}(d) \bar{\varphi}_F^{pl} \rangle}{\sqrt{\langle \bar{\varphi}_{lb}^2 \rangle \langle (\bar{\varphi}_F^{pl})^2 \rangle}}. \quad (10)$$

Here is $d = |\rho_0| / R_0$. The accounts were executed for model of a spectrum atmospheric turbulence [21-25]

$$\Phi_n(\kappa, \xi) = 0,033 C_n^2(\xi) \kappa^{-11/3} (1 - \exp(-\kappa^2 / \kappa_0^2)), \quad (11)$$

where $\kappa_0^{-1}(\xi)$ is the outer scale atmospheric turbulence.

Under calculations in paper [18] of factor of correlation $K(d)$ the outer scale of atmospheric turbulence was set as constant size for the whole atmosphere. Hardly it is justified for all cases. Let's take advantage of several models [26, 27] of a vertical structure of outer scale:

model A0

$$\kappa_0^{-1}(\xi) = 0.4\xi,$$

model B

$$\kappa_0^{-1}(\xi) = \begin{cases} 0.4\xi, & \xi \leq 25 M \\ 2\sqrt{\xi}, & \xi > 25 M \end{cases},$$

model C

$$\kappa_0^{-1}(\xi) = \begin{cases} 0.4\xi, & \xi \leq 25 M \\ 2\sqrt{\xi}, & 25 M < \xi \leq 1000 M \\ 2\sqrt{1000}, & \xi > 1000 M \end{cases},$$

model D

$$\kappa_0^{-1}(\xi) = \frac{5}{1 + \left[\frac{\xi - 7500}{2000} \right]^2},$$

model E

$$\kappa_0^{-1}(\xi) = \frac{4}{1 + \left[\frac{\xi - 8500}{2500} \right]^2}.$$

Efficiency of application of such models was already shown earlier. On Figs.1 and 2 as five fragments (for models A, B, C, D, E) the accounts of factor of correlation $K(d)$ as function of the space of axes of the focused laser beam and telescope $d = |\rho_0| / R_0$ for two heights X LGS formation, accordingly 10 and 100 kms are given. The meanings of parameter $b = a_0 / R_0$ were set equal 0.1, 0.3, 0.7, 1.0, 3.0, 5.0. It is necessary to note, that the best correlation the jitter of a center of gravity of the focused beam and the jitter of a center of gravity of the image of a plane wave is achieved with size of the ratio $b = 1$. If $b = a_0 / R_0$ is not large, i.e., $a_0 < R_0$, then has a place asymptotical behaviour $K(d, b) \approx (2b)^{1/6}$, and when $a_0 > R_0$ is received, that $K(d, b) \approx (2/b)^{1/6}$.

Using expression (10) for factor of correlation $K(d)$ with $d = 0$, it is possible to write down expression (9) in the following kind:

$$\beta = 1 - \frac{K^2(0)}{\left\{ 1 + \langle (\bar{\varphi}_F^{ss})^2 \rangle / \langle \bar{\varphi}_{lb}^2 \rangle \right\}}. \quad (12)$$

Thus, the efficiency correction of general inclination of wave front for bistatic scheme [18] will be determined by value $K^2(0)$ and the ratio $\langle (\bar{\varphi}_F^{ss})^2 \rangle / \langle \bar{\varphi}_{lb}^2 \rangle$.

For the wide focused laser beam having the initial size a_0 , the variance laser beam jitter in approximation from paper [28] is given

$$\begin{aligned}
\langle \varphi_{lb}^2 \rangle = & 2\pi^2 0,033 \Gamma(1/6) 2^{1/6} \int_0^X d\xi C_n^2(\xi) (1 - \xi/X)^2 \\
& \times \left\{ \left[a_0^2 (1 - \xi/X)^2 \right]^{-1/6} - \left[a_0^2 (1 - \xi/X)^2 + 2\kappa_0^{-2} \right]^{-1/6} \right\}.
\end{aligned} \tag{13}$$

The variance of jitter of the image of an extended source was studied rather well earlier by number of the authors [29-31, 11]. We use expression for $\langle (\bar{\varphi}_F^{ss})^2 \rangle$ from paper [11], written down for a spectrum (11). Then to within 5% of accuracy we receive for ratio

$$\begin{aligned}
\langle (\varphi_F^{ss})^2 \rangle / \langle \varphi_{lb}^2 \rangle = & \int_0^X d\xi C_n^2(\xi) (1 - \xi/X)^2 \left\{ \left[a_b^2 (\xi/X)^2 + R_a^2 (1 - \xi/X)^2 \right]^{-1/6} - \right. \\
& \left. - \left[a_b^2 (\xi/X)^2 + R_a^2 (1 - \xi/X)^2 + 2\kappa_0^{-2} \right]^{-1/6} \right\} \\
& \times \left[\int_0^X d\xi C_n^2(\xi) (1 - \xi/X)^2 \left\{ \left[a^2 (1 - \xi/X)^2 \right]^{-1/6} - \left[a^2 (1 - \xi/X)^2 + 2\kappa_0^{-2} \right]^{-1/6} \right\} \right]^{-1}
\end{aligned} \tag{14}$$

Here a_b is seen linear size of an extended "secondary" source, R_a is the size of the aperture of an additional telescope. The accounts of the ratio of variances $\langle (\bar{\varphi}_F^{ss})^2 \rangle / \langle \varphi_{lb}^2 \rangle$ for various ratio of sizes a_b , R_a , a_0 were executed. The model of a high-altitude profiles of $C_n^2(\xi)$ was taken from paper [32], appropriate the "average" conditions of vision through an atmosphere are used. Some models for the description of a high-altitude profiles of outer scale atmospheric turbulence are used: models C and E, and also fixed meanings $\kappa_0^{-1} = 3, 10, 100$ and 1000 meters. The accounts were carried out for several meanings of the apertures of the main telescope $R_0 = 1, 4$ and 10 meters. The results are given on Figs.3 and 4 (as a set of function $f(e) = \langle (\varphi_F^{ss})^2 \rangle / \langle (\varphi_{lb})^2 \rangle$ for $X = 10$ and $X = 100$ km) as six fragments each, the left column of figures corresponds to meaning $R_a / R_0 = 0.1$, and right - $R_a / R_0 = 1$. The ratio of the seen size extended "

secondary " of a source a_b to the initial size of a laser beam (parameter $e = a_b / a_0$) was set in an interval from 0.1 up to 1000. Thus we have all necessary characteristics for an estimation of efficiency of correction of a general inclination of wave front.

Let us to compare the efficiency this scheme (use Eq.(12)) with a case, when the "secondary" source is seen from the aperture of an additional telescope as dot ($a_b < R_a$), then $\langle (\bar{\varphi}_F^{ss})^2 \rangle / \langle \bar{\varphi}_{lb}^2 \rangle = (a_0 / R_a)^{1/3}$. In this case for level of residual fluctuations is received in the next form

$$\beta_0 = 1 - \frac{K^2(0)}{1 + (R_0 / R_a)^{1/3}}. \quad (15)$$

To compare efficiency of correction of a general inclination of wave front for extended and dot LGS, we use specific digital meanings of parameters which are included in the formulas (12), (14), (15). Let's consider $R_0 = 4$ i, $a_b = 400$ i, $X = 100$ km, model $C_n^2(\xi)$ - "average", model $\kappa_0^{-1}(\xi)$ - model C, the additional telescope has the aperture $R_a = 0.1R_0$, $R_a = R_0$. Using curves on Fig.2, we receive $K(0) = -0,7$ for meaning $R_a = 0.1R_0$ and $K(0) = -0,95$ for meaning $R_a = R_0$, and using fragments of the second line on Fig.3 we come to the following results:

$$\beta = 0,57, \beta_0 = 0,84 \text{ for } R_a = 0.1R_0, \beta = 0,31, \beta_0 = 0,71 \text{ for } R_a = R_0.$$

Taking into account all this, it is possible to recommend construction LGS not for a separate telescope, but for separately taken observatory (for example, at top of a volcano Mauna Kea). Thus it is supposed, that in observatory there are some telescopes with the various sizes of the apertures. Thus the largest telescope is used as main illuminator. This telescope forms for itself monostatic LGS. With formation of such star by the full aperture of the main telescope ($a_0 = R_0$) the monostatic star appears practically motionless [7, 10], but this star can be used for measurement high-order aberations of a phase of wave front. In too time for smaller telescopes operating in observatory, such

guide star will be act as bistatic one (see (7)), and thus parameter $b = a_0 / R_0$ will be larger than 1.

1.5. Hybrid scheme LGS

Already the idea [11, 18, 19] of application the hybrid scheme repeatedly expressed. The hybrid scheme of LGS have been assumed monostatic and bistatic schemes operating simultaneously. In such scheme the simultaneous measurement of an angular position of the image of the monostatic (is offered with $a_0 < R_0$) star in the main telescope

$$\bar{\varphi}_{mono} = \bar{\varphi}_{lb} + \bar{\varphi}_F^{sp}(R_0)$$

and angular position of the bistatic star in focal a plane of an additional telescope (size of the additional telescope aperture R_a)

$$\bar{\varphi}_{bi} = \bar{\varphi}_{lb} + \bar{\varphi}_F^{ss}(R_a).$$

We use for correction a difference of these two measurements

$$\bar{\Delta} = \bar{\varphi}_{mono} - \bar{\varphi}_{bi} = \bar{\varphi}_F^{sp}(R_0) - \bar{\varphi}_F^{ss}(R_a).$$

Efficiency of correction of a general inclination of wave front for "optimum" algorithm of correction is given

$$\beta = 1 - \frac{\langle \bar{\varphi}_F^{pl}(R_0) \bar{\varphi}_F^{sp}(R_0) \rangle^2}{\langle (\bar{\varphi}_F^{pl}(R_0))^2 \rangle \left\{ \langle (\bar{\varphi}_F^{sp}(R_0))^2 \rangle + \langle (\bar{\varphi}_F^{ss}(R_a))^2 \rangle \right\}}. \quad (16)$$

For enough large height of formation LGS practically is received

$$\beta \approx 1 - \frac{1}{\left\{ 1 + \langle (\bar{\varphi}_F^{ss}(R_a))^2 \rangle / \langle (\bar{\varphi}_F^{sp}(R_0))^2 \rangle \right\}}. \quad (17)$$

If to compare this expression with (12), we receive, that for the hybrid scheme the efficiency of correction of a general inclination of wave front (Eq.(17)) does not depend on parameters of a laser beam forming a star. It is possible also to show, that the hybrid

scheme has larger efficiency. For the same parameters, as earlier, i.e., $R_0 = 4$, $a_b = 400$, $X = 100$ kms, we receive

$$\beta = 0,38 \text{ for } R_a = 0.1R, \beta = 0,24 \text{ for } R_a = R_0.$$

However hybrid scheme assumes presence of two wave front sensors [33].

The given hybrid scheme can be it carried out on pair of telescopes constructed with opportunities of realization of idea of a telescope - interferometer, as on an example, pair of 10-meter telescopes - ESO-I and ESO-II, or pair 8-meter telescopes from family of a telescope - interferometer VLTI.

References for Chapter 1

1. V.P.Linnik, "About a basic opportunity of reduction of influence of an atmosphere on the star image", Optics and spectroscopy. **25**, N4, N.401-402, 1957.
2. J.Hardy, IEEE, **66**, N7. N.31-85, 1978.
3. Robert Q.Fugate and Walter J.Wild, "Untwinkling the Stars - Part I.", Sky and Telescope, pp.25-32, May 1994.
4. V.P.Lukin, V.F.Matyukhin, "Adaptive correction of the image", Quantum Electronics, **10**, N.12. pp.2465-2473, 1983.
5. Special Issue on Adaptive Optics, Lincoln Laboratory Journal, **5**. N.1. 170 p., Spring 1992.
6. V.P.Lukin, "Limiting resolution of adaptive telescope with the use of artificial star", Proc. ICO-16, "Active and Adaptive optics", pp.521-524, 1993.
7. R.Fugare, "Laser beacon adaptive optics", Optics and Photonics News, pp.14-19, 1993.
8. R.Ragazzoni, "Absolute tip-tilt determination with laser beacons", Astron. Astrophys., **305**, pp. L13-L16, 1996.
9. R.Ragazzoni, S.Esposito, E.Marchetti, "Auxiliary telescopes for the absolute tip-tilt determination of a laser guide star", Mon. Not. R.Astron. Soc., **276**, pp. L76-L78, 1995.
10. M.S.Belen'kii, "Full aperture tilt measurement technique with a laser guide star", Proc. SPIE, **2471**, pp.289-296, 1995.
11. M.S.Bele'kii, "Tilt angular correlation and tilt sensing techniques with a laser guide star", Proc. SPIE, **2956**, pp.206-217, 1996.
12. V.P.Lukin, B.V.Fortes, "Efficiency of adaptive correction of images in a telescope using an artificial guide star", OSA Techn. Digest, **23**, pp.192-194, 1995.

13. V.P.Lukin, "Laser beacon and full aperture tilt measurements", Adaptive Optics, Techn. Digest Series, **13**, pp.35-1-35-5, 1996.
14. V.P.Lukin, "Adaptive formation of beams and images in turbulent atmosphere", Atmospheric and Oceanic Optics, **8**, pp.301-341, 1995.
15. V.P.Lukin, B.V.Fortes, "Limiting opportunities and applicability of various ways of formation of laser guide stars", Atmospheric and Oceanic Optics, **10**, pp.34-41, 1997.
16. V.P.Lukin, "Observation of random angular displacement of optical beams", V All-Union Symposiums on distribution of laser radiation in an atmosphere. Proc. Tomsk., Part II, pp.33-36, 1979.
17. V.P.Lukin, "Correction of random angular displacement of optical beams", Quantum Elektronik., **7**, pp.1270-1279, 1980.
18. V.P.Lukin, "Monostatic and bistatic schemes and an optimal algorithms for tilt correction in ground-based adaptive telescopes", Applied Optics, **37**, N21, pp.4634-4644, 1998.
19. V.P.Lukin, "The hybrid scheme of formation of a laser guide star", Atmospheric and Oceanic Optics, **10**, pp.975-979, 1997.
20. V.P.Lukin, "Distinction and similarity of two schemes of formation laser guide star", Atmospheric and Oceanic Optics, **11**, N.11. pp.1253-1257, 1998.
21. R.E.Good, R.R.Beland, E.A.Marphy, J.H.Brown, And E.M.Dewan, "Atmospheric models of optical turbulence", Proc. SPIE, **928**, pp.165-186, 1988.
22. T.S.McKechnie, "Atmospheric turbulence and the resolution limit of large ground-based telescopes", J.Opt. Soc. Am. A., **9**, pp.1937-1954, 1992.
23. V.P. Lukin, "Optical measurements of outer scale of atmospheric turbulence", Atmospheric and Oceanic Optics, **5**, pp.354-377, 1992.
24. V.P.Lukin, "Research of some features of structure large-scale atmospheric turbulence", Atmospheric and Oceanic Optics, **5**, pp.834-840, 1992.

25. V.P.Lukin, "Comparison of models of spectra atmospheric turbulence", *Atmospheric and Oceanic Optics*, **6**, pp.1102-1107, 1993.
26. V.P.Lukin, A.A.Nosov, "Effective outer scale atmospheric turbulence", *Atmospheric and Oceanic Optics*, **10**, pp.162-171, 1997.
27. V.P.Lukin, "Models and measurements of atmospheric turbulence characteristics and their impact on AO design", *Adaptive Optics-96, Technical Digest Series*, **13**, pp.150-152, 1996.
28. V.I.Klyatskin, *The statistical description of dynamic systems with fluctuation parameters*, Science, Moscow, 1975.
29. V.M.Orlov, I.V.Samokhvalov, G.G.Matvienko, M.L.Belov, *Elements of the theory lightscattering and optical remote sensing*,. Science, Novosibirsk .
30. M.A.Kallistratova, A.I.Kon, "Fluctuations of angles of arrival of light waves from an extended source in turbulent atmosphere", *Izv. Vuzov. Radiophysics*, **9**, N6, pp.1100-1107, .1966.
31. V.L.Mironov, V.V.Nosov, S.N.Chen, "Correlation of displacement of the image of optical laser beams in turbulent atmosphere", *Izv. Vuzov. Radiophysics*, **25**, N12, pp.1467-1471, 1982.
32. M.A.Gracheva, A.S.Gurvich, "Simple model of turbulence, *Izv. AS USSR. Atmospheric and Oceanic Physics*, **16**, pp.1107-1111, 1980.
33. V.P.Lukin, B.V.Fortes, *Adaptive formation of beams and images in atmosphere*,
SB RAS Press, Novosibirsk, 1999.

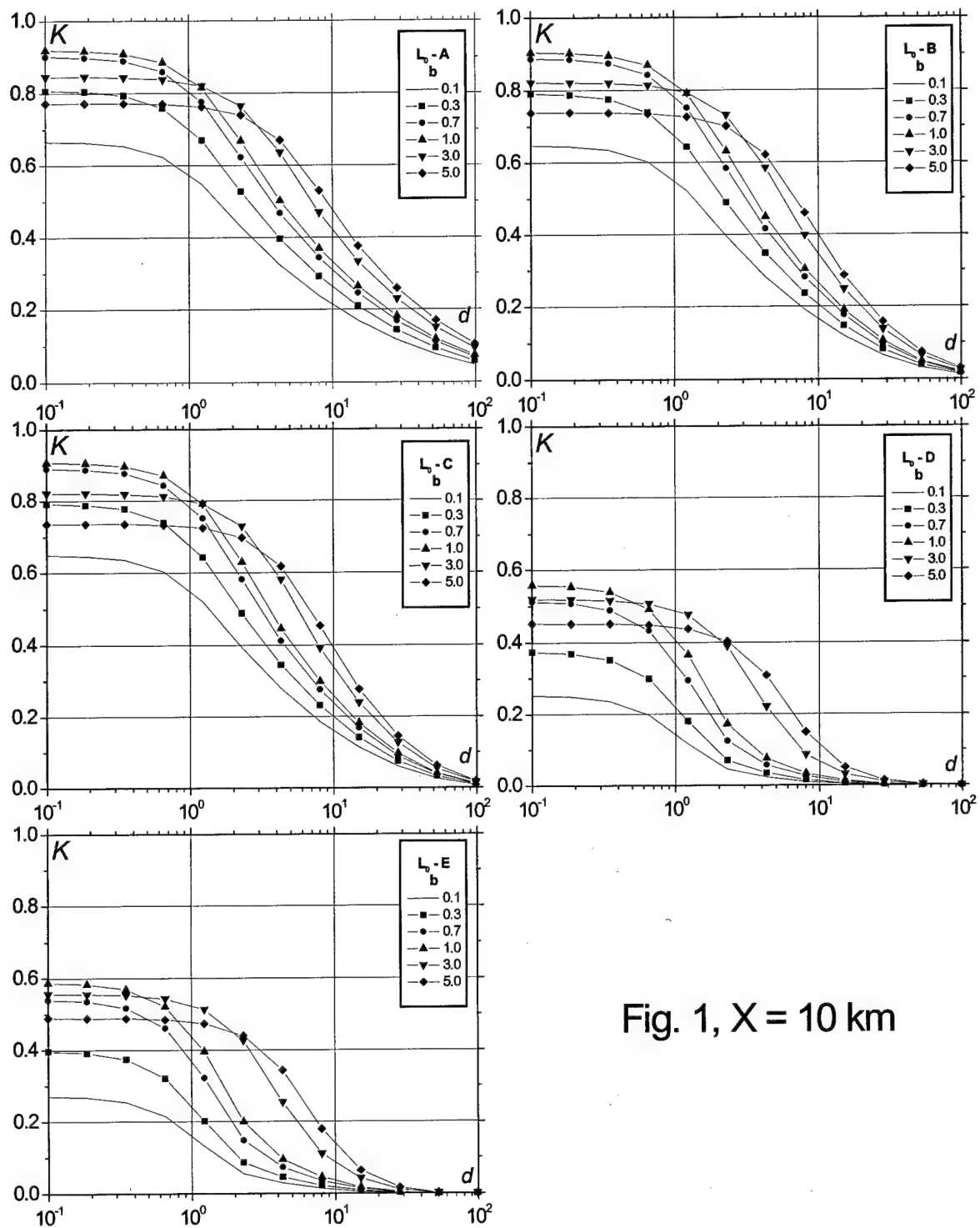


Fig. 1, $X = 10$ km

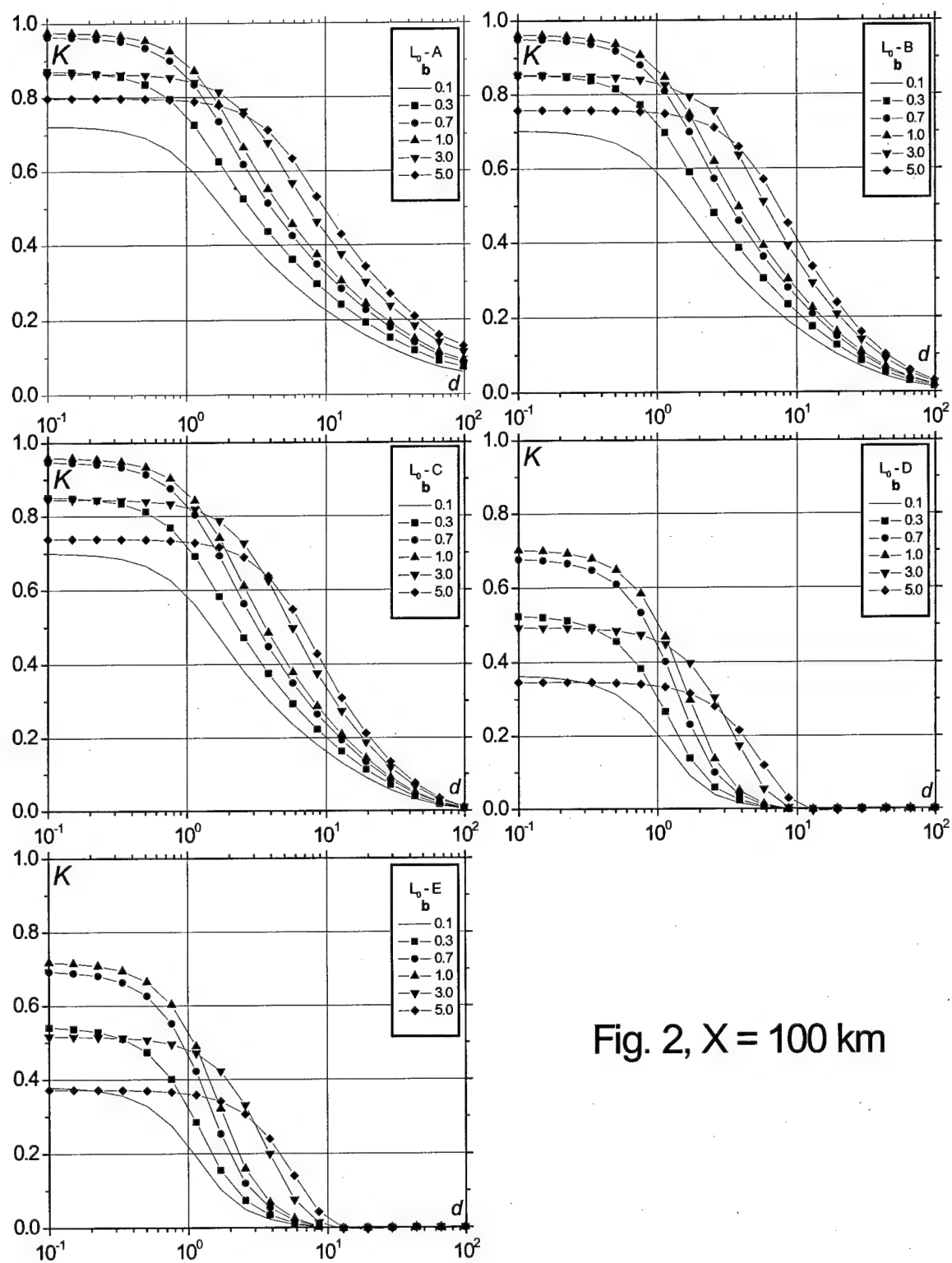


Fig. 2, $X = 100$ km

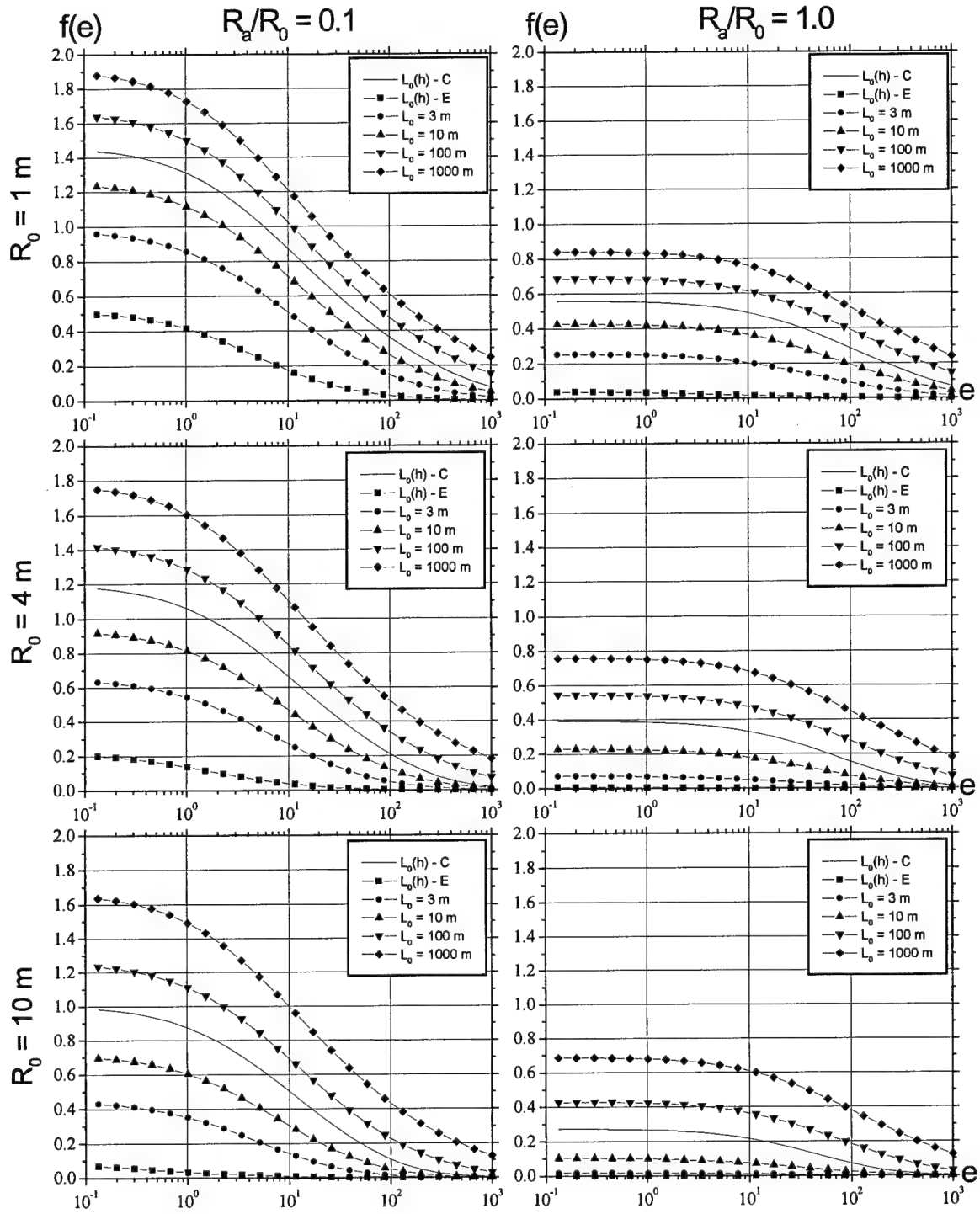


Fig. 3, $X = 10\text{ km}$

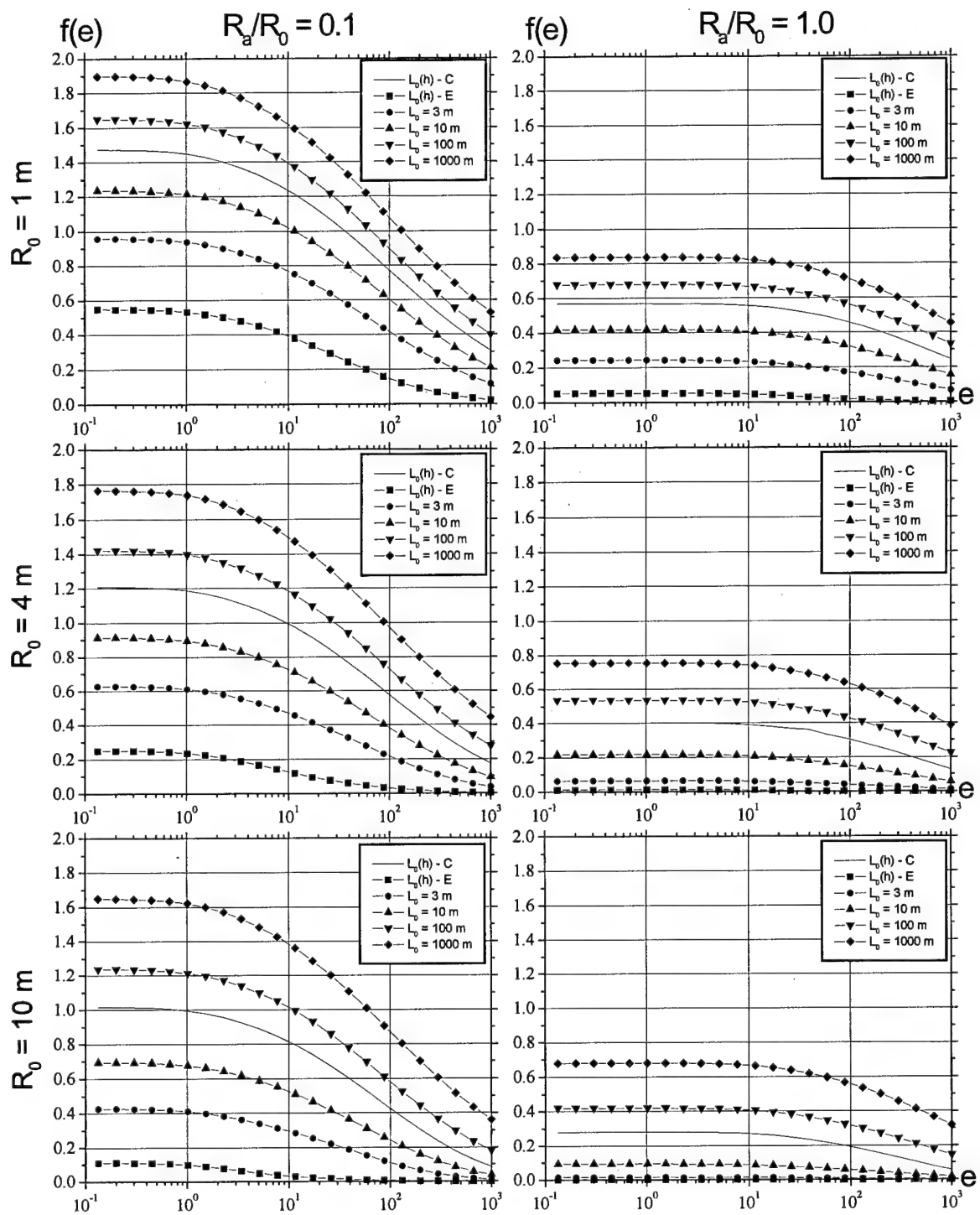


Fig. 4, $X = 100 \text{ km}$

Chapter 2. Adaptive correction of the focused beam in conditions strong fluctuations of intensity

2.1. Introduction

Long time the terms "phase correction" and "wavefront correction" were considered as interchangeable concepts, and "phase corrector" and "corrector of wavefront" - synonyms. The adaptive correction was frequently treated as straightening of wavefront, if deal with recieving of the deformed wave. For adaptive focusing of beams the correction was considered as predistortion of wavefront.

On the other hand, the stricter mathematical consideration within the framework of wave optics describes focusing of a beam or image as addition of eigen waves with of their phase fluctuations. From this point of view the adaptive element phases eigen waves and provides the maximal intensity in focus of optical system.

In usual conditions, if the wavefront is rather smooth surface, both approaches really are practically equivalent. However with infringement of a condition smoothness of wavefront, the situation varies. It occurs, for example, in turbulent atmosphere, when fluctuations of intensity caused the fluctuations of a parameter of refraction, are rather strong.

It is known, that dislocations of wavefront conterminous to points where instant meaning of intensity equal to zero, arise with distances approximately equal diffraction length $L_d = kr_0^2$, where r_0 - coherence radius for a plane wave.

With presence of such points the wavefront of a reference wave cannot be determined as a smooth one-coherent surface, therefore efficiency of adaptive systems with flexible mirrors begins to be reduced.

At the same time, the numerical experiment with model of a compound phase corrector has shown, that its efficiency practically does not change with transition in area of strong fluctuations of intensity. These results were stated in previous reports [1], the calculations were carried out for a plane wave, and the adaptive system operated as a "receiving system".

2.2. Comparison cases for plane wave and gaussian beam

Before to consider the results received for a focused wave beam in adaptive system, working as a "transmitter system", i.e. on formation of the focused beam, we shall remind the most important results received for a plane wave.

We have found out, that the efficiency of adaptive system with a compound corrector does not vary with transition from area weak fluctuations of intensity in area strong fluctuations. This conclusion has seemed to us at first little bit paradoxical, as we expected, that the presence of the special points of a phase and breaks of wavefront will require application of an adaptive corrector with large number of elements. However it has not taken place. From the point of view on adaptive system as on system of phasing of eigen waves, and should be.

Is valid, the transformation of phase distortions in peak, with transition from short optical path to long path, does not result at all in reduction of the size of area of coherence, and even on the contrary, results in some increase of it size. Therefore having a compound mirror with the size of an element equal to radius of coherence, we can to adjust among themselves these coherent areas and by that ensure coherent addition of waves in focus of telescope.

From this point of view, it is easy to explain another result for a plane wave: the dependence of efficiency of adaptive system on delay in circuit of correction practically does not vary with transition from weak fluctuations to area strong fluctuations.

A task of the given work was researches of a more interesting case - a wave as a focused gaussian beam. We wanted to check up, whether it will be possible to receive the same high quality of correction for a beam, as for a plane wave. Besides in this case adaptive system works as a "transmeter system", that too can result in other results.

It is known, that for "ideal" adaptive system in such system the high quality of correction of the focused beam is possible. It was shown in works P.A.Konyaev and Prof. V.P.Lukin. The "ideal" means, that the phase corrector has the indefinitely small size of an element and the boundary conditions describing a field on the radiating aperture of adaptive system look like:

$$U(\vec{\rho}) = A_0(\vec{\rho}) \exp(-\arg u(\vec{\rho})) \quad (2.1)$$

In our case the phase corrector has the finite size of an element equal in our numerical experiments to Fried's radius of coherence for a plane wave.

Let's consider at first results for the "ideal" wavefront sensor and corrector. Here it is interesting to compare the schemes for plane wave and focused beam. Result of calculations shown on Fig.2.1. In both cases the system works in a mode as a "transmeter system", i.e., the irradiated wave at first is modulated by an adaptive phase corrector, and then is distributed through inhomogeneous index of refraction. In case of focused gaussian beam a measure of quality of correction is the average intensity in focus, and in case of a plane wave - intensity in a distant zone, i.e., in focus of a lens, located on the other end, in a plane $z = L$. This approximately

correspond wide collimated beam, or wide beam focused far beyond a layer randomly non-uniform media.

As follows from a Figure 2.1. we have essentially different result for the focused beam and plane wave. We changed length of a path L in a range from $1/10$ up to $10 L_d$ and have not found out essential decrease of efficiency correction for a case of a plane wave. Other result has turned out for gaussian beam. Already with $L = 2L_d$ focal intensity is reduced twice, with $L = 5L_d$ - in three times, and with $L = 7L_d$ - in four times in comparison with the diffraction-limited meaning. From here follows, that there is a principal restriction on pure phase correction of turbulent broadening of the focused beam. What was not adaptive system, completely to compensate turbulent effects on long paths it will be not possible. For presentation in following Table such is shown, that in this case means a long path. Here are simply counted meaning L_d for $r_0 = 10 \text{ m}$ and $\lambda = 0.5 \text{ mm}$ and for presentation the mentioned above meanings of lengths of paths are shown.

Table 1

L_d	$2 L_d$	$5 L_d$	$7 L_d$
$L = 125 \text{ km}$	$L = 250 \text{ km}$	$L = 625 \text{ km}$	$L = 825 \text{ km}$
$SR = 0,68$	$SR = 0,48$	$SR = 0,33$	$SR = 0,25$

The calculation was executed for the size of the aperture $D = 10r_0$, i.e., $D \gg r_0$. For $D > 10r_0$ it is possible to expect the approximately same dependence SR from L/L_d at least for $0.1 < SR < 1$.

Now we shall consider other variant - correction only the potential part of phase distortions. Here a concept of the two parts of phase fluctuations are introduced: vortex and potential components of phase. This variant corresponds to adaptive

system of a traditional type with a flexible mirror and wavefront sensor, which using standard algorithm of reconstruction of a phase from its differences. In previous report [1] we represented result for a plane wave, that now is interesting to compare them to results of calculations for the focused beam. They are shown in a Fig. 2.2.

Is unexpected a little on the first glance that a system effectiveness with a plane wave decreases faster (in a case shown in a Fig.2.1. it was on the contrary - intensity in focus of a beam decreased faster). However it is easy for understanding if to take into account that in system with the focused beam as a reference radiation is the divergent wave. And in a divergent wave the fluctuations of intensity develop slower on large distances. It is obvious if to compare expressions for scintillation index for a plane wave

$$\beta_0^2 = 1.24 C_n^2 k^{7/6} L^{11/6} \quad (2.2)$$

and for divergent spherical wave

$$\beta_0^2 = 0.42 C_n^2 k^{7/6} L^{11/6} . \quad (2.3)$$

From these formulas follows, that in a divergent wave the given meaning of scintillation index will be on a path almost twice longer for equal meanings $C_n^2 k^{7/6}$. With equal L in a divergent spherical reference wave phase dislocations will be less and efficiency of correction - higher.

Thus we have compared efficiency of adaptive correction for a plane wave and focused beam and have found out that in case of correction all aberrations (including phase dislocations) with growth of length of a path is reduced focal efficiency for the focused beam, and with correction smoothed (potential) of a part only phase aberrations - on the contrary faster. The truth the scales of lengths of paths thus differ almost on the order. Let's notice that in both cases the spatial resolution of adaptive

system was necessary infinite, i.e., we considered that the sizes of elements of the wavefront sensor and corrector d much less than Fried's radius of coherence r_0 .

Further us interests efficiency of adaptive system with the finite size of an element, for example, let us to take $d = r_0$. As we have shown in previous reports [1], it is quite enough for a plane wave of such spatial resolution of adaptive correction both in the field of weak, and in the field of strong fluctuations of intensity. Let's check up so whether it for the focused beam.

Let's remind, that we determine a phase on an element of the subaperture by the size d through average complex amplitude

$$\varphi_{ij} = \arg(\bar{U}); \bar{U} = \frac{1}{d^2} \iint_d U(x, y) dx dy \quad (2.4)$$

Roughly speaking, we interchange the position operation of averaging on a subaperture and operation of calculation *arctang* function (more precisely - main meaning of argument). Thus we avoid trouble the definitions, connected to a problem, of a continuous phase on the aperture with presence phase dislocations. Other question - what type of the optical wavefront sensor is capable to execute such measurement. Let's postpone while its decision. Let's notice, that using such model of adaptive system, we avoid a question about it physical realization, but thus to allow to keep in mathematical model parameter describing the spatial resolution of adaptive correction - the size d . In our case this size is the same as for the wavefront sensor, and as element of a compound corrector.

Let's consider results of numerical modeling presented on Fig.2.3. Three curves here are shown: one for the infinite spatial resolution ($d = 0$) and two for $d = r_0$ (only in for first case is corrected only average phase, and in the second case - additionally and local inclination). It is seen that in a general the difference between

these three variants not so principal. And though the efficiency of adaptive system with the infinite spatial resolution is higher, the greater meaning has length of a path.

2.3. Two-colour adaptive system

The completely new character is got in light of occurrence phase dislocations with a task about two-color adaptive correction. The problem arises owing to necessity of scaling phase aberrations from length of a wave of reference radiation λ_r on length of a wave of corrected radiation λ . If the correction on length of a wave λ_r equal $\varphi_r + 2n\pi$ is determined, even in case of complete absence fluctuations of intensity reference indifinition composed $2n\pi$ essentially influences on result of phase correction. Really if the compound mirror brings in an additional optical difference of a path, determined as

$$\Delta l = (\lambda_r / 2\pi)(\varphi_r + 2n\pi),$$

that on other length of a wave we in result shall receive change of a phases, equal

$$\varphi = (\lambda_r / \lambda)(\varphi_r + 2n\pi).$$

Let's notice for clearness that the sizes φ , φ_r and n are functions of cross coordinates (x, y) , which here for brevity are omitted. If, for example $(\lambda_r / \lambda) = 1/2$, the difference of phases between edges of break of wavefront equal 2π for a reference wave turns in π for corrected wave, i.e., the fluctuations which would develop in a sinphase will become to develop in contraphase. Thus indefinition composed 2π , not having any meaning on length of a wave λ_r , can result in cardinal consequences with transition to other length of a wave.

Thus already statement of a task about use of reference radiation with other length of a wave is coordinated to algorithm incorporated in the wavefront sensor. Basically, in two-colour adaptive system it is more logical to measure just aberrations of wavefront describing fluctuations of the differences of optical length of the way Δl ,

instead of fluctuations of a difference of phases. However to measure optical length of a way directly we can not, and calculation Δl as product of the size of the subaperture d on the measured local inclination s give large mistake in the range of strong fluctuations. Even if we shall determine a surface of wavefront of a reference wave, the presence of points dislocations and lines of breaks of wavefront again results us to exact to the same problem.

As the task of two-colour correction is complex and itself multifactors, we shall not to complicate it by introduction of additional spatial scale - size of a beam. Let's consider while some results of numerical experiment with a plane wave.

Here are results for several variants of system. Among themselves they differ by measurable values (local inclination, or "average" complex amplitude). The second difference it is a algorithm of reconstruction, which give way for determination composed 2π .

Numerical "sensor" of wavefront calculates average complex amplitude on each subaperture U_{ij} , then appropriate phase (argument of complex number) and matrix of differences of phases between the next subapertures:

$$\varphi_{ij} = \arg(U_{i,j}); \Delta_{ij}^x = \varphi_{i+1,j} - \varphi_{i,j}; \Delta_{ij}^y = \varphi_{i,j+1} - \varphi_{i,j}.$$

The calculation of differences of phases seems by a superfluous step, as we as are going to calculate a phase. However we should from any reasons attribute $2\pi m_{ij}$ by each ij subaperture and just for it we calculate differences of phases and processable received file Δ_{ij} with the help of algorithm of reconstruction of a phase.

The main lack of this approach - possible passing of an integer of lengths of waves even in absence fluctuations of intensity, as the function \arg returns meanings in a range $[0, 2\pi]$, that corresponds $[0, \lambda]$ in the terms of optical length of a way. However nobody guarantees that an optical difference of a course between beams has

carried out on distance d less λ . If (as in our case) $d = r_0$, the structural function on such distance is equal $D_s(\rho = d) = 6,88 (d/r_0)^{5/3} = 6,88 \text{ rad}$. The accordingly root-mean-square of a difference of a path expressed in lengths of waves, is equal $(6,88)^{1/2}/2\pi = 0,4\lambda$. Situations thus are quite probable when the optical difference of a path is equal, we shall about $1,1\lambda$ and the sensor of a difference of phases give meaning $0,1 \cdot 2\pi = 0,628 \text{ rad}$.

Single way to find out that actually difference of an optical course was more length of a wave - to reduce the size of an element of the sensor d , we shall tell in 2-3 times, and make sum the received differences of phases. Other way - to measure a local inclination of wave front and multiply it on the size d . However last way give a mistake, which value quickly grows in the field of strong fluctuations of intensity.

To illustrate our reasonings we shall consider results of numerical modeling submitted in a Fig. 4-6. All of them are executed for a plane wave with the following ratio between the size of a focusing lens D , radius coherent r_0 and size of the subaperture d : $D/r_0 = 10$, $d = r_0$. Randomly non-uniform media was simulated by 10 random screens and intensity in focal plane of a lens averaging on 10 random realizations. Length of a path was set equal $L/L_d = 0,01$, i.e. fluctuations of intensity on an exit from random media practically are absent.

We varied length of a wave of reference radiation, λ_r . Let's notice that length of a wave enters into the formulas for L_d and r_0 . As in our task two radiations with different lengths of waves now are examined, it is necessary to concretize, what length of a wave enters in normalization of parameters of a task. We have decided to use for normalization fixed length of a wave of corrected radiation λ . Therefore it is necessary to mean, that normalized length of a path L/L_d and size of the aperture D/r_0 for reference radiation with length of a wave λ_r will differ. In the descriptions

of results of numerical modeling we always indicate sizes the waves, appropriate to initial length, λ .

On Fig.4 is shown dependence of the normalized intensity SR (Strehl parameter) in focus of a lens from the ratio λ_r/λ . In a figure are two diagrams - they are given differ by a way of definition of a array of differences of phases $\Delta\phi_{ij}$. In one case (curve \dot{a}) a difference of phases were determined through the *argument* of average complex amplitude U , and in the other - as product of a local inclination on the size of the subaperture (the local inclination also is calculated through U and *gradient* U) [1].

In both cases used algorithm based on the decision MNE (modified normal equation) offered in [2, 3] and used by us in previous reports those of [1]. In this case it gives the same result as algorithm based on the decision UNE (unmodified normal equation), as fluctuations of intensity negligible are small ($L/L_d = 0.01 \ll 1$).

As we also expected, the direct measurement of a difference of phases with scaling on longer length of a wave results in fast reduction of efficiency of correction. Already with $\lambda_r = 0.8\lambda$ parameter Strehl SR falls twice, and with reduction λ_r up to 0.5λ the meaning SR is reduced simply catastrophically. At the same time second variant of the wavefront sensor, which uses meanings of local inclinations, works practically equally well in all range of calculations $0.5\lambda < \lambda_r < 1.5\lambda$. Some reduction SR with $\lambda_r < \lambda$ is explained by small growth fluctuations of intensity in reference radiation with reduction of length of a wave λ_r .

It is interesting to look in what ranges the efficiency of correction for system with the sensor of local inclinations will be kept. Let's consider longer paths. Let's set normalized length $L/L_d = 0.25 \dots 1.0$ and also we shall vary reference length of a wave λ_r in wider ranges - from 0.5λ up to 10λ . The results of numerical modeling

are represented on Fig.4. We see, what even with equal lengths of waves, i.e. with $\lambda_r = \lambda$, the normalized intensity of focal spot is less than the diffraction-limited meaning. As we know, it is caused by that in system with the local inclinations sensor under growth fluctuations of intensity the mistake of estimation of a difference of phases is fast increasing.

With reduction of length of a wave of reference radiation the fluctuations of intensity in it grow and accordingly efficiency of correction quickly falls. With change λ_r from λ up to 0.7λ parameter Strehl decreases almost twice. Increase of length of a wave the reference radiation results at first in some increase of meaning SR with change λ_r from λ up to 2λ and with transition on more long wavelength reference radiation, the efficiency of adaptive correction begins to decrease, however it is enough slowly. Parameter Strehl decreases approximately twice, with increasing λ_r up to 6λ and three times with increase λ_r up to 8λ .

Thus use as reference more long wavelength radiation results in insignificant change of efficiency of correction with $\lambda_r = \lambda \dots 3\lambda$, and with transition to the longer waves - to slow reduction of efficiency of correction. To make here, apparently, already anything it is impossible, as it is connected not with fluctuations of intensity (they decrease with growth λ) or unsuccessful choice of the sensor of distortions, and it is simple with diffraction. With growth of length of a wave the phase distortions pass in faster peak and it does not result in growth fluctuations of intensity only because phase distortions decrease with increase of length of a wave.

References for Chapter 2

1. Previous report for contract SPC 98-4041 (second stage).
2. Takajo H., Takanashi T. //J.Opt.Soc.Am.A, **5**, No.3, pp.416-425, 1988.

3. Takajo H., Takanashi T. //J.Opt.Soc.Am.A, **5**, No.11, pp.1818-1827, 1988.

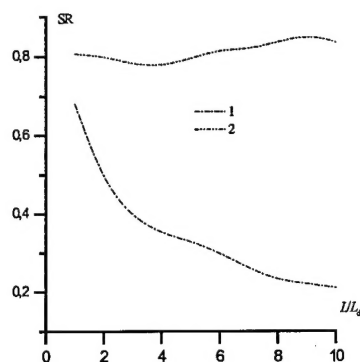


Fig.2.1. Dependence of parameter Strehl from normalized length of a path. $D/r_0 = 10$, 1 - Plane wave, 2 - Focused gaussian beam.

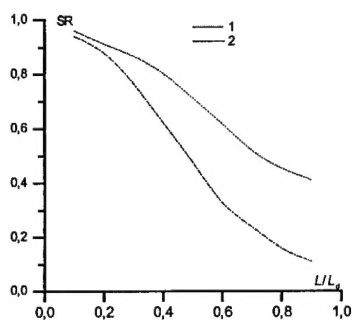


Fig.2.2. Dependence of parameter Strehl from normalized length of a path with correction "potential part" of phases. The wave-front sensor of complex amplitude uses algorithm based on the decision NE, $d \ll r_0$.

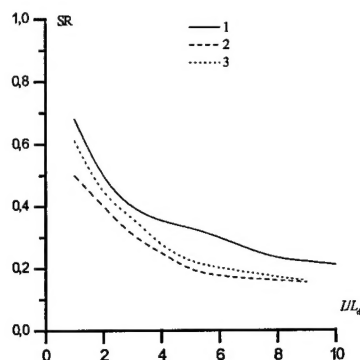


Fig.2.3. Dependence of parameter Strehl from normalized length of a path with correction with the finite size of an element adaptive system. The sensor of complex amplitude uses algorithm based on the decision MNE, 1 - $d \ll r_0$, 2 - $d = r_0$, correction "average" phases and inclination, 3 - correction only "average" phases.

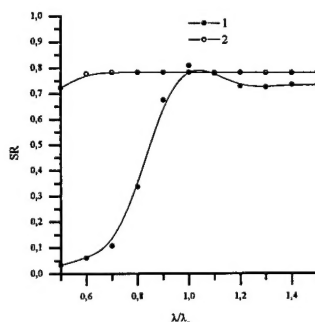


Fig.2.4. Dependence of parameter Strehl from normalized length of reference radiation for two types of the wave-front sensor: A - sensor of a "average" phase, \hat{A} - sensor of a local inclination.

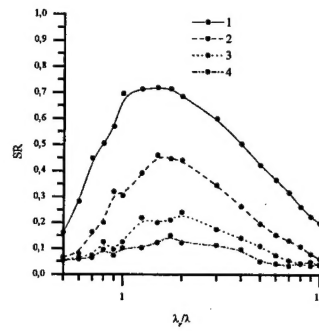


Fig.2.5. Dependence of the normalized intensity (parameter Strehl) from length of a wave of reference radiation. Meanings of normalized length of a path L/kr_0^2 (normalized on length of a wave of corrected radiation): 1 - 0.25, 2 - 0.5, 3 - 0.75, 4 - 1.0.

REPORT DOCUMENTATION PAGE

Form Approved OMB No. 0704-0188

Public reporting burden for this collection of information is estimated to average 1 hour per response, including the time for reviewing instructions, searching existing data sources, gathering and maintaining the data needed, and completing and reviewing the collection of information. Send comments regarding this burden estimate or any other aspect of this collection of information, including suggestions for reducing this burden to Washington Headquarters Services, Directorate for Information Operations and Reports, 1215 Jefferson Davis Highway, Suite 1204, Arlington, VA 22202-4302, and to the Office of Management and Budget, Paperwork Reduction Project (0704-0188), Washington, DC 20503.

1. AGENCY USE ONLY (Leave blank)		2. REPORT DATE 1999	3. REPORT TYPE AND DATES COVERED Final Report	
4. TITLE AND SUBTITLE Laser Beams And Images Adaptive Correction, Including Laser Guide Star Schemes For Formation And The Tip-Tilt Problem			5. FUNDING NUMBERS F61775-98-	
6. AUTHOR(S) Prof Vladimir P. Lukin				
7. PERFORMING ORGANIZATION NAME(S) AND ADDRESS(ES) Institute of Atmospheric Optics RAS Av. Akademicheskii, 1 Tomsk 634055 Russia			8. PERFORMING ORGANIZATION REPORT NUMBER N/A	
9. SPONSORING/MONITORING AGENCY NAME(S) AND ADDRESS(ES) EOARD PSC 802 BOX 14 FPO 09499-0200			10. SPONSORING/MONITORING AGENCY REPORT NUMBER SPC 98-4041	
11. SUPPLEMENTARY NOTES				
12a. DISTRIBUTION/AVAILABILITY STATEMENT Approved for public release; distribution is unlimited.			12b. DISTRIBUTION CODE A	
13. ABSTRACT (Maximum 200 words) This report results from a contract tasking Institute of Atmospheric Optics RAS as follows: The contractor will investigate optical wave propagation in the atmosphere, atmospheric propagation model development, and codes describing the operation of various components of an adaptive system. Especially they will develop a 4D computer code for calculating the parameters of optical waves propagating in both inhomogeneous layers and random-inhomogeneous stratified media under the conditions of thermal blooming.				
14. SUBJECT TERMS EOARD, Atmospheric Propagation, Atmospheric, Atmospheric Science, laser atmospheric propagation, Modelling & Simulation, Turbulence Modeling, Turbulence			15. NUMBER OF PAGES 188	
			16. PRICE CODE N/A	
17. SECURITY CLASSIFICATION OF REPORT UNCLASSIFIED	18. SECURITY CLASSIFICATION OF THIS PAGE UNCLASSIFIED	19. SECURITY CLASSIFICATION OF ABSTRACT UNCLASSIFIED	20. LIMITATION OF ABSTRACT UL	

NSN 7540-01-280-5500

DTIC QUALITY INSPECTED 4Standard Form 298 (Rev. 2-89)
Prescribed by ANSI Std. Z39-18
298-102